TRANSCRIPTIONAL RESPONSES TO TOXIC LEVELS OF CARBONYL CYANIDE P-(TRIFLUROMETHOXY) PHENYLHYDRAZONE [FCCP], AN UNCOUPLER OF OXIDATIVE PHOSPHORYLATION

By

SABU KURUVILLA
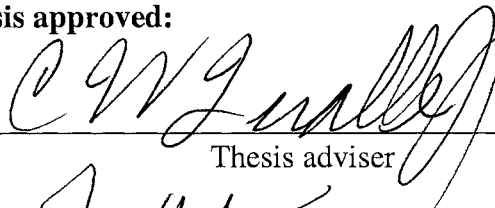
Bachelor of Veterinary Sciences and Animal
Husbandry
Kerala Agricultural University
Trichur, India
1976

Master of Veterinary Sciences
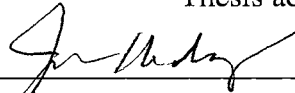University of Agricultural Sciences
Bangalore, India
1980

Submitted to the Faculty of the
Graduate College of the
Oklahoma State University
In partial fulfillment of
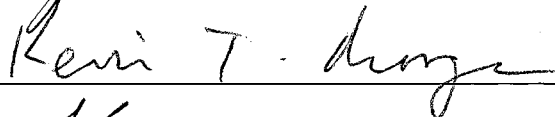the requirements for
the Degree of
DOCTOR OF PHILOSOPHY
May, 2003

TRANSCRIPTIONAL RESPONSES TO TOXIC LEVELS OF CARBONYL CYANIDE P-(TRIFLUROMETHOXY) PHENYLHYDRAZONE [FCCP], AN UNCOUPLER OF OXIDATIVE PHOSPHORYLATION
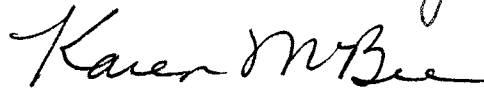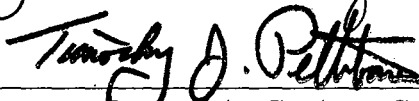
Thesis approved:

Thesis adviser

Dean of the Graduate College

ACKNOWLEDGEMENTS

TABLE OF CONTENTS

LIST OF TABLES

LIST OF FIGURES

CHAPTER 1

THESIS INTRODUCTION

The common bioenergy currency, ATP, is synthesized in energy-transducing

membranes such as those of mitochondria, chloroplasts, and various microorganisms.

The energy to drive the uphill reaction (phosphorylation) for synthesis of ATP from ADP

and inorganic phosphate (Pi) by ATP synthase is supplied by the sequential oxidation-

reduction chain reactions in electron transporting systems. During oxidative

phosphorylation in the mitochondria, the respiratory chain supplies this energy. Thus,

ATP is synthesized by coupling of two reactions, electron transport and phosphorylation.

Uncouplers of oxidative phosphorylation inhibit ATP synthesis by preventing this

coupling reaction in such a fashion that the energy produced by redox reactions cannot be

used for phosphorylation. Thus, in the presence of an uncoupler, the activities of electron

flow and ATP synthase are not inhibited, but ATP synthesis can not take place. A wide

variety of compounds are known to be uncouplers of oxidative phosphorylation in

mitochondria. Most of them are hydrophobic weak acids that possess protonophoric

activities, that is, activities for transporting hydrogen ions (H^+) through a H^+-

impermeable membrane. According to the chemiosmotic theory of Mitchell (Lehninger,

1997), direct energy for ATP synthesis in the form of the chemical potential of H^+

(proton motive force) across H^+-impermeable energy-transducing membranes is supplied

1

by redox reactions. ATP is synthesized from ADP and Pi when H^+ enters the mitochondria via ATP synthase, which consists of the catalytic site F_1 projecting from the membrane and a connecting hydrophobic protein F_0 buried in the membrane. Thus a protonophoric action to collapse the H^+ chemical potential by transport of H^+ into the mitochondria via the membrane is regarded as essential for uncoupling action. Furthermore, since the proton motive force across membranes consists of a pH difference (ΔpH) and a membrane potential ($\Delta \Psi$), any compound or physical force such as osmotic shock and aging that dissipates the pH difference and membrane potential can cause uncoupling (Terada, 1990).

Phenols, benzimidazoles, N-phenylanthranilates, salicylanilides, phenylhydrazones, salicylic acids, acyldithiocarbazates, cumarines and aromatic amines are known to induce uncoupling. These compounds are all weak acids, and their uncoupling is thought to be attributable to their protonophoric actions (Hanstein et al., 1976). The simplest mechanism of the protonophoric action of a weakly acidic uncoupler is as follows. At the membrane-water interface, the anionic form of the uncoupler, U^-, traps H^+ and becomes the neutral form of UH. UH traverses the membrane to the opposite side where it releases H^+. U^- then returns to the original interface where it again traps H^+. By this uncoupler cycle, H^+ is transported into inner side of mitochondria through the H^+ impermeable membrane, thus dissipating the H^+ gradient across the membrane, which results in uncoupling. Some compounds, such as hydrophobic cations and hydrophobic anions, that do not possess an acid dissociable group are also known to induce uncoupling, but their activities are weaker than protonophoric uncouplers (Terada, 1990).

Endogenous uncouplers have also been well recognized in the recent years. The ability of hibernators, cold-adapted rodents and new-born mammals to produce heat and increase standard metabolic rate (SMR) by non-shivering thermogenesis results from the activity of uncoupling protein 1 (UCP1) in mitochondria of brown adipose tissue (BAT) (Nedergaard et al., 2001). UCP1 is restricted to the brown adipocytes, and was originally thought to be the only transporter capable of uncoupling mitochondria. However, UCP1 probes occasionally gave weak signals in other tissues (Ricquier et al., 2000), suggesting the presence of homologues. UCP2 was discovered because of its relatively high sequence identity to UCP1. UCP2 mRNA has been found in many tissues, including cardiac muscle, BAT, white adipose tissue, skeletal muscle, kidney, non-parenchymal liver cells, lung, placenta, pancreatic cells and the immune system. UCP2 protein however, was not detected in heart, skeletal muscle, liver or BAT (Pecqueur et al., 2001). Human UCP3 is 59% identical to human UCP1 and 72% identical to human UCP2. UCP3 is restricted to BAT and skeletal muscle (Sivitz et al., 1999), both tissues that make a major contribution to thermogenesis, making it a more enticing target for drug development than UCP2. Evidence that UCP2 and UCP3 are responsible for basal proton conductance comes from experiments employing high expression of mammalian UCP2 and UCP3 in yeast (Hinz et al., 1999) and transgenic over-expression of human UCP3 in mice (Clapham et al., 2000). Such high expression lowers mitochondrial membrane potential and increases state 4 respiration, indicating uncoupling. The UCPs remain important potential targets for specific pharmacological uncoupling as a treatment for obesity. Other members of the mitochondrial carrier family have also been implicated in the uncoupling of mitochondria. In particular, the adenine nucleotide transporter is

responsible for uncoupling by free fatty acids (Skulachev et al., 1998) and these carriers may also be potential drug targets.

There has been considerable interest within the pharmaceutical industry in developing specific β_3-adrenoceptor agonists that would selectively lead to the activation of uncoupling through UCP1 in brown fat. The activity of the β_3-adrenoceptor to activate lipolysis in both white and brown fat leading to a consequent activation of UCP1 mediated lipolysis in brown fat is now well understood (Nicholls et al., 1999). Rodent studies provide excellent evidence that activation of uncoupling by brown fat represents an important potential human therapeutic target. Unfortunately, clinical studies have yet to provide proof of concept in humans, though clinical trials are still in progress. It has proved particularly difficult to develop β_3-adrenoceptor agonists that lack activity against 1 and 2-adrenoceptors (Weyer et al., 1999). This difficulty, coupled with the very low levels of brown fat in adult humans has made the results of the various clinical trials difficult to interpret. However, if β_3-adrenoceptor agonists prove capable of reactivating dormant brown fat, or if conversion of white to brown adipose tissue becomes possible, then a suitably selective agent may show relevant activity in humans.

Thyroid hormones have a long history in the treatment of obesity (Byrom, 1993) and are positively correlated with basal metabolic rate (BMR). At the cellular level, hepatocytes isolated from hyperthyroid rats have twice the respiration rate of euthyroid controls and at the subcellular level, mitochondria prepared from the liver of hyperthyroid animals have increased proton permeability compared with those from euthyroid animals (Brand et al., 1992). There are now two main hypotheses for the stimulation of respiration and proton conductance in mitochondria and cells by thyroid

4

hormones. In the first hypothesis, thyroid hormones act directly at the membrane level, rigidifying the bilayer and leading to a compensatory change in the fatty-acyl composition of the phospholipids. Alternatively, thyroid hormones could alter membrane composition through transcriptional regulation of desaturases and other enzymes. In either case, the change in phospholipid fatty acyl composition alters the proton conductance and degree of uncoupling of the mitochondrial inner membrane. In support of this hypothesis, the polyunsaturation of mitochondrial phospholipid acyl chains increases in hyperthyroidism (Hulbert, 2000), and liver mitochondrial proton conductance correlates with polyunsaturation of mitochondrial phospholipid acyl chains (Brookes et al., 1998). Changes in the area of mitochondrial inner membrane are also implicated in the change in measured proton conductance (Brand et al., 1992). In the second hypothesis, thyroid hormones act through transcriptional regulation and affect proton conductance through expression of specific proteins (Soboll, 1993). For example, the levels of UCP2 and UCP3 mRNA increase in response to thyroid treatment (Masaki et al., 1997; Lanni et al., 1999). Supra-physiological doses of thyroid hormones are no longer used in the treatment of obesity because of unwanted side-effects such as tachycardia, increased heart weight (Klein et al., 1984), thyroid atrophy (Mittleman et al., 1984) and a negative nitrogen balance, that is a loss of lean body mass (muscle) (Kyle et al., 1996). They may cause loss of water and muscle rather than loss of fat and adipose tissue.

Leptin has also been a target for drug development. Leptin is an adipocyte hormone that functions as the afferent signal in a negative feedback loop regulating body weight. In addition, leptin functions as a key link between nutrition and the function of most, if

not all other physiologic systems. When at their set point, individuals produce a given amount of leptin and in turn maintain a state of energy balance. Weight gain results in an increased plasma leptin level, which elicits a biologic response characterized in part by a state of negative energy balance. Weight loss among both lean and obese subjects results in decreased plasma levels of leptin, which lead to a state of positive energy balance and a number of other physiologic responses. In humans, both the intrinsic sensitivity to leptin and its rate of production vary and both appear to contribute to differences in weight (Friedman, 2002).

Historically, Mitochondrial uncoupling has been widely seen as a potential target for development of pharmaceutical drugs for treatment of clinical obesity. Obesity is a disease resulting from a prolonged positive imbalance between energy intake and energy expenditure resulting in the storage of fat. The rapidly increasing world-wide incidence of obesity and its association with serious pathological conditions means that it is beginning to replace under-nutrition and infectious diseases as the most significant contributor to ill health in the developed world (Kopelman, 2000). Weight loss, induced by dieting, has been shown to be successful in reducing the health consequences of obesity but unfortunately large percentage of individuals who lose weight through dietary control eventually return to their original weight (Wadden, 1993). Pharmacological treatment may therefore be desirable for those patients with associated morbid conditions who have been unable to control their obesity through diet and exercise.

Any treatment for obesity has to reduce energy intake, increase energy expenditure or combine both effects. Current therapies for obesity predominantly lead to decreased energy intake either by acting at satiety centers in the brain, or by reducing the efficiency

of intestinal absorption. Sibutramine is an example of a drug in the former class (Luque et al., 2002), and orlistat is an example of a drug in the latter class (Ballinger et al., 2001). Exercise is the most practical and potentially easiest way to increase energy output. The main benefit of exercise is to increase resting metabolic rate, and overall energy expenditure, by a greater amount than that resulting directly from the exercise (Poehlman, 1989). Pharmacological agents that increase metabolic rate by increasing uncoupling of mitochondrial oxidative phosphorylation are likely to mimic this beneficial effect of exercise on resting metabolic rate and could provide a useful adjunct to agents acting to reduce satiety.

Basal metabolic rate (BMR) is the minimal caloric requirement for normal life in an organism in the absence of external stimulation, work and growth. It is measured under defined conditions at thermo-neutrality, in a post-absorptive state. Basic physiological processes continue in this minimal state, including ventilation and blood circulation. At the cellular level, the reactions that make up BMR include protein turnover, ion cycling across the plasma membrane, turnover of nucleic acids and lipids, and proton cycling across the mitochondrial inner membrane (uncoupling) (Brand, 1990). Resting metabolic rate (RMR) is measured as BMR but not in the post-absorptive state (Blaxter, 1989). These measurements are not suitable in animals; therefore standard metabolic rate (SMR) is a more useful measure of metabolic rate in animals. SMR is measured under defined conditions, which are not necessarily those of BMR; in particular, temperature may vary. SMR varies considerably between species. It is primarily dependent on body mass and so mass-specific SMR decreases as body mass increases. For example, the SMR per gram of a mouse (body mass 0.05 kg) is approximately 10-fold higher than the SMR per gram of

a horse (body mass 500 kg). (Harper et al., 2001). The differences in mass-specific SMR between species indicate the existence of regulatory mechanisms that may be amenable to pharmacological manipulation. Some of these differences in SMR may be caused by differences in mitochondrial proton cycling (Harper et al., 2001).

Skeletal muscle represents a particularly attractive target for directed uncoupling due to the large muscle mass, which in humans, accounts for approximately 15-20% of SMR (Rolfe et al., 1999). The maximal aerobic capacity of a human is generally estimated to be up to 12 times SMR. Most of this increase can be directly attributed to skeletal muscle respiratory activity and it is clear that muscle can greatly increase its metabolic activity. Doubling metabolic rate by modestly uncoupling skeletal muscle should produce few adverse side effects as this increase would only be comparable to mild exercise (Blaxter, 1989). Indeed, support for this view has been obtained using proteins (uncoupling proteins 1 and 3) that may naturally uncouple mitochondria. High expression of human UCP3 in transgenic mouse skeletal muscle led to decreased weight gain despite increased food intake (Clapham et al., 2000).

Mitochondria are normally responsible for 90% of cellular oxygen consumption and the majority of adenosine triphosphate (ATP) production. The flow of electrons from reduced substrate to oxygen is coupled by a proton electrochemical gradient across the mitochondrial inner membrane to the synthesis of ATP. However, not all of the available energy is coupled to ATP synthesis. Instead, much is lost by uncoupled reactions when protons move from the inter-membranous space back into the mitochondrial matrix via pathways, which circumvent the ATP synthase. There are two sorts of uncoupling. Basal (mild) uncoupling is not tightly regulated and is present in all mitochondria, whereas

inducible proton conductance is catalyzed by proteins, tightly regulated, and found in discrete cell types.

Proton cycling is a major contributor to SMR, responsible for around 26% of the oxygen consumed in resting rat hepatocytes and about 52% in perfused, resting rat skeletal muscle. Multiplication of these values by the contribution of each tissue to SMR suggests that proton cycling account for 20-25% of rat SMR (Rolfe et al., 1996). This makes proton cycling the largest single contributor to SMR. It would be helpful to understand how protons re-enter the mitochondrial matrix without passing through the ATP synthase. Diffusion of protons through the phospholipid bilayer is one mechanism of basal proton conductance, although certain properties of the membrane, such as the presence of proteins, are important in determining the conductance (Brookes et al., 1997). Mitochondrial membranes containing a higher ratio of polyunsaturated fatty acyl groups (PUFA) to monounsaturated fatty acyl groups (MUFA) may allow a higher molecular activity of membrane proteins, so membrane acyl composition could affect metabolic rate. In particular, ω-3 PUFAs have been strongly linked to SMR (Hulbert et al., 1999). As described above, mammals with a smaller body mass have higher mass-specific SMR and higher mitochondrial proton conductance than larger mammals. Surface area and fatty acyl composition of mitochondria both vary with body mass (Porter et al., 1996), so either factor could affect proton conductance. Around two-thirds of the difference in proton conductance of mitochondria from mammals of different body mass is due to the amount of mitochondrial membrane, and one-third is due to some difference (protein or phospholipid) in membrane composition (Porter et al., 1996). Dietary fatty acids can alter the fatty acyl composition of the mitochondrial inner membrane (Pehowich, 1999), and it

is conceivable that diet, or pharmaceutical agents that alter the PUFA: MUFA ratio of fatty acyl groups in the membrane, could affect mitochondrial uncoupling and hence modify BMR and weight gain. For example, fish oil high in ω-3 PUFA has been suggested to limit obesity (Hun et al., 1999). Oils that contain high levels of ω-3 fatty acids and claimed to be beneficial are already on the market, although evidence that they effect weight loss is lacking.

The artificial uncoupler 2,4-dinitrophenol (DNP) has been used in the treatment for obesity for many years (Parascandola, 1974). DNP is a lipid-soluble weak acid which acts as a protonophore because it can cross membranes protonated, lose its proton and return as the anion, then reprotonate and repeat the cycle. In this way, it increases the basal proton conductance of mitochondria and uncouples. The effect of DNP derivatives was first noted in 1885 when scientists saw thermogenic effects of Martius Yellow (a dinitro-alpha-napthol), a coal tar dye used in the 19th century to give the impression that food was rich in eggs (Harper et al., 2001).

The use of DNP to treat obesity was stimulated by observations of its effect in French ammunition workers during World War I. They commonly used a mixture of 40% dinitrophenol and 60% trinitrophenol for their munitions. DNP was introduced as a drug in the 1930s and used with considerable success, though reports of side-effects such as cataracts, and some deaths from overdose led to it being removed from the market due to pressure from the US Food and Drug Administration (FDA) in 1938 (Harper et al., 2001).

The most extensive controlled trials with DNP were carried out during the 1930s at Stanford University, CA. Interpretation of this work can be complicated, as the doses of DNP had to be optimized for each patient (due to the steep dose response and patient to

patient variability) and were usually increased as the studies progressed. Doses up to about 5 mg/ kg were generally well tolerated. Between about 5-10 mg/ kg, patients reported profuse sweating but, surprisingly, there was no evidence of increased body temperature or heart rate. Doses above 10 mg/ kg led to increased heart rate, respiration rate and excessive body temperature rises. Single doses of 3-5 mg/ kg produced an increase in resting metabolic rate of 20-30% within the first hour. This was maintained for 24 h after which a gradual fall became apparent. Daily dosing of 3-5 mg/ kg produced a gradual increase of efficacy - an average 40% increase in metabolic rate was observed after a few weeks that was then maintained, with no sign of tolerance, for at least 10 weeks (Harper et al., 2001).

Weight loss in these studies, where no attempt was made to control diet, was reported to be variable. Of 170 treated patients, a mean of 7.8 kg weight loss was recorded, averaging 0.64 kg week 1. There were no clearly reported effects on food consumption. In contrast to the use of thyroid extract (also in common use at the time to treat obesity), DNP did not promote urinary nitrogen excretion, so the assumption was made that weight loss could be attributed to a specific loss of fat. One potential complication in the interpretation of weight loss data is the ability of the drug to promote edema. This effect was reported to account for a common apparent failure to continue to lose weight in the face of a maintained increase in metabolic rate. For some patients, withdrawing DNP led to a rapid weight loss that was attributed to loss of excess body water after which DNP dosing could be resumed with its former effectiveness. Therapeutic doses of DNP had no effects on blood pressure or heart rate in normal patients. Interestingly, a subset of 30 hypertensive patients exhibited average falls of 9.4

mm Hg in systolic and 12.6 in diastolic blood pressure. These improvements in hypertension were also noted at doses of DNP insufficient to cause weight loss. Some studies were also performed in diabetic patients with inconsistent results but there did appear to be improvements in glucose tolerance after long-term dosing (Harper et al., 2001).

This ability of DNP to produce significant reductions in body weight, without the need for dietary restriction, led to its widespread use to treat obesity. In the absence of formal regulatory controls it is not surprising that inexperienced physicians soon prescribed it with no access to the metabolic rate measurements necessary to determine optimal doses. DNP was even included in a variety of anti-obesity preparations that could be used by the public without medical consultation. By 1934 it was estimated that a total of 100,000 patients had been treated (Harper et al., 2001).

Given the steep dose dependence of metabolic rate for DNP and its the widespread use, it is perhaps not surprising that a number of deaths in the 1930s were attributed to accidental or deliberate overdose. A number of cases of cataracts were reported in women in 1935. In 1938 the FDA acquired more powers to prosecute manufacturers of misbranded therapies and announced that the use of a variety of patent medicines, including DNP, could lead to prosecution. These threats led to a withdrawal, in 1938, of the DNP-containing nostrums from the market as well as an end to the official clinical use of DNP (Parascandola et al., 1974).

Antony et al. (2001) re-evaluated the effects of DNP in rats and confirmed the relative insensitivity of this species and the particularly steep dose response to increase metabolic rate. In contrast to humans, DNP did not significantly increase metabolic rate

in rats when dosed orally at 10 mg/ kg, but a good comparatively long lasting increase was seen at 30 mg/ kg that was comparable in magnitude to a rodent β_3-adrenoceptor agonist. It has been unambiguously established however, that uncoupling can increase energy expenditure without compensatory mechanisms increasing food intake to the extent that they nullify the uncoupling.

Using pharmacological agents to uncouple all mitochondria throughout the body may be a high-risk treatment, because it might compromise energy homeostasis in tissues such as heart and brain. On the other hand, active tissues like these may be less susceptible to mild uncoupling than less active ones like resting muscle or resting BAT because proton conductance has much less control over respiration rate in active mitochondria (Hafner et al., 1990). The small difference between the effective and the fatal doses of DNP, as well as side-effects resulting from its non-selective actions, mean that more research needs to be done to understand the mechanisms of actions associated with such compounds on the various biochemical circuitries.

It was against this historical backdrop that the present study was undertaken to investigate the various mechanisms of toxicity associated with supra-pharmacological doses of DNP using large-scale differential gene expression (DGE) technology. Skeletal muscle, being the potential target tissue for anti-obesity drug development, was selected as the cell line of choice for the study. One of the early experiments in the study involved measuring mitochondrial uncoupling by DNP, using a J-aggregate forming probe, 5,5', 6,6'-tetrachloro-1, 1', 3,3'-tetraethylbenzimidazolylcarbocyanine iodide (JC-1), in vitro. Carbonyl cyanide p- (trifluromethoxy) phenylhydrazone [FCCP], also a classical protonophoric uncoupler with similar mode of action as DNP, was used as a positive

control in such assays. Ironically, after several months of work in standardizing the assay, the positive control yielded consistent and reproducible results, but the results obtained from DNP were inconsistent and non-reproducible, and the decision was made to abandon DNP and pursue the work using FCCP. It was not clear as to why DNP gave unreliable results - the selected rhabdomyosarcoma cell line (RD) could be insensitive to uncoupling by DNP or the assay may have required different sets of conditions.

Various methods are available for detecting and quantitating gene expression levels, including Northern blots and differential display. The new arrivals to this arena are two array based technologies – cDNA and oligonucleotide arrays. These allow one to study expression levels in parallel, thus providing static information about gene expression (that is, in which tissues the gene is expressed) and dynamic information (that is, how the expression pattern of one gene relates to those of others) (Duggan et al., 1999).

Although both cDNA and oligonucleotide arrays are capable of producing patterns of gene expression, fundamental differences do exist between the methods. Hybridization of nucleic acids (one of which is immobilized on a matrix) provides a core capability of molecular biology. This method provides high sensitivity and specificity of detection as a consequence of exquisite, mutual selectivity between complimentary strands of nucleic acid. Transcript abundance is assayed by immobilizing mRNA or total RNA on membrane and then incubating in a radioactively (or fluorescently) labeled, gene specific target. If multiple RNA samples are immobilized on the same matrix, as done in oligonucleotide arrays with different fluorescent labeling for each sample, one obtains simultaneous information about the quantity of a particular message present in each RNA pool. Many gene-specific polynucleotides derived from the 3' end of RNA transcripts are

individually arrayed on a single matrix such as nylon. This matrix is then probed with radioactively tagged cDNA representations of total RNA pool from test and reference cells, allowing one to determine the relative amount of transcript present in the pool by the type or amount of signals generated. The adaptive nature of the fabrication and hybridization methods allows the techniques to be widely applied. Production of arrays begins with the selection of the 'probes' to be printed on the array. In many cases, these are chosen directly from databases including GenBank and UniGene. Additionally, full-length cDNAs, collections of partially sequenced cDNAs (ESTs), or randomly chosen cDNAs from any library of interest can be used. cDNA arrays are produced by spotting PCR products (of approximately 0.6 - 2.4 kb) representing specific genes onto a matrix. Typically, the PCR products are purified by precipitation or gel-filtration to remove unwanted salts, detergents, PCR primers and proteins present in the PCR cocktail. A robot that spots a sample of each gene product carries out printing on to the solid matrix. The types of membranes commonly used are nitrocellulose and charged nylon. Glass-based arrays are most often made on microscope slides, which have low inherent fluorescence. In most cases, DNA is cross-linked to the matrix by ultraviolet irradiation. The targets for the microarray are labeled representations of cellular mRNA pools. Typically, reverse transcription from an oligo-dT primer is used. This has the virtue of producing a labeled product from the 3' end of the gene, directly complimentary to immobilized targets synthesized from ESTs. Frequently, total RNA pools (rather than mRNA selected on oligo-dT) are labeled, to maximize the amount of message that can be obtained from a given amount of tissue. The purity of RNA is a critical factor in hybridization performance (Duggan, 1999).

Rapid progress in genome sequencing and in the development of platforms to assess gene and protein expression has made these tools readily accessible to research teams. This is the era when genomic technology promises to revolutionize research in drug discovery and toxicology. The power of large-scale DGE is that the mRNA levels in cells can be obtained for thousands of genes in a single experiment. Traditionally, research has been on a 1-gene-1-protein at a time basis (the vertical approach). In the genomic era, horizontal investigations involve functional characterization of a large portion of genes in a genome using single high-throughput tools. The horizontal and vertical approaches are complementary. Horizontal approaches offer the advantage of global analyses but do not provide conclusive answers. The vertical approach is more appropriate to investigation of specific hypothesis, which though lacks efficiency can answer questions raised by horizontal studies. Structural genomics is directed towards understanding of the physical make up of genomes, while functional genomics studies the function of the genes and gene products. Toxicogenomics is a subdiscipline of functional genomics using genomic tools to evaluate toxicity caused by pharmaceutical or environmental chemicals (Boorman et al., 2002).

Since microarray technology is still an emerging field and remains somewhat unproven, and since changes in transcription can not be equated to changes in functional pathways, because transcripts have to be translated and proteins may require post-translational modifications in order to become functional, changes in mRNA expression profiles observed in the study could not be accepted as such, to indicate changes in biochemical functions. Hence appropriate functional biochemical assays and

morphological evaluations were performed as and when necessary throughout the entire

study to support gene expression data.

REFERENCES

Anthony, D.M., Dickinson, K., Jones, R.B. and Heal, D.J. (2001). Metabolic actions of 2,4-dinitrophenol: a re-evaluation of activity in-vitro and in-vivo. In Obesity Regulation Energy Homeostasis Keystone Symposia. Keystone Symposia, Silverthorne, CO. 218-224.

Ballinger, A., Peikin, S.R. (2002). Orlistat: its current status as an anti-obesity drug. *Euro. J. Pharmacol.* **440**, 109-117.

Blaxter, K. (1989). *Energy Metabolism in Animals and Man.* Cambridge University Press, Cambridge, UK.

Boorman, G.A., Anderson, S.P., Casey, W., Brown, R.H., Crosby, L., Gottschalk, K., Easton, ., Ni, H., and Morgan, K. (2002). Toxicogenomics, drug discovery, and the pathologist. *Toxicol. Pathol.* **30**, 15-27.

Brand, M.D. (1990). The contribution of the leak of protons across the mitochondrial inner membrane to standard metabolic rate. *J. Theor. Biol.* **145,** 267-286.

Brand, M.D., Steverding, D., Kadenbach, B., Stevenson, P.M., and Hafner, R.P. (1992). The mechanism of the increase in mitochondrial proton permeability induced by thyroid hormones. *Eur. J. Biochem.* **206**, 775-781.

Brookes, P.S., Hulbert, A.J., and Brand, M.D. (1997). The proton permeability of liposomes made from mitochondrial inner membrane phospholipids: no effect of fatty acid composition. *Biochim. Biophys. Acta.* **1330,** 157-164.

Brookes, P.S., Buckingham, J.A., Tenreiro, A.M., Hulbert, A.J., and Brand, M.D. (1998). The proton permeability of the inner membrane of liver mitochondria from ectothermic and endothermic vertebrates and from obese rats: correlations with standard metabolic rate and phospholipid fatty acid composition. *Comp. Biochem. Physiol. B. Biochem. Mol. Biol. 119, 325-334.*

Byrom, F.B. (1933). Nature of myxoedema. *Clin. Sci.* **1,** 273-285.

Clapham, J.C., Arch, J.R., Chapman, H., Haynes, A., Lister, C., Moore, G.B., Piercy, V., Carter, S.A., Lehner, I., Smith, S.A., Beeley, L.J., Godden, R.J., Herrity,.N., Skehel,M.,

Changani, K.K., Hockings, P.D., Reid, D.G., Squires, S.M., Hatcher, J., Trail, B., Latcham, J., Rastan, S., Harper, A.J., Cadenas, S., Buckingham, J.A., Brand, M.D., and Abuin, A. (2000). Mice overexpressing human uncoupling protein-3 in skeletal muscle are hyperphagic and lean. *Nature.* **406,** 415-418.

Duggan, D.J., Bittner, M., Chen, Y., Meltzer, P., and Trent, J.M. (1999). Expression profiling using cDNA microarrays. *Nat. Genet.* **21,** 10-14.

Friedman, J.M. (2002). The function of leptin in nutrition, weight, and physiology. *Nutr. Rev.* **60,** 1-14.

Hafner, R.P., Brown, G.C., and Brand, M.D. (1990). Thyroid-hormone control of state-3 respiration in isolated rat liver mitochondria. *Biochem. J.* **265,** 731-734.

Hanstein, W.G. (1976). Uncoupling of oxidative phosphorylation. *Biochim. Biophys. Acta.* **456,** 129-148.

Harper, J.A., Dickinson, K., and Brand, M.D. (2001). Mitochondrial uncoupling as a target for drug development for the treatment of obesity. *Obes. Rev.* **2,** 255-265.

Hinz, W., Faller, B., Gruninger, S., Gazzotti, P., and Chiesi, M. (1999). Recombinant human uncoupling protein-3 increases thermogenesis in yeast cells. *FEBS Lett.* **448,** 57-61.

Hulbert, A.J. (2000). Thyroid hormones and their effects: a new perspective. *Biol. Rev. Camb. Philos. Soc.* **75,** 519-631.

Hulbert, A.J., and Else, P.L. (1999). Membranes as possible pacemakers of metabolism. *J. Theor. Biol.* **199,** 257-274.

Hun, C.S., Hasegawa, K., Kawabata, T., Kato, M., Shimokawa, T., and Kagawa, Y. (1999). Increased uncoupling protein 2 mRNA in white adipose tissue, and decrease in leptin, visceral fat, blood glucose, and cholesterol in KK-Ay mice fed with eicosapentaenoic and docosahexaenoic acids in addition to linolenic acid. *Biochem. Biophys. Res. Commun.* **259,** 85-90.

Klein, I., and Levey, G.S. (1984). New perspectives on thyroid hormone, catecholamines, and the heart. *Am. J. Med.* **76,** 167-172.

Kopelman, P.G. (2000). Obesity as a medical problem. *Nature.* **404,** 635-643

Kyle, L.H., Ball, M.F., and Doolan, P.D. (1966). Effect of thyroid hormone on body composition in myxedema and obesity. *N. Engl. J. Med.* **275,** 12-17.

Lanni, A., Beneduce, L., Lombardi, A., Moreno, M., Boss, O., Muzzin, P., Giacobino, J.P., and Goglia, F. (1999). Expression of uncoupling protein-3 and mitochondrial

activity in the transition from hypothyroid to hyperthyroid state in rat skeletal muscle. *FEBS Lett.* **444**, 250-254.

Lehninger, A.L., Nelson, D.L., and Cox, M.M. (1997). *Principles of Biochemistry.* Worth publishers, NY.

Luque, C.A., and Rey, J.A. (2002). The discovery and status of sibutramine as an anti-obesity drug. *Eur. J. Pharmacol.* **440**, 119-128.

Masaki, T., Yoshimatsu, H., Kakuma, T., Hidaka, S., Kurokawa, M., and Sakata, T. (1997). Enhanced expression of uncoupling protein 2 gene in rat white adipose tissue and skeletal muscle following chronic treatment with thyroid hormone. *FEBS Lett.* **418**, 323-326.

Mittleman, R.E., Goldberg, R.B., and Nadji, M. (1984). Severe thyroid atrophy due to prolonged ingestion of thyroid hormone for treatment of obesity. *South. Med. J.* **77**, 268-270.

Nedergaard, J., Golozoubova, V., Matthias, A., Asadi, A., Jacobsson, A., and Cannon, B. (2001). UCP1: the only protein able to mediate adaptive non-shivering thermogenesis and metabolic inefficiency. *Biochim. Biophys. Acta.* **1504**, 82-106.

Nicholls, D.G. and Rial, E. (1999). A history of the first uncoupling protein, UCP1. *J. Bioenerg. Biomembr.* **31**, 399-406.

Parascandola, J. (1974). Dinitrophenol and bioenergetics: a historical perspective. *Mol. Cell. Biochem.* **5**, 69-77.

Pecqueur, C., Alves-Guerra, M.C., Gelly, C., Levi-Meyrueis, C., Couplan, E., Collins, S., Ricquier, D., Bouillaud, F., and Miroux, B. (2001). Uncoupling Protein 2, in vivo distribution, induction upon oxidative stress, and evidence for translational regulation. *J. Biol. Chem.* **276**, 8705-8712.

Poehlman, E.T. (1989). A review: exercise and its influence on resting energy metabolism in man. *Med. Sci. Sports Exerc.* **21**, 515-525.

Porter, R.K., Hulbert, A.J., and Brand, M.D. (1996). Allometry of mitochondrial proton leak: influence of membrane surface area and fatty acid composition. *Am. J. Physiol.* **271**, R1550-R1560.

Ricquier, D. and Bouillaud, F. (2000). The uncoupling protein homologues: UCP1, UCP2, UCP3, StUCP and AtUCP. *Biochem. J.* **345**, 161-179.

Rolfe, D.F.S., and Brand, M.D. (1996). Contribution of mitochondrial proton leak to skeletal muscle respiration and to standard metabolic rate. *Am. J. Physiol.* **271**, C1380-C1389.

Rolfe, D.F.S., Newman, J.M., Buckingham, J.A., Clark, M.G., and Brand, M.D. (1999). Contribution of mitochondrial proton leak to respiration rate in working skeletal muscle and liver and to SMR. *Am. J. Physiol.* **276**, C692-C699.

Sivitz, W.I., Fink, B.D., and Donohoue, P.A. (1999). Fasting and leptin modulate adipose and muscle uncoupling protein: divergent effects between messenger ribonucleic acid and protein expression. *Endocrinology.* **140**, 1511-1519.

Skulachev, V.P. (1998). Uncoupling: new approaches to an old problem of bioenergetics. *Biochim. Biophys. Acta.* **1363**, 100-124.

Soboll, S. (1993). Thyroid hormone action on mitochondrial energy transfer. *Biochim. Biophys. Acta.* **1144**, 1-16.

Terada, H. (1990). Uncouplers of oxidative phosphorylation. *Environ. Health Perspect.* **87**, 213-218

Wadden, T,A. (1993). Treatment of obesity by moderate and severe caloric restriction. Results of clinical research trials. *Ann. Intern. Med.* **119**, 688-693.

Weyer, C., Gautier, J.F., Danforth, E. (1999). Development of β_3-adrenoceptor agonists for the treatment of obesity and diabetes-an update. *Diabetes. Metab.* **25**, 11-21.

CHAPTER 2

EFFECTS OF MINIMALLY TOXIC LEVELS OF CARBONYL CYANIDE
P-(TRIFLUOROMETHOXY) PHENYLHYDRAZONE [FCCP],
ELUCIDATED THROUGH DIFFERENTIAL GENE
EXPRESSION WITH BIOCHEMICAL AND
MORPHOLOGICAL CORRELATIONS.

Sabu Kuruvilla[1,2], Charles W. Qualls Jr.[2], Ronald D. Tyler[2], Sam M. Witherspoon[2], Gina R. Benavides[2], Lawrence W. Yoon[2], Karen Dold[2], Roger H. Brown[2], Subbiah Sangiah[1] and Kevin T. Morgan[2,3]

[1]*Oklahoma State University, Stillwater, OK 74078*
[2]*GlaxoSmithKline Inc.,5 Moore drive, Research Triangle Park, NC 27709*
[3]*Present address: Aventis Pharmaceuticals, Raleigh, NC 27612*

ABSTRACT

Uncouplers of oxidative phosphorylation have relevance to bioenergetics and obesity. The mechanisms of action of chemical uncouplers of oxidative phosphorylation on biological systems were evaluated using differential gene expression. The transcriptional response in human rhabdomyosarcoma cell line, RD, was elucidated following treatment with FCCP, a classical uncoupling agent.

Changes in mitochondrial membrane potential were used as the biological dosimeter. There was an increase in membrane depolarization with increasing concentrations of FCCP. The concentration at 75% uncoupling (20 μM) was chosen to study gene expression changes, using cDNA based large-scale differential gene expression (LSDGE) platforms. At the above concentration, subtle light microscopic and clear gene expression changes were observed at 1, 2 and 10 h. Statistically significant transcriptional changes were largely associated with protein synthesis, cell cycle regulation, cytoskeletal proteins, energy metabolism, apoptosis and inflammatory mediators. Bromodeoxyuridine (BrdU) and Propidium iodide (PI) assays revealed cell cycle arrest to occur in the G_1 and S phases. There was a significant initial decrease in the intracellular ATP concentrations. The following 7 genes were selected as potential molecular markers for chemical uncouplers: seryl-tRNA synthetase (Ser-tRS), glutamine-hydrolyzing asparagine synthetase (Glut-HAS), mitochondrial bifunctional methylenetetrahydrofolate dehydrogenase (Mit BMD), mitochondrial heat shock 10-kDa protein (Mit HSP 10), proliferating cyclic nuclear antigen (PCNA), cytoplasmic beta-actin (Act B) and growth arrest & DNA damage-inducible protein 153 (GADD153). Transcriptional changes of all 7 genes were later confirmed with RT-PCR. These results suggest that gene expression changes may provide a sensitive indicator of uncoupling in response to chemical exposure.

Key words:

FCCP, uncoupling agent, gene expression, molecular marker, cell cycle, protein synthesis.

INTRODUCTION

Oxidative phosphorylation is the process by which most of the energy is produced in an animal cell. In aerobic organisms, all the catabolic pathways involved in energy metabolism converge on oxidative phosphorylation or cellular respiration. Electrons are donated by NADH (reduced nicotinamide adenine dinucleotide) and FADH2, which are produced by oxidation of nutrients including carbohydrate, fat and protein. These electrons flow down a redox gradient along the electron transport chain located in the inner mitochondrial membrane and are ultimately transferred to molecular oxygen, yielding energy for generation of ATP from ADP and inorganic phosphate (Pi). Our current understanding of synthesis of ATP in energy transducing membranes, such as those of mitochondria is based on the chemiosmotic theory, introduced in 1961 by Peter Mitchell in which transmembrane differences of proton concentrations are central to energy transduction. (Lehninger et. al., 1997).

The transfer of electrons along the respiratory chain is accompanied by outward pumping of protons (H^+) across the inner mitochondrial membrane, which results in transmembrane differences in proton concentration (gradient). The proton-motive force is subsequently used to drive the synthesis of ATP, as H^+ flow passively back into the matrix through proton pores formed by ATP synthase, another enzyme complex system in the inner mitochondrial membrane. Thus, ATP is synthesized by coupling two reactions, electron transport and phosphorylation. Endogenous uncouplers, called uncoupling proteins (UCPs), uncouple oxidative phosphorylation by forming channels in the inner mitochondrial membranes, allowing passive movement of H^+ back into mitochondrial matrix, thus disrupting proton-motive force with dissipation of oxidative

energy as heat. The function of biological uncouplers is assumed to be two-fold: (a) thermogenesis, in brown fat of neonates, cold adapted rodents and hibernators; (b) possible protective role in the antioxidant system (Skulachev, 1998).

Certain synthetic compounds classified as uncoupling agents inhibit ATP synthesis by preventing the above coupling reaction by permitting H^+ to bypass ATP synthesis, functionally akin to endogenous uncouplers. In the presence of an uncoupler, respiration proceeds until virtually all of the available oxygen is reduced and rapid oxidation of substrates proceed with little or no phosphorylation of ADP. In other words, these compounds uncouple oxidation from phosphorylation. A large number of uncouplers have been discovered. Predominant classes are either hydrophobic weak acids that act as protonophores (Terada, 1990), or divalent organic cations (Shinohara et al., 1998), capable of transferring H^+ into the matrix space across inner mitochondrial membrane, thereby disrupting the membrane potential.

Although chemical uncouplers have been known from the early 1900's and their potential use in treating clinical obesity has been understood, they have not been successfully developed as therapeutic agents. One of the important reasons is that the full spectrum of their effect on various biochemical circuitry, besides uncoupling, is not well documented. The present study was undertaken to understand the effect of chemical uncoupling on metabolic pathways and to identify potential molecular markers for uncoupling, by analyzing gene expression profiles in the RD cell line using minimally toxic levels of FCCP, a classical weak acid uncoupler (Starkov, 1997).

MATERIALS AND METHODS

Chemicals:

FCCP, a classical uncoupler of oxidative phosphorylation, was selected for these studies because (a) it has been extensively employed to induce uncoupling of mitochondrial oxidative phosphorylation in many cell types, including cardiac myocytes (Hool and Aurthur, 2002), (b) the mode of action of FCCP in the inner mitochondrial membrane is known (Terada, 1990), (c) FCCP has been used as a model compound for the development of high-throughput approaches to the detection of effects on mitochondrial membrane potential in other in vitro systems (Wong and Cortopassi, 2002). FCCP was procured from Sigma Chemical Company (St Louis, MO) and was at least 98% pure by thin layer chromatography. Ten mg of the compound was initially dissolved in 786.8µl of 95% ethyl alcohol, due to its poor solubility in tissue culture media, and subsequent dilutions were made in media. Other chemicals and reagents were obtained from Clontech Laboratories (Palo Alto, CA), Molecular Probes (Eugine, OR), Calbiochem-Novabiochem Corporation (San Diego, CA), Invitrogen Life Technologies (Carlsbad, CA), CN Biosciences (San Diego, CA) and Perkin Elmers Life Sciences (Boston, MA).

Cell culture:

Skeletal muscle represents a particularly attractive target for directed uncoupling due to the large muscle mass, which in humans, account for approximately 15 - 20% of standard metabolic rate (Rolfe et al., 1999). The maximal aerobic capacity of a human is

generally estimated to be up to 12 times SMR. Most of this increase can be directly attributed to skeletal muscle respiratory activity and it is clear that muscle can greatly increase its metabolic activity. Doubling metabolic rate by modestly uncoupling skeletal muscle should produce few adverse side effects as this increase would only be comparable to mild exercise (Blaxter, 1989). Indeed, support for this view has been obtained using proteins (uncoupling proteins 1 and 3) that may naturally uncouple mitochondria. High expression of human UCP3 in transgenic mouse skeletal muscle led to decreased weight gain despite increased food intake (Clapham et al., 2000). Thus, skeletal muscle being the potential target tissue for anti-obesity drug development, based on availability at the time, the rhabdomyosarcoma cell line was chosen for this study. RD cells (ATCC, CCL-136), obtained from American Type Culture Collection (ATCC), Rockville, MD were grown in Dulbeco's Modified Eagles Medium (DMEM) with Glutamax and 10% fetal bovine serum (FBS), without antibiotics and incubated at 37°C with 5% CO_2. They were cultured in collagen coated 'T175 Biocoat vented flasks' (Collagen I Cellware, Becton Dickinson Labware) and fed every 2 days, for subculture and stock expansion. For RNA preparations the cells were grown in Biocoat 150 mm diameter petri dishes (Collagen I cellware, Becton Dickinson Labware) with 25 ml medium, and containing a numbered collagen coated glass microscope coverslip for light microscopic evaluation of cell morphology. For RNA extraction, cells were seeded at a density of 1x 10^7 in 3 control and 3 treated dishes. They were fed at 24 and 38 h, and were dosed at 48 h after seeding. For RNA extraction, cells were harvested at multiple time points, from 0 to 24 h post-treatment.

Mitochondrial membrane potential assay:

Changes in mitochondrial membrane potential ($\Delta\Psi$m) of intact cells were measured with a J-aggregate-forming lipophilic, cationic probe, 5,5', 6,6'-tetrachloro-1, 1', 3,3'-tetraethylbenzimidazolylcarbocyanine iodide (JC-1), procured from Molecular Probes, using a FACScan flow cytometer (Becton-Dickinson, San Jose, CA), as per the method described by Cossarizza et al. (1993). JC-1 is a carbocyanine with a delocalized positive charge and is capable of selectively entering mitochondria. It exists as a green-fluorescent monomer at lower concentrations (lower membrane potential), emitting at 530 nm upon exciting at 490 nm; and as red-fluorescent "J-aggregates" emitting at 590 nm at higher (above 0.1 μM) concentration (higher membrane potential) [Smiley et. al., 1991; Salvioli et al., 1997]. The cells were adjusted to 1×10^6 cells/ ml and suspended in DMEM. They were then dosed with 100 nM to 64 μM FCCP and incubated at 37^0C for 1 h. JC-1 was then added at 10 μg/ ml to the cell suspension and incubated in the dark for 20 min. At the end of 20 min, they were put on ice to cool for 15 min and then washed twice and resuspended in PBS containing appropriate concentrations of FCCP. JC-1 fluorescence emission data was acquired from the flow cytometer. Differences between control and treated groups for each time point were expressed as mean ($\pm$ SD) and significance was assessed using a 2 tailed t-test at $p < 0.05$ or $p < 0.01$.

Experimental design:

For gene expression studies, 57 tissue culture dishes, with one coverslip each, were seeded with 1×10^7 cells. There were 10 time points, with 3 control and 3 treated dishes

per time point, except 0 h that had only control dishes. A second set of 30 dishes, 3 per time point, was used as controls for compound concentration assay. A third set of 54 dishes, 6 (3 control and 3 treated) per time point, was used for the ATP assay. The media was changed at 24 h post seeding and then again 10 h prior to dosing. The treatment group was dosed with the compound at 48 h after seeding. The cultures were incubated under standard conditions and cells harvested at the following time points for gene expression analysis: 0, 0.5, 1, 2, 4, 6, 8, 10, 12 and 24 h after dosing. For each of the applicable time points, samples were also collected for media chemistry, compound concentration and ATP analysis.

Compound concentration assay:

Aliquots of the media were collected at the various time points from both treated dishes and a set of control dishes that contained only media with FCCP and no cells. The samples were immediately frozen and subsequently analyzed using HPLC to evaluate compound degradation over time. Differences between control and treated groups for each time point were expressed as mean ($\pm$ SD) and significance was assessed using a 2 tailed t-test at $p < 0.05$ or $p < 0.01$.

Media chemistry:

Media samples at each time point, for both control and treated, were centrifuged at 3200xg for 15 min at 4°C to remove floating cells and the supernatant stored at -20°C prior to analysis for glucose, lactate and lactate dehydrogenase (LD) using a Hitachi 911 analyzer (Roche Diagnostics). Glucose was assayed by a hexokinase method, LD assayed

at 37°C by a modified kinetic procedure, lactate assayed at 37°C by a UV method catalyzed by lactate oxidase and peroxidase. Differences between control and treated group for each time point were expressed as mean (± SD) and significance was assessed using a 2 tailed t-test at $p < 0.01$ or $p < 0.05$.

Morphology:

Coverslips were removed from the dishes at each time points and fixed in 95% ethanol. They were then stained with hematoxylin and eosin (H&E) and evaluated by light microscopy. Five representative 20x fields from each of the 3 controls and 3 treated coverslips were captured with a digital camera mounted on a microscope and imported into Imagepro plus™ software. The images were then enlarged as necessary and the cells from each 20x field were counted to obtain separate values for cell counts and mitotic figures.

ATP assay:

Changes in intracellular ATP concentrations were measured for both control and treated cells at each time point, using Luciferin-Luciferase as per Karamohamed et al. (1999) and Ford et al. (1996). Bioluminescent somatic cell assay kits were purchased from Sigma Chemical Company. The cells were suspended in their original media and adjusted to 5×10^5 cells/ ml. The cells were treated with ATP releasing agent, which allowed rapid release of small molecules such as ATP, while larger molecules remained trapped inside the cells, affording protection from the ATPases. The free ATP was allowed to react with Luciferin-Luciferase and the light released was measured using a

Turner Designs 20/20 luminometer. The luminescences associated with serial dilutions of known ATP standards were separately measured to generate a standard curve. A regression line fitted to the standard curve was used to derive the ATP concentrations. Differences between control and treated groups for each time point were expressed as mean ($\pm$ SD) and statistical significance was assessed using a 2 tailed t-test at $p < 0.01$ or $p < 0.05$.

Gene expression assays:

CCL-136 tissue culture cells, after removal of media, were lysed in situ, with Trizol Reagent™ (Gibco BRL, MD) and the lysate was stored at -80°C until use. Total RNA was isolated by chloroform/ isopropanol/ ethanol extraction and RNA quality and quantity were assessed using agarose gel electrophoresis and spectrophotometric 260/ 280 nm absorbency. For the initial exposure-time Vs. gene expression analysis, ^{33}P-labelled cDNA probes were prepared with one pooled RNA sample each, from 3 controls and 3 treated dishes and hybridized to Clontech Atlas™ human 1.2-1 cDNA microarray. From the array comparison report generated, $\log_2$ ratios of adjusted intensity were created and 165 genes relating to energy metabolism were graphed for all the time points using Microsoft Excel™ to identify time points with the most transcriptional changes. Accordingly 1, 2 and 10 h time points were selected for further investigation.

For the detailed investigation, ^{33}P-labelled cDNA probes were prepared with total RNA from each of the triplicate samples of both control and treated groups for the three time points selected, using a modified Clontech protocol, and hybridized to Clontech Atlas™ human 1.2-1, 1.2-3 and 1.2-toxicology microarrays with 1176 genes per array,

30

with an estimated 5 - 10% overlap of genes among various arrays. Clontech Atlas™ arrays are nylon-membrane based cDNA arrays used for broad-scale differential gene expression profiling. The broad-coverge arrays profile many crucial cellular pathways and functions in a specific species. The human 1.2-1 array contains genes associated largely with cell cycle, oncogenes, ion channels, growth factors, signal transduction, DNA metabolism, cell to cell adhesion, cytokines, stress signals and apoptosis. The 1.2-3 array contains genes associated with RNA metabolism, protein metabolism, carbohydrate metabolism, lipid metabolism, energy metabolism, cell surface antigens, transcriptional activation, cytokines, oncogenes, extracellular matrix, membrane channels and signal transduction. The 1.2-toxicology array contains genes associated with xenobiotic metabolism, drug resistance, stress response, apoptosis, cell cycle, cell surface antigens, transcriptional activation, oncogenes, cytokines, signal transduction, cytoskeleton, energy metabolism and DNA metabolism.

Denaturation and annealing (4µl) was carried out at 94^0C for 10 sec and 70°C for 10 min using 6 µg total RNA and 1 µl CDS Atlas specific primers (0.2 µM each). The extension reaction (22 µl, 35 min at 49°C) contained 0.5 mM each dATP, dGTP, dTTP; 50 mM Tris-HCl pH 8.3; 75 mM KCl; 3 mM $MgCl_2$; 4.5 mM DTT; 100 µCi ^{33}P-α-dCTP (3000 Ci/ mmol, 10 µCi/ µl, NEN) and 200 units Super Script II™ reverse transcriptase (Gibco-BRL, MD). Extension was terminated by heating to 94°C for 5 min. Unincorporated ^{33}P-α-dCTP was removed using G_{50} Microspin columns (Amersham Biosciences, Inc., Piscataway, NJ). Pre-hybridization was carried out at 64°C for 1 h, in 6.5 ml MicroHybe™, 3.25 µl poly-dA (1µg/ µl, ResGen) and 6.5 µl Human Cot 1 DNA (1 µg/ µl, Clontech). Heat denatured ^{33}P-cDNA weas added and hybridization carried out

for 16 h. Arrays were washed at 64° following manufacturer's instructions. The membranes were exposed to a phosphor imager screen for 60 h and optical density was acquired using Optiquant™ and a Cyclone scanner (Packard Biosciences Co., Meridian, CT). Image files generated from phosphor imager scans were analyzed using Clontech Atlas Software™. After background subtraction, data were normalized and statistically analyzed using Normalization and Local Regression (NLR) software. NLR processed text files were used to compare control with treated groups, generate p-values, mean log intensity (MLI), and ratio of differences between groups. The NLR output files were again subjected to data manipulation with Microsoft Excel™ to find changes through ranking by ratios, p-values or MLI. The NLR software uses local regression analysis to estimate the normalized expression differences between two groups of arrays, such as control versus treated. The underlying mathematics of NLR, which is described in detail by Kepler et al. (2002), is based upon the assumption that the 'large majority' of gene expression levels do not change in response to treatment. This program takes text files of transcript signal intensity data, generated in this study by the Clontech AtlasImage software, and outputs an intergroup fold change for each transcript, a p-value for this change, and the 'mean log intensity' (MLI) for each transcript. The MLI provides an indication of mean signal intensity for the gene of interest compared to the average signal of all genes in the data set in the form of the log of the ratio of the mean intensity for the gene of interest to the mean of the intensity of the entire data set. Thus an MLI of '0' represents a ratio of '1' with the gene of interest expressed at the average level of the entire gene list examined. The MLI of more or less highly expressed transcripts will lie to the right or left of zero for the sample set, respectively. The MLI calculation is applied to

all samples, including controls and treated, and thus it only provides a crude indication of expression level for each set of genes. It is strongly recommended during more detailed analyis that one plot the normalized signal intensity for individual genes of interest, or use the group-by-group variance tables, which are also output by NLR. We routinely use Microsoft Excel spreadsheets for the examination of individual sample data as an adjunct to interpretation of statistical outputs. It is strongly recommended that the implicit assumptions and other characteristics of NLR be understood when applying this method.

<u>Real Time Quantitative RT-PCR (TaqMan™):</u>

Seven genes were selected from the 10 h array data to serve as molecular markers for 80% chemical uncoupling and were analyzed by real time quantitative RT-PCR (TaqMan™) for confirmation. Total RNA was DNAase treated (Ambion DNAase I) according to the manufacturer's protocol. RNA was quantified using Molecular Probes Ribogreen™ assay with a Cytofluor 2350 fluorometer. Samples were diluted to 10 ng/ μl prior to TaqMan™ (Perkin Elmer ABI Prism 7700 Sequence Detection system) analysis. Primers were designed with the use of Perkin Elmer Primer Express™ software. A 96-well assay was arranged to detect mRNA expression of 7 genes in 3 control and 3 treated RNA samples, using probes and primers from Keystone Biosource. The arrangement of the plate included one row for each gene and one row for 18S ribosomal RNA (rRNA) internal control. RNA samples were then arranged column-wise, with 3 pairs of control and 3 pairs of treated samples, in duplicate to fill the 12 columns of the plate. Forward and reverse primers were diluted to 9 μM and probe to 2 μM, and 20 μl of each was aliquoted to make the probe/ primer master mix. The master mix for the remaining

components were prepared according to the manufacturer's protocol (without probes and primers) and 35 μl was aliquoted per well. Fifteen μl of probe/ primer mix was then added using a multichannel pipette, the plate was sealed with optical grade caps, and the reaction was carried out as follows: 48°C for 30 min (reverse transcriptase or RT step), 95°C for 10 min (Amplitaq activation and RT denaturation), 40 cycles of 94°C for 15 sec and 60°C for 1 min. Values of fold change in expression were graphed for comparison purpose. Statistical significance was determined for control vs. treated groups using a 2 tailed t-test at $p < 0.05$ or $p < 0.01$.

Cell cycle assay:

The stages of cell cycle arrest and the proportion of dead cells at 2, 10, 24, 36 and 48 h post treatment with 20 μM FCCP were determined by flow cytometric assay with BrdU and PI. BrdU cell proliferation assay kit was purchased from CN Biosciences and PI was obtained from Calbiochem-Novabiochem Corporation. Thirty minutes prior to each of the above time points, cells were treated with BrdU at a ratio of 1 BrdU: 100 media (to obtain a final concentration of 10 μM), incubated for 30 minutes, then trypsinized and resuspended in PBS, and fixed in 47% methyl alcohol (1 ml cell suspension in PBS + 2 ml 70% methyl alcohol). Following storage at -20°C, the cells were prepared for flow cytometric analysis. The cellular DNA was partially unwound by incubating cells in 2 N hydrochloric acid / 0.05% Triton ZX-100 for 30 min at room temperature. The acid was neutralized by washing the cells with 0.1 M sodium borate. The cells were then incubated with 100 μl anti-BrdU-FITC (diluted at 1: 5 in 0.5% Tween20, 1% BSA in PBS) per sample. PI, a fluorescent dye that intercalates into DNA, was used to measure total

cellular DNA. The samples were incubated in PI at 5 μg/ ml in PBS. They were then analyzed on a Becton Dickinson's FACS flow cytometer, with laser excitation at 488 nm, as per Dolbeare et al. (1983). Simultaneous measurement of the amount of BrdU incorporated into DNA and cellular DNA content were taken at various time points, up to 48 h. Cells with DNA content of 2N were considered to be in G_1/G_0 phase, 4N in G_2/M phase, 2 to 4N in S phase and < 2N was considered to be dead cells. For a review of the terminology and mechanism associated with cell death, the suggested reading is Trump et al. (1997). Statistical significance of the difference between control and treated groups were assessed using a 2 tailed t-test at $p < 0.05$ or $p < 0.01$.

RESULTS (Data are presented in appendices IA and IB)

Characterization of RD cells:

This human embryonal rhabdomyosarcoma cell line was established in 1968 from a malignant embryonal rhabdomyosarcoma of the pelvis of a seven-year old girl (McAllister et al., 1969). The line consists of cells of two cytological features - poorly differentiated spindle cells and larger multinucleated cells. No contractile myofilaments could be demonstrated by light or electron microscopy and immunohistochemical staining failed to reveal the presence of significant amounts of either myosin or myoglobin (data not shown). The cells grew as a monolayer and showed occasional 'whorling' patterns when grown on collagen coated plastic tissue culture dishes.

Mitochondrial membrane potential:

There was an increase in the depolarized cell population with increasing concentrations of FCCP. Approximately 11% of cells were normally depolarized. The response to treatment was linear up to 2 μM and plateaued at around 32 μM. At 20 μM FCCP, there was approximately 75% depolarization (fig. 1.1).

Cell morphology:

On light microscopic examination of the H&E stained coverslips, the treated cells at 10 and 24 h were elongated rather than polyhedral and were generally smaller (attenuated) (fig. 1.2). There was a 100% and 55 % decrease in mitotic figures and cell counts, respectively, in the treated group at 24 h relative to time matched controls (data not shown).

Compound concentration assay:

FCCP, at 20 μM, was very stable in solution with no appreciable degradation for up to 12 hours in media, and when exposed to cells, approximately 50% and 75% of the compound was taken up / metabolized by the cells in 2 and 5 hours, respectively (fig. 1.3).

Gene expression arrays:

Fig. 1.4 shows the $\log_2$ ratios of adjusted intensity between pooled control and treated groups for 9 time points involving 165 genes. The genes are associated with energy metabolism and were selected from the Clontech 1.2-3 microarray. Based on the

log$_2$ ratios, 1, 2 and 10 h time points were found to exhibit the greatest degree of transcriptional dysregulation and hence the above time points were chosen for detailed investigations. The data in fig. 1.4 was only used as a guideline to help narrow down the time points to be studied and was not included in any further analysis. All the analyses hence forth were based on 3 controls and 3 treated at each time point, using appropriate statistical methods. Table 1.1 contains data pertaining to detailed analyses of Clontech human 1.2-1, 1.2-3 and 1.2-toxicology arrays for 1, 2 and 10 h, as NLR output files. The genes that changed in a significant manner (p < 0.05) are listed along with the ratios of normalized treated and control intensities of the transcripts (fold changes) and MLI. Statistically significant transcriptional changes were largely associated with protein synthesis, cell cycle regulation, cytoskeletal proteins, energy metabolism, apoptosis, muscle specific proteins and inflammatory mediators

At 1 h, the transcriptional response indicated a down-regulation of anabolic pathways, evidenced by the pronounced down-regulation of amino acid synthesis genes (glutaminyl-tRNA synthetase, methyonyl-tRNA synthetase), and early sign of cell cycle arrest, suggested by the down-regulation of cullin homolog 1 (CUL-1). At 2 h, the transcriptional profile showed continued slow-down of anabolic processes like protein synthesis, with down regulation of glutaminyl-tRNA synthetase and ribosomal proteins. Several electron transport chain genes including cytochrome c oxidase polypeptides and electron transfer flavoprotein beta-subunit were down regulated. Disassembly of cytoskeletal proteins (tubulin beta-2 chain, beta tubulin) was observed with down-regulation of extracellular and matrix protein genes (Collagen VII alpha 1 subunit, matrix metalloproteinase 9). DNA damage was suggested by up-regulation of DNA damage

37

genes and DNA ligase. By 10 h, there were two distinct sets of transcriptional response, one set of genes showed recovery of metabolic processes, evidenced by marked up-regulation of protein synthesis transcripts (asparagine synthetase, seryl-tRNA synthetase). There is also up-regulation of glycolysis (pyruvate kinase) with simultaneous down-regulation of pyruvate dehydrogenase. More genes of toxicological importance (Glutathione S-transferases, cytochrome P450 4A11, cytosolic superoxide dismutase 1) and stress proteins (heat shock proteins) showed down-regulation. There is up-regulation of cell to cell adhesion and extracellular proteins. Electron transport chain genes also show a partial recovery, as fewer genes are down-regulated compared to 2 h. The second set of genes showed marked cell cycle arrest and apoptotic activity. Among the down-regulated genes were PCNA, G1/S specific cyclin E, G1/S specific cyclin D3, DNA primase large subunit, DNA polymerase epsilon subunit B, The up-regulated genes included caspases 3 and 4. Uncoupling protein 2 was down regulated at this point.

Markers for FCCP uncoupling [Quantitative RT-PCR (TaqMan™)]:

Seven genes were selected from the 10 h array data to serve as molecular markers for uncoupling with FCCP. These genes were chosen to represent pathways that were transcriptionally most active and showing high levels of statistical significance. The selected genes were Ser-tRS, Glut-HAS, Mit-BMD, Mit-HSP10, PCNA, Act B and GADD153. The fold expression all 7 genes were statistically significant ($p < 0.01$; $p < 0.05$) and the changes in directions and magnitudes were in good agreement with the microarrays results (fig. 1.5).

<u>Cell cycle assay:</u>

The results of BrdU and PI time course assay from 2 to 48 h, for 20 μM FCCP is presented in fig. 1.6. The response of the cell cycle machinery to treatment is time dependent. There was a change in the rate of BrdU incorporation as early as 2 h in response to the treatment. The S phase change occurred in two dimensions. The percentage of cells that incorporated BrdU (BrdU+S) significantly decreased with time. In addition, the amount of BrdU incorporated into each cell per 30 min pulse also decreased in a time dependant manner. The BrdU-S cells were BrdU negative cells that were in S phase with respect to DNA content (they fill the space between the G_1 and the G_2 populations). By 24 - 48 h, there were very few cells incorporating BrdU, while 10-15% of the cells were in BrdU-S phase. These cells were arrested in S phase. There was a concomitant increase in the percentage of cells in G_1/G_0 and G_2/M phases as the percentage of cells in S phase decreased. The G_2/M compartment of the treated cells increased with time to 24 h and then began to decrease at the 36 - 48 h time points, meaning that the cells were not arrested in G2/M, but were passing through G_2/M to G_1/G_0. In the treated group, cells in G_1/G_0 continued to increase throughout the time course while no cells were in S phase, indicating a G_1 arrest. Cell death was not evident until 24 h, when a very small (1.3% over the controls), but statistically significant ($p < 0.01$) population of cells underwent death. The dead cells gradually increased to 2.4% ($p < 0.01$) at 48 h.

Media chemistry:

Results of media glucose and lactate time course assays are presented in fig.1.7. There was a time dependant decrease in media glucose and increase in media lactate in both control and treated groups. However, the changes in the treated groups were more marked and statistically significant ($p < 0.01$) across most time points, and the pattern was evident as early as 2 h.

ATP assay:

Results of the time course ATP assay are presented in fig. 1.8. There was a downward trend in the intracellular ATP concentrations of the control group from 0 to 24 h. The treated group presented a different picture. There was a 19 and 40% decrease in ATP at 15 min and 30 min, respectively. However, starting at 1 h, there was an upward trend and at 4 h, the treated group was at the same level as the controls. At 6 h, they were above the controls and stayed at a higher level until the end of the experiment.

Mechanistically important genes [Quantitative RT-PCR (TaqMan™)]:

A separate set of 11 genes were chosen from the 10 h array data for RT-PCR quantitation (fig. 1.9). These genes were chosen to represent pathways that were important in the proposed mechanism of action of FCCP, as outlined in fig. 1.10. The selected genes were: Beta 1 catenin (β catenin), PRB-binding protein E2F1 (E2F1), fas antigen ligand (FasL), growth arrest and DNA damge-inducible protein 45 (GADD 45), cyclin dependant kinase inhibitor 1A (CDKI 1A/ p21), cyclin dependant kinase 4 inhibitor 2 (p16), replication protein A 14 kDa (RP-A), caspase 3 (casp3), growth arrest

and DNA damage-inducible protein 45 gamma (Gadd45g) mitogen activated protein kinase 8 (MAPK8) and N-myc proto-oncogene (N-myc). RT-PCR was performed with triplicate samples and the statistical significance of the fold changes were determined. In general, there was good agreement in both direction and magnitude between the array result and RT-PCR.

DISCUSSION

The use of microarrays for comprehensively evaluating changes in RNA expression is a promising new methodology. Technical developments that offer increased sensitivity, the prospect that large numbers of genes for a given organism could be scrutinized in this way, and a general appreciation of the need to integrate information obtained from more traditional and reductionist approaches to biology make microarray-based expression analysis a powerful tool (Bowtell, 1999).

The overall sequence of molecular events observed in this study were reminiscent of ischemic (hypoxic) cell injury and are consistent with the expected effect of chemical uncouplers on cell systems, as uncouplers essentially reverse the physiological role of oxygen, creating a 'hypoxic' environment.

In living organisms, the first point of hypoxia is the cell's aerobic respiration, that is, mitochondrial oxidative phosphorylation. As the oxygen tension decreases there is loss of oxidative phosphorylation and decreased generation of ATP, resulting in widespread effects on many systems, including decreased activity of plasma membrane sodium pump, alteration of energy metabolism by switching from oxidative phosphorylation to

glycolysis with increased lactic acid production, disassociation of ribosomes from rough

endoplasmic reticulum leading to structural disruption of protein synthesis apparatus

resulting in reduced protein synthesis and morphological deterioration causing

cytoskeletal disruption. If hypoxia continues, there is further deterioration and the

cytoskeleton disperses, resulting in the loss of ultrastructural features like microvilli and

formation of 'blebs' at the cell surface. Myelin figures derived from plasma as well as

organellar membranes, may be seen within the cytoplasm (Cotran et al. 1999).

It is appreciated that the current study was with cells in culture and not the whole

animal. Nevertheless, important changes in patterns of gene expression were evident.

Dose response relationships and time courses are important parameters that must be

considered in these complex analyses. The proposed sequence of the molecular events

following FCCP treatment are diagramatically represented in fig. 1.10. The central event

in this study is the sharp decrease in ATP, which presumably led to DNA damage.

Collapse of mitochondrial membrane potential is known to occur rapidly upon exposure

to FCCP (Sagi-Eisenberg et al. 1983). In the present study, membrane depolarization was

followed by drop in ATP as early as 15 min post treatment.

One of the early events that followed drop in ATP was down-regulation of protein

synthesis, which is consistent with the effect of hypoxia (Cotran, 1999). However,

whether this effect on protein synthesis is a direct result of hypoxia-mediated

disassociation of ribosomes, negative feed back from cell cycle arrest or as a result of

metabolic shut down of energy metabolism, is not clear. The up-regulation of GADD153

at 2 h, as per both microarray and RT-PCR are suggestive of DNA damage during the

early part of the time course. GADD153 is a negative regulator of the transcription factor

C/EBP, which causes a G_1 and S phase cell cycle arrest through binding with CDK2/4–Cyclin D2/3 complex. (Ron et al., 1992; Wang et al., 2001). S phase arrest has been biochemically confirmed (fig. 1.6). Examination of gene expression profile for the same period reveals that genes associated with cell proliferation show both up and down regulation. It is easy to see that cell cycle arrest and cell proliferation activities do concurrently occur in the same population of cells illustrating the often difficult nature of interpreting gene array data sets. This also attests to the fact that transcriptional response is never clear–cut and such studies need to be supplemented with biochemical and / or morphologic assays to be able to draw meaningful conclusions.

Eventually, DNA damage is presumed to have led to regulatory modification of several pathways important in cell cycle regulation, as suggested by morphological evaluations (figs. 1.2) and the transcriptional response of genes in the following discussion. GADD45 is a DNA damage inducible gene that binds to PCNA and cyclin dependant kinases (CDKs) leading to S phase cell cycle arrest and stimulation of DNA excision repair (Smith et al., 1994). GADD 45 may also directly interacts with p21, a cell cycle inhibitor (Kearsey et al., 1995). Up-regulation of GADD45 was supported by RT-PCR (fig. 1.9) and S phase arrest was demonstrated by the cell cycle assay (fig. 1.6). Increased activity of DNA excision repair was evident from the transcriptome. GADD 45g (supported by RT-PCR in direction) and GADD45 are inducible by both cytokines and DNA damage, and is important initiator of the SPAK/JNK and p38 pathway, mediated through MAPK8 (supported by RT-PCR in direction) [Takekawa et al., 1998]. Upregulation of P21/ Waf1 (supported by RT-PCR) is mediated through p53, consequent to DNA damage (El-Deiry et al., 1993), and p21 binds with CDK 4/6 (Ahmad et al.,

2001) and PCNA (Chen et al., 1996) to effect G_1 phase cell cycle arrest. In the event the cell is unable to repair the DNA damage in spite of the p53 mediated G_1 arrest, it turns on the p53 mediated apoptotic pathway. Here, this pathway is presumed to be mediated though Fas (supported by RT-PCR in direction) signaling and caspase 3 (supported by RT-PCR in direction). Fas mediated apoptosis upon FCPP treatment has been reported by earlier workers (Linsinger et al. 1999). p16 (supported by RT-PCR in direction) is known to specifically bind CDKs 4 and 6 to mediate G_1 phase arrest (Stott et al., 1998). Replication protein A (supported by RT-PCR) is a DNA damage responsive protein and its down-regulation causes S phase arrest through down-regulation of DNA polymerase (Lohrer, 1996). PCNA (supported by RT-PCR) is involved in DNA synthesis, DNA repair, as a cofactor for DNA polymerase δ (Bravo, 1986), and its down-regulation is responsible for S phase arrest and altered DNA repair. Down-regulation of the transcription factor E2F1 (supported by RT-PCR) through undetermined pathways is presumed to have contributed to S phase arrest via DNA polymerase α (Dynlacht et al., 1994). Down-regulation of β-catenin and N-myc (both supported by RT-PCR), also through undetermined pathways, may have contributed to G_1 phase arrest through interaction with cyclins D, E and F. The transcriptional changes found in this study are in agreement with reports in literature suggesting that the postulated DNA damage is mediated via P21, P16, PCNA and replication protein A (Lohrer, 1996).

A comprehensive gene expression study with FCCP, such as this, has not been attempted before and hence extensive gene expression data is not available in literature. It is of interest to note that rotentone, which blocks electron flow through mitochondrial complex I has been found to induce dose-dependant cell cycle arrest at G_2/M phase and

apoptosis (Armstrong et al., 2001). Disassembly of cytoskeletal proteins subsequent to FCCP treatment, a notable event in this study, has been observed previously by other workers (Bergstorm-Porter et al., 1979; Maro et al., 1982).

An interesting observation is the diversion from oxidative to glycolytic metabolism as oxidative phosphorylation becomes less efficient due to the effect of uncoupling. This trend is transcriptionally evident by the up-regulation of glycolysis with simultaneous down-regulation of pyruvate dehydrogenase, channeling pyruvate into anaerobic metabolism at 10 h. This is supported by clinical chemistry results showing increasing concentrations of media lactate in treated group, with each time point (fig. 1.7). The ATP assay result (fig. 1.8) in this study was particularly unexpected. By 6 h post- treatment, ATP levels in the treated cells increased to a higher level than the control. This suggests that, after the initial decline in ATP consequent to treatment, the cells responded by up-regulating ATP synthetic pathways and at the same time, down-regulating pathways that expend energy. It may also be recalled that at least 60% of the compound was taken up (and presumably metabolized) in the first 4 hours and hence the reduced availability of the compound in the later time-points could have potentially allowed the recovery of the cells. Also, with a population of cells that were undergoing cell cycle arrest and limited cell death, there was further reduction in utilization of ATP, contributing to an overall excess. Creatine phosphate is a major energy reserve in muscle cells and provides readily available high-energy phosphate, which can be used to generate ATP from ADP, the reaction being catalyzed by creatine kinase (Murray et al., 1996). Creatine phosphate may also have contributed to the increase in ATP levels.

All 7 genes proposed as biological markers for FCCP mediated uncoupling of oxidative phosphorylation gave good Taqman™ confirmation, both in direction and fold changes (fig. 1.5), and it was concluded that gene expression changes may be used as a sensitive indicator of uncoupling due to chemical exposure. Since DGE technology is still in the early stages and not yet a widely used technology, every effort has been made in this study to interpret cautiously after rigorous statistical analyses. Further, biochemical assays, quantitative RT-PCR and morphological evaluations were performed to confirm transcriptional data and to test biological end-points.

ACKNOWLEDGEMENTS

REFERENCES

Ahmad, N., Adhami, V.M., Afaq, F., Feyes, D.K., and Mukhtar, H. (2001). Resveratrol causes WAF-1/p21-mediated G(1)-phase arrest of cell cycle and induction of apoptosis in human epidermoid carcinoma A431 cells. *Clin. Cancer Res.* **7**, 1466-1473.

Armstrong, J.S., Hornung, B., Lecane, P. jones, D.P., and Knox, S.J. (2001). Rotenone-induced G2/M cell cycle arrest and apoptosis in a human B lymphoma cell line PW. *Biochem. Biophys. Res. Commun.* **289** (5), 973-978.

Beisker, W., Dolbeare, F., and Gray, J.W. (1987). An improved immunocytochemical procedure for high sensitivity detection of incorporated bromodeoxyuridine. *Cytometry* **8,** 235-239.

Bergstrom-Porter, B., and Shelton, E. (1979). Effect of uncouplers of oxidative phosphorylation on microtuble location and surface structure in murine mast cells. *Anat. Rec.* **195,** 375-386.

Blaxter, K. (1989). Energy Metabolism in Animals and Man. Cambridge University Press, Cambridge, UK..

Bowtell, D.D.L. (1999). Options available-from start to finish-for obtaining expression data by microarray. *Nat. Genet. supplement.* **21,** 25-32.

Bravo, R. (1986). Synthesis of nuclear protein cyclin (PCNA) and its relationship with DNA replication. *Exp. Cell Res.* **163,** 287-293.

Campo, M.L., Tedeschi, H., Muro, C., and Kinnally, K.W. (1997). Effects of carbonyl cyanide phenylhydrazones on two motochondrial ion channels activities. *J. Bioenerg. Biomembr.* **29,** 223-231.

Chen, J., Peters, R., Saha, P., Lee, P., Theodoras, A., Pagano, M., Wagner, G., and Duta, A. (1996). A 39amino acid fragment of the cell cycle regulator p21 is sufficient to bind PCNA and partially inhibit DNA replication in vivo. Nucleic Acids Res. **24,** 1727-1733.

Clapham, J.C., Arch, J.R., Chapman, H., Haynes, A., Lister, C., Moore, G.B., Piercy, V., Carter, S.A., Lehner, I., Smith, S.A., Beeley, L.J., Godden, R.J., Herrity,.N., Skehel,M., Changani, K.K., Hockings, P.D., Reid, D.G., Squires, S.M., Hatcher, J., Trail, B., Latcham, J., Rastan, S., Harper, A.J., Cadenas, S., Buckingham, J.A., Brand, M.D., and Abuin, A. (2000). Mice overexpressing human uncoupling protein-3 in skeletal muscle are hyperphagic and lean. Nature. 406, 415-418.

Cossarizza, A., Baccarani-Contri, M., Kalashnikova, G. and Franceschi, C. (1993). A new method for the cytofluorimetric analysis of mitochondrial membrane potential using the J-aggregate forming lipophilic cation 5,5',6,6'-tetrachloro-1,1',3,3'-tetraethylbenzimidazolcarbocyanine iodine (JC-1). *Biochem. Biophys. Res. Commun.* **197,** 40-45.

Cotran, R.S., Kumar, V., and Collins, T. (1999). *Robbins Pathologic Basis of Disease.* W.B. Saunders Co., Philadelphia, PA..

Dolbeare, F., Gratzner, H.G., Pallavicini, MG, and Gray, J.W. (1983). Flow cytometic measurement of total DNA content and incorporated bromodeoxyuridine. *Proc. Natl. Acad. Sci. USA.* **80**, 5573-5578.

Dolbeare, F., Pallavicini, M. G., Vanderlaan, M., and Gray, J.W. (1985). Cytochemistry for bromodeoxyuridine/DNA analysis: stoichiometry and sensitivity. *Cytometry.* **6**, 521-530.

Dynlacht, B.D., Brook, A., Dembski, M., Yensh, L. and Dyson, N. (1994). DNA binding and transactivation properties of Drosophila E2F and DP proteins. *Proc. Natl. Acad. Sci. U S A.* **91**, 6359-63.

El-Deiry, W.S., Tokino, T., velculescu, V.E., Levy, D.B., Parsons,R., Trent, J.M., Lin, D., Mercer, E., Kinzler, K.W., and Vogelstein, B. (1993). Waf 1, a potential mediator of p53 tumor suppression. *Cell.* **75**, 817-825.

Ford, S.R., Chenault, K.H., Bunton, L.S., Ginger, H.J., McCarty, J., Hall, M.S., Pangburn, S.J., Buck, L.M. and Leach, F.R. (1996). Use of firefly luciferase for ATP measurement for ATP measurement: other nucleotides enhance turnover. *J. Biolumin. Chemilumin.* **11**, 149-167.

Harper, J.A., Dickinson, K., and Brand, M.D. (2001). Mitochondrial uncoupling as a target for drug development for the treatment of obesity. *Obes. Rev.* **2**, 255-265.

Hool , L.C., Arthur, P.G. (2002). Decreasing cellular hydrogen peroxide with catalase mimics the effects of hypoxia on the sensitivity of the L-type Ca2++ channel to beta-adrenergic receptor stimulation in cardiac myocytes. *Circ. Res.* **91**, 601-609.

Karamohamed, S., Nordstrom, T. and Nyren, P., (1999). Real-time bioluminometric method for detection of nucleoside diphosphate kinase activity. *Biotechniques.* **26**, 728-734.

Kearsey, J.M., Coates, P.J., Prescott, A.R., Warbrick, E., and Hall, P.A. (1995). *Oncogene.* **11**, 1675-1683.

Kepler, T.B., Crossby, L., and Morgan, K.T. (2002). Normalization and analysis of DNA microarray data by self-consistency and local regression. *Genome biology.* **3**, 1-12.

Lehninger, A.L., Nelson, D.L., and Cox, M.M. (1997). *Principles of biochemistry.* Worth publishers, NY.

Li, C.X., and Poznansky, M.J. (1990). Effect of FCCP on tight junction permeability and cellular distribution of ZO-1 protein in epithelial (MDCK) cells. *Biochim. Biophys. Acta.* **1030**, 297-300.

Linsinger, G., Wilhelm, S., Wagner, H. and Hacker, G. (1999). Uncouplers of oxidative phosphorylation can enhance a Fas death signal. *Mol. Cel. Biol.* **19**, 3299-3311.

Lohrer, H.D. (1996). Regulation of the cell cycle following DNA damage in normal and Ataxia telangiectasia cells. *Experimentia.* **52**, 316-28.

Maro, B., Marty, M.C., and Bornens, M. (1982). In vivo and in vitro effects of the mitochondrial uncoupler FCCP on microtubules. *EMBO J.* **1**, 1347-1352.

McAllister, R.M., Melnyk, J., Finkelstein, J.Z., Adams, E.C. and Gardner, M.B. (1969).Cultivation in vitro of cells derived from a human rhabdomyosarcoma. *Cancer.* **24**, 520-526.

Mousses, S., Ozcelik, H., Lee, P.D., Malkin, D., Bull, S.B., and Andrulis, I.L. (1995). Two variants of the CIPI/WAF1 gene occur together and are associated with human cancer. *Hum. Molec. Genet.* **4**, 1089-1092.

Murray, R.K., Granner, D.K., Mayes, P.A. and Rodwell, V.W. (1996). *Harper's Biochemistry.* Appleton and Lange, Stamford, Connecticut.

Oyaizu, N., McCloskey, T.W., Than, S., Hu, R., Kalyanaraman, V.S., and Pahwa, S. (1994). Cross-linking of CD4 molecule upregulates Fas antigen expression in lymphocytes by inducing interferon-γ and tumor necrosis factor-α secretion. *Blood* **84**, 2622-2631.

Rolfe, D.F.S., Newman, J.M., Buckingham, J.A., Clark, M.G., and Brand, M.D. (1999). Contribution of mitochondrial proton leak to respiration rate in working skeletal muscle and liver and to SMR. *Am. J. Physiol.* **276**, C692-C699.

Ron, D., and Hanener, J.F. (9192). CHOP, a novel developmentally regulated nuclear protein that dimerizes with transcription factors C/EBP and LAP and functions as a dominant-negative inhibitor of gene transcription. *Genes Dev.* **6**, 439-453.

Sagi-Eisenberg, R. and Pechat, I. (1983). Membrane potential changes during IgE-mediated histamine release from rat basophilic leukemia cells. *J. Membr. Biol.***75**, 97-104.

Salvioli, S., Ardizzoni, A., Franceschi, C. and Cossarizza, A. (1997). JC-1, but not DiOC₆(3) or rhodamine 123, is a reliable fluorescent probe to assess ΔΨ changes in untact cells: implications for studies on mitochondrial functionality during apoptosis. *FEBS Lett.* **411**, 77-82.

Shinohara, Y., Shidzuko, B., Shinichi, K., Seiichiro, K., Shuuji, I. and Hiroshi, T. (1998). Cationic uncouplers of oxidative phosphorylation are inducers of mitochondrial phosphorylation are inducers of mitochondrial permeability transition. *FEBS Lett.* **428**, 89-92.

Skulachev, V.P. (1998). Uncoupling: new approaches to an old problem of bioenergetics. *Biochim. Biophys. Acta.* **1363**, 100-124.

Smiley, S.T., Reers, M., Motola-Hartshorn, C., Lin, M., Chen, A., Smith, T.W., Steele, G. and Chen, L.B. (1991). Intracellular heterogeneity in mitochondrial membrane potentials revealed by a J-aggregate-forming lipophilic cation JC-1. *Proc.Natl. Acad. Sci. USA.* **88**, 3671-3675.

Smith, M.L., Chen, I.T., Zhan, Q., Bae, I., Chen, C.Y., Glimer, T.M., Kastan, M.B., O'Connor, P.M., and Fornace, A.J. Interactionof the p53 regulated protein Gadd45 with proliferating cell nuclear antigen. (1994). *Science* **266**, 1376-1380.

Starkov, A.A. (1997). "Mild" uncoupling of mitochondria. *Biosci. Rep.* **17**, 273-279.

Stott, F.J., Bates, S., James, M.C., McConnell, B.B., Starborg, M., Brookes, S., Palmero, I., Ryan, K., Hara, E., Vousden, K.H. and Peters, G. (1998). The alternative product from the human CDKN2A locus, p14(ARF), participates in a regulatory feedback loop with p53 and MDM2. *EMBO J.* **17**, 5001-5014.

Takekawa, M., and Saito, H. (1998). A family of stress-inducible Gadd45-like proteins mediate activation of the stress-responsive MTK1/MEKK4 MAPKKK. *Cell.* **95**, 521-530.

Terada, H. (1990). Uncouplers of oxidative phosphorylation. *Environ. Health Perspect.* **87**, 213-218.

Wang, H., Iakova, P., Wilde, M., Welm, A., Goode, T., Roesler, W.J., and Timchenko, N.A. (2001). *Mol. Cell* **8**, 817-828.

Wong, A., Cortopassi, G.A. (2002). High-throughput measurement of mitochondrial membrane potential in a neural cell line using a fluorescence plate reader. *Biochem. Biophys. Res. Commun.* **298**, 750-754.

Yu, Z.K., Gervais, J.L., and Zhang, H. (1998). Human CUL-1 associates with the SKP1/SKP2 complex and regulates p21 (CIPI/WAF1) and cyclin D proteins. *Proc. Natl. Acad. Sci. USA.* **95**, 11324-11329.

Table 1. 1:

Differential gene expression profile. NLR output for Clontech Atlas™ human 1.2-1, 1.2-3 and 1.2-toxicology cDNA microarrays, showing important genes that have changed significantly ($p \leq 0.05$), at 1, 2 and 10 h post FCCP treatment. In column 2, '1' denotes down-regulation and '2' denotes up-regulation. Fold changes represents the ratio of treated/ control. MLI is mean log intensity. Genes included on the molecular marker panel for FCCP (Fig. 1.5) are boldfaced and italicized. Genes selected as mechanistically important (Fig. 1.10) are non-boldfaced italicized.

Genes	1 = down 2 = up	Fold change	MLI	p-value
1h				
Protein synthesis				
glutaminyl--RNA synthetase	1	1.55	0.446	2.71E-03
methionyl-tRNAarna synthetase	1	1.47	1.78	1.80E-02
threonyl-tRNA synthetase, cytoplasmic	1	1.38	0.629	3.07E-02
lysyl-RNA synthetase	1	1.4	1.8	3.94E-02
Electron transport				
cytochrome c oxidase polypeptide iv precursor	2	1.43	2.78	4.94E-02
Cell proliferation				
cullin homolog1 (CUL-1)	1	2.34	0.687	4.35E-08
ATP synthesis				
voltage-dependent anion-selective channel protein 2	2	2.35	-3.33	1.43E-03
2 h				
Protein synthesis				
glutaminyl-tRNA synthetase	1	1.43	0.151	4.28E-02
elongation factor 1 alpha 2	1	1.5	1.7	3.24E-02
60S ribosomal protein l15	1	2.81	1.49	5.72E-07
60S ribosomal protein l35a	1	1.93	1.67	1.42E-03
60S ribosomal protein l12	1	1.84	3.75	2.43E-03
40S ribosomal protein s12	1	1.8	2.48	2.82E-03
40S ribosomal protein s6	2	1.58	3.84	2.32E-02
40S ribosomal protein s14	2	1.51	3.92	3.91E-02
Gluconeogenesis				
malate dehydrogenase	1	1.51	2.19	4.26E-02

Genes	1 = down 2 = up	Fold change	MLI	p-value
Glycolytic pathway				
malate dehydrogenase	1	2.01	-1.69	6.70E-04
6pf-2-k/fru-2,6-p2ase brain/placenta-type	1	1.41	-0.392	4.28E-02
Mitochondrial electron transport				
electron transfer flavoprotein beta-subunit	1	2.04	-1.09	3.24E-04
cytochrome c oxidase polypeptide iv precursor	1	2.14	0.723	9.20E-06
cytochrome c oxidase polypeptide viii-liver/heart	1	1.68	2.09	1.15E-02
cytochrome oxidase assembly factor.	1	1.52	0.166	1.90E-02
cytochrome c oxidase polypeptide -liver	1	1.5	1.76	4.65E-02
ATP synthase lipid-binding protein p2 precursor	1	1.49	2.21	4.87E-02
Cell cycle				
jun proto-oncogene	2	1.83	2.01	1.71E-03
c-fos proto-oncogenen	2	3.44	-2.36	1.98E-06
CDC-like kinase 1 (CLK1)	2	2.08	0.452	3.24E-04
early growth response protein 1 (EGR1)	2	1.85	2.97	3.14E-03
mitogen-activated protein kinase 6 (MAPK 6)	2	1.64	1.32	1.57E-02
early growth response protein 1 (hEGR1)	2	2.7	2.56	8.55E-07
cell division protein kinase 9 (CDK9)	2	1.55	2.38	3.23E-02
dual-sp.mitogen-activated protein kinase kinase1	2	1.49	3.95	3.66E-02
fos-related antigen (FRA1)	2	1.55	1.45	3.75E-02
PRB-binding protein E2F1	1	2.59	0.849	8.42E-12
protein kinase C zeta type (NPKC-zeta)	1	1.72	-2.08	2.86E-02
fos-related antigen 2 (FRA2)	1	1.65	-1.28	3.20E-02
s-interacting upstream stimulatory factor 2 (USF2)	1	1.48	2.04	4.03E-02
cell division protein kinase 7 (CDK7)	1	2.77	0.997	4.03E-06
G1/S-specific cyclin D2 (CCND2)	1	1.54	2.18	3.62E-02
Cytoskeleton				
tubulin beta-2 chain.	1	2.08	2.82	1.48E-04
beta tubulin.	1	2.24	1.58	9.01E-05
kinesin-related motor protein eg5	1	2.12	1.96	2.92E-04
p60 katanin.	2	1.74	0.071	1.92E-03
Muscle specific				
myosin-ie (fragment)	2	2.02	-4	1.26E-02
kiaa0647 protein	2	1.43	0.397	4.51E-02
troponin i, slow-twitch isoform	1	2.54	-0.945	1.76E-06
myosin light chain 2	1	1.7	-0.198	2.10E-03

Genes	1 = down 2 = up	Fold change	MLI	p-value
10 h				
Protein synthesis				
asparagine synthetase	2	4.91	0.606	1.96E-24
seryl-tRNA synthetase	2	2.62	1.83	6.55E-10
cysteinyl-tRNAsynthetase	2	2.25	0.455	1.19E-07
methionyl-tRNA synthetase	2	2.08	2.01	1.33E-06
alanyl-tRNA synthetase	2	1.95	0.416	1.19E-05
multifunctional aminoacyl-tRNA synthetase	2	1.62	0.631	1.41E-03
isoleucyl-tRNA synthetase, cytoplasmic	2	1.58	1.89	2.77E-03
threonyl-tRNA synthetase, cytoplasmic	2	1.52	0.928	4.31E-03
glutamine-hydrolyzing asparagine synthetase	2	10.4	1.66	3.32E-60
60S ribosomal protein L13A	1	1.44	4.83	3.04E-02
60S ribosomal protein L3	2	1.56	3.99	6.22E-03
histidyl-tRNA synthetase homolog	1	1.34	0.073	1.53E-02
40S ribosomal protein S9	1	16.3	1.2	8.45E-76
bifuncttional methylenetetrahydrofolate dehydrogenase	2	3.42	2.73	3.28E-12
Glycolytic pathway				
pyruvate kinase R/L (PKLR)	2	1.74	1.67	9.07E-05
Anaerobic glycolysis				
dihydrolipoamide acetyltransferase (pyruvate dehydrogenase)	1	1.42	0.477	2.19E-02
Toxicologic				
glutathione S-transferase MU 5	1	1.4	-1.38	4.91E-02
cytochrome P450 IVA11 (CYP4A11)	1	1.97	-2.01	4.19E-04
microsomal glutathione S-transferase 1 (MGST1)	1	1.51	0.201	4.43E-04
plasma glutathione peroxidase (GPXP)	1	1.75	-1.72	1.60E-03
thioredoxin peroxidase 2 (TDPX2)	1	1.5	2.52	4.93E-03
microsomal glutathione S-transferase 2 (MGST2)	1	1.49	-0.64	5.48E-03
quinone oxidoreductase; NADPH:quinone reductase	1	1.49	-0.639	5.73E-03
xanthine dehydrogenase/oxidase	1	2.08	-2.95	5.75E-03
microsomal glutathione S-transferase 3 (MGST3)	1	1.4	-0.214	7.95E-03
cytosolic superoxide dismutase 1 (SOD1)	1	1.38	2.36	2.32E-02
glutathione S-transferase theta 1 (GSTT1)	2	1.32	1.39	3.43E-02
thioredoxin peroxidase 2 (TDPX2)	1	1.5	2.52	4.93E-03
dimethylaniline monooxygenase (N-oxide forming)	2	4.35	-2.06	1.92E-02

Genes	1 = down 2 = up	Fold change	MLI	p-value
glutathione S-transferase A1 (GTH1)	2	1.69	1.2	9.33E-05
copper-zinc superoxide dismutase3 (Cu-Zn SOD3)	2	1.59	-1.52	6.76E-03
cytochrome P450 IA2 (CYP1A2)	2	1.54	-1.8	1.76E-02
Stress related				
heat shock 70-kDa protein 1 (HSP70.1)	1	2.91	0.806	3.55E-15
heat shock cognate 71-kDa protein	1	2.67	3.73	1.90E-09
stress-induced phosphoprotein 1 (STIP1)	1	1.62	1.7	2.24E-04
heat shock cognate 71-kDa protein	1	<u>4.52</u>	3.16	3.92E-02
90-kDa heat-shock protein A (HSP90A)	1	1.47	3.22	1.14E-02
110-kDa heat-shock protein (HSP110)	1	1.39	0.97	1.65E-02
heat shock-related 70-kDa protein 2	1	1.43	-1.56	3.83E-02
mitochondrial heat shock 10-kDa protein (HSP10)	1	1.6	1.9	6.72E-03
protein kinase/endoribonulcease	2	3.2	-0.722	3.02E-12
70-kDa heat shock protein 5 (HSPA5)	2	2.06	4.57	1.79E-05
C-reactive protein precursor	2	5.65	-0.81	4.97E-02
heat shock 40-kDa protein 3 (HSP40-3)	2	1.42	-0.476	1.14E-02
heat shock transcription factor 4 (HHSF4)	2	1.67	-2.57	3.37E-02
Extra cellular & cell to cell adhesion				
type V collagen alpha 2 subunit	2	1.53	3.11	5.04E-03
collagen III alpha 1 subunit (COL3A1)	2	1.62	5.47	5.20E-03
collagen XV alpha 1 subunit (COL15A1)	2	1.42	-0.096	4.74E-03
collagen VI alpha 1 subunit (COL6A1)	2	1.42	0.877	9.91E-03
collagen-binding protein 1 (CBP1)	2	1.45	3.67	2.01E-02
collagen IV alpha 2 subunit (COL4A2)	2	1.33	1.55	2.51E-02
occludin	2	2.05	-1.53	2.83E-05
tight junction protein 1 (TJP1)	2	1.56	0.231	1.65E-04
annexin IV (ANX4)	2	1.36	0.018	1.01E-02
annexin III (ANX3)	2	1.4	2.6	2.04E-02
metalloprotease/disintegrin/cysteine-rich protein	2	1.33	1.01	3.91E-02
annexin VI (ANX6)	1	2.45	2.37	4.93E-10
enamelysin	1	1.48	-0.469	1.15E-02
matrix metalloproteinase 2 (MMP2)	1	1.75	0.286	2.63E-06
intercellular adhesion molecule 2 (ICAM2)	1	1.81	-2.77	2.11E-02
Electron transport				
electron transfer flavoprotein beta-subunit (beta-etf)	1	1.4	-0.678	3.65E-02
ATP synthase lipid-binding protein p3 precursor	1	1.34	1.19	4.82E-02
NADH dehydrogenase 1 alpha s.comp. 2 (NDUFA2)	1	1.46	-0.64	8.12E-03

54

Genes	1 = down 2 = up	Fold change	MLI	p-value
DNA replication				
DNA primase large subunit (DNA primase 58 kD)	1	1.53	-0.681	8.64E-03
DNA polymerase epsilon subunit B	1	1.96	-0.839	6.02E-06
MCM3 DNA replication licensing factor	1	5.58	-0.212	1.77E-02
MCM5 DNA replication licensing factor	1	5.39	0.428	2.64E-02
replication protein A 14-kDa subunit (RP-A)	1	6.27	1.7	5.99E-03
DNA primase small subunit (DNA primase 49-kDa)	1	1.65	0.629	7.32E-05
DNA polymerase delta catalytic subunit	1	1.66	1.33	1.43E-04
DNA topoisomerase I (TOP1)	2	1.7	2.77	3.37E-04
histone 2AZ (H2AZ)	1	1.46	1.03	6.07E-03
DNA topoisomerase III alpha (TOP3A)	1	1.37	-0.081	1.10E-02
DNA topoisomerase II alpha (TOP2A)	1	1.36	2.14	2.81E-02
chromosome condensation protein 1 (CHC1)	1	1.72	0.92	7.66E-05
DNA repair				
DNA mismatch repair protein MSH6	1	2.47	1.16	4.99E-11
DNA mismatch repair protein MSH2	1	2.42	1.24	6.63E-11
DNA damage repair & recomb. protein 51 (RAD51)	1	2.3	-0.587	6.72E-09
DNA damage repair & recomb. protein 54 (RAD54)	1	2.06	-0.812	9.91E-07
DNA repair protein RAD 51 Homolog 2	1	1.73	-0.257	1.76E-05
DNA mismatch repair protein MSH3	1	1.45	-0.783	1.15E-02
DNA recombination & repair protein HNGS1	1	1.38	-0.564	2.19E-02
endonuclease III homolog 1	2	1.42	6.12	4.73E-02
ATP-dependent DNA ligase I (LIG1)	1	1.86	1.21	4.31E-06
DNA ligase III (LIG3)	2	6.42	1.15	7.88E-03
UV excision repair protein RAD 23A (RAD23A)	2	1.74	2.62	1.58E-04
DNA damage				
growth arrest & DNA damage 153 (GADD153)	2	6.99	1.96	9.14E-41
growth arrest & DNA damage 45 (GADD45)	2	2.99	1.74	2.78E-16
growth arrest & DNA damage 45g (GADD45 g)	2	2.52	0.99	2.75E-11
Cell cycle and signal transduction				
proliferating cyclic nuclear antigen (PCNA)	1	4.1	0.904	1.78E-23
cyclin-dependent kinase inhibitor 1A (CDKN1A/ p21)	2	3.34	0.971	4.31E-07
cell division cycle 25 homolog A (CDC25A)	1	2.59	1.04	7.63E-12
G1/S-specific cyclin E (CCNE)	1	2.38	0.56	8.58E-12
cyclin F (CCNF)	1	2.32	-0.465	1.60E-09

Genes	1 = down 2 = up	Fold change	MLI	p-value
jun proto-oncogene	2	2.06	1.79	5.21E-08
G2/mitotic-specific cyclin B1 (CCNB1)	1	2	1.57	8.13E-08
G1/S-specific cyclin D3 (CCND3)	1	1.96	2.12	1.25E-06
junD proto-oncogene	2	1.84	-0.185	1.30E-06
cyclin-dependent kinase 10 (CDK10)	2	1.82	0.488	1.58E-06
mitogen-activated protein kinase kinase 3 (MAPKK 3)	1	2.01	-0.749	1.66E-06
mitogen-activated protein kinase kinase 6 (MAPKK 6)	1	1.99	-1.12	1.95E-05
cyclin-dependent kinase inhibitor 2C (CDKN2C)	1	1.95	-1.13	3.42E-05
cyclin D1 (CCND1)	1	1.73	1.38	3.47E-05
mitotic feedback control protein MADP2 homolog	1	1.64	0.289	3.49E-05
N-myc proto-oncogene	1	2.1	-1.88	6.75E-05
mitogen-activated protein kinase 9 (MAPK9)	2	1.73	2.19	8.87E-05
cell division control protein 2 homolog (CDC2)	1	1.7	1.95	1.01E-04
cyclin A1 (CCNA1)	2	1.76	-0.9	1.95E-04
cyclin-dependent kinase 5 activator	1	1.7	-0.724	2.34E-04
mitogen-activated protein kinase 6 (MAPK 6)	2	1.61	1.14	4.62E-04
cyclin-dependent kinase 4 inhibitor 2 (p16-INK4)	2	1.57	1.39	6.28E-04
mitogen-responsive phosphoprotein DOC2	2	1.57	-0.733	1.94E-03
early growth response protein 2 (EGR2)	2	1.44	0.258	2.13E-03
catenin delta 1 (CTNND1)	1	1.39	0.47	8.01E-03
cyclin-dependent kinase inhibitor 3 (CDKN3)	1	1.33	0.392	1.77E-02
mitogen-activated protein kinase 7 (MAPK 7)	2	1.33	0.601	2.46E-02
cell division cycle 20 homolog (CDC20)	1	1.38	2.64	2.93E-02
mitogen-activated protein kinase 8 (MAPK8)	2	1.31	-0.186	3.19E-02
fos-related antigen 2 (FRA2)	2	1.37	-0.883	3.61E-02
beta 1 catenin (CTNNB)	1	1.31	1.23	4.15E-02
mitogen-activated protein kinase 12 (MAPK 12)	1	1.26	0.286	4.74E-02
c-fos proto-oncogene	2	1.61	-2.55	4.76E-02
ras-related protein RAB2	2	1.37	0.359	9.09E-03
Apoptosis				
caspase 4 (CASP4)	2	2.11	0.304	6.50E-10
BCL2/adenovirus E1B 19-kDa-inter. Prot. 3 (BNIP3)	1	1.69	0.234	7.38E-06
caspase 3 (CASP3)	2	1.51	1.83	1.96E-03
fas antigen ligand (FASL)	2	9.36	-0.614	7.11E-03

Genes	1 = down 2 = up	Fold change	MLI	p-value
bcl-2 interacting killer (BIK)	2	3.64	-1.76	4.76E-02
apoptosis regulator bcl-x	2	1.51	1.14	2.53E-03
BCL2-like 2 (BCL2L2)	2	1.38	1.32	1.43E-02
casper, a FADD- and caspase-rel. inducer of apoptosis	2	1.31	0.206	2.11E-02
caspase & RIP adaptor with death domain (CRADD)	2	1.31	-0.339	4.06E-02
caspase 2 (CASP2)	1	2.07	1.33	4.57E-08
apoptotic protease activating factor 1 (APAF1)	1	1.36	-0.0051	1.19E-02
fas-associated via death domain protein (FADD)	1	1.39	-1.09	3.86E-02
Cytoskeleton				
cytoplasmic beta-actin (ACTB)	1	1.87	5.01	1.09E-05
lamin b1	1	1.91	1.52	3.07E-05
tubulin beta-2 chain	1	1.78	2.9	3.90E-05
beta tubulin	1	1.82	1.73	1.40E-04
tubulin alpha-4 chain	1	1.65	2.88	3.22E-04
lamin b2 (fragment)	1	1.43	0.495	1.75E-02
brain-specific tubulin alpha 1 subunit (TUBA1)	1	1.38	4.33	2.17E-02
lamin b receptor	1	1.45	-1.04	2.95E-02
cytoplasmic beta-actin (ACTB)	1	2.94	4.72	3.90E-10
tubulin alpha 1 (TUBA1)	1	1.62	5.19	4.77E-03
cytovillin 2; villin 2 (VIL2)	1	4.29	1.28	3.09E-02

Fig. 1. 1:

JC-1 assay showing changes in membrane potential as a response to treatment with 0.1 to 64 μM FCCP for 1 h, in RD cells. There is a dose-dependant increase of uncoupled cells subsequent to treatment, reaching a plateau at 32 μM. 20 μM FCCP which yielded approximately 75% uncoupling, was selected as the exposure concentration for the present studies.
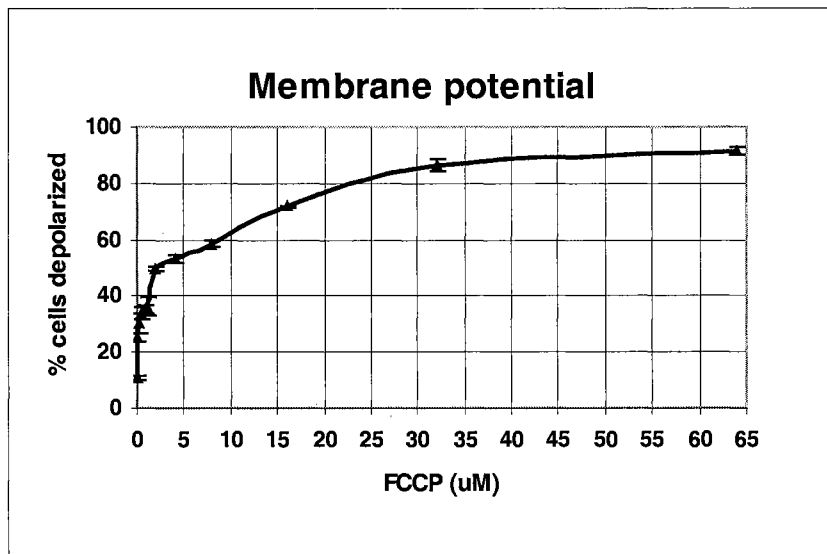
Fig. 1. 2:

Photomicrographs of H&E stained RD cells treated with 20 μM FCCP for 2, 10 and 24 h along with time-matched controls. The cell cycle arrest is evidenced by the decrease in the number of cell in the treated group as time progressed. Histologically, the treated cells were smaller and attenuated.
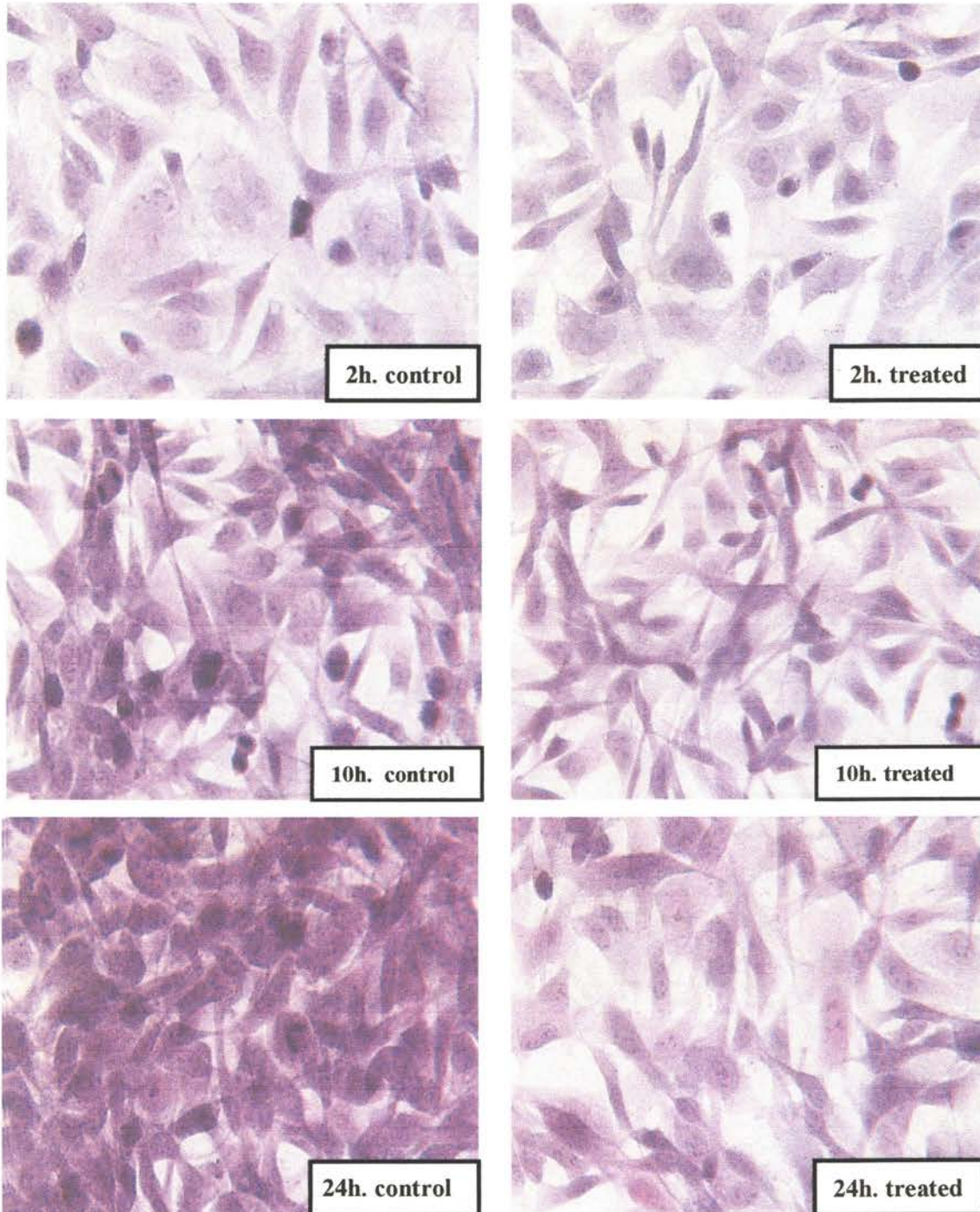
Fig. 1. 3:

Compound concentration assay. HPLC measurement of the concentration of FCCP in the media, from 0 to 24 h. The compound was stable for up to 24 h in the control group, which had only media and no cells. In the treated group however, the compound was taken up by the cells almost completely by 24 h.
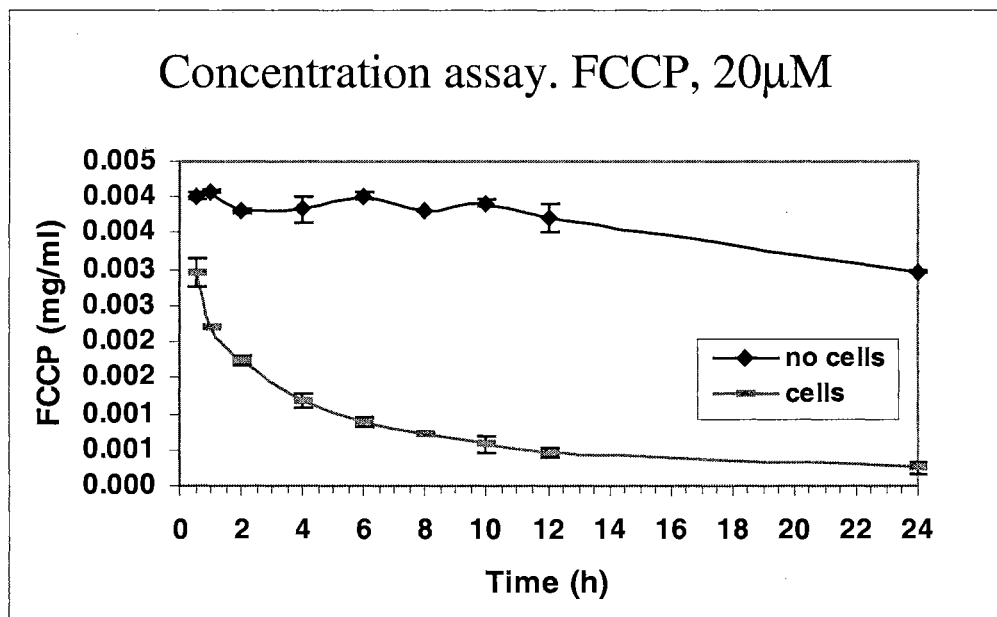

Concentration assay. FCCP, 20µM

X-axis: Time (h) — 0, 2, 4, 6, 8, 10, 12, 14, 16, 18, 20, 22, 24

Y-axis: FCCP (mg/ml) — 0.000, 0.001, 0.001, 0.002, 0.002, 0.003, 0.003, 0.004, 0.004, 0.005

Legend: no cells, cells

Fig. 1. 4:

Time course data showing $\log_2$ ratios (treated/control) of adjusted intensities of mRNA expression of 165 genes associated with energy metabolism, in response to treatment with 20 µM FCCP. The lines in the graph represent individual genes and the data was obtained from Clontech™ Atlas human 1.2-3 microarray using poled RNA (Within each time point, RNA samples obtained from each of the 3 replicate were combined to yield a single pooled sample each for control and treated). Transcriptioanl dysrergulations were most pronounced at 1, 2 and 10 h.

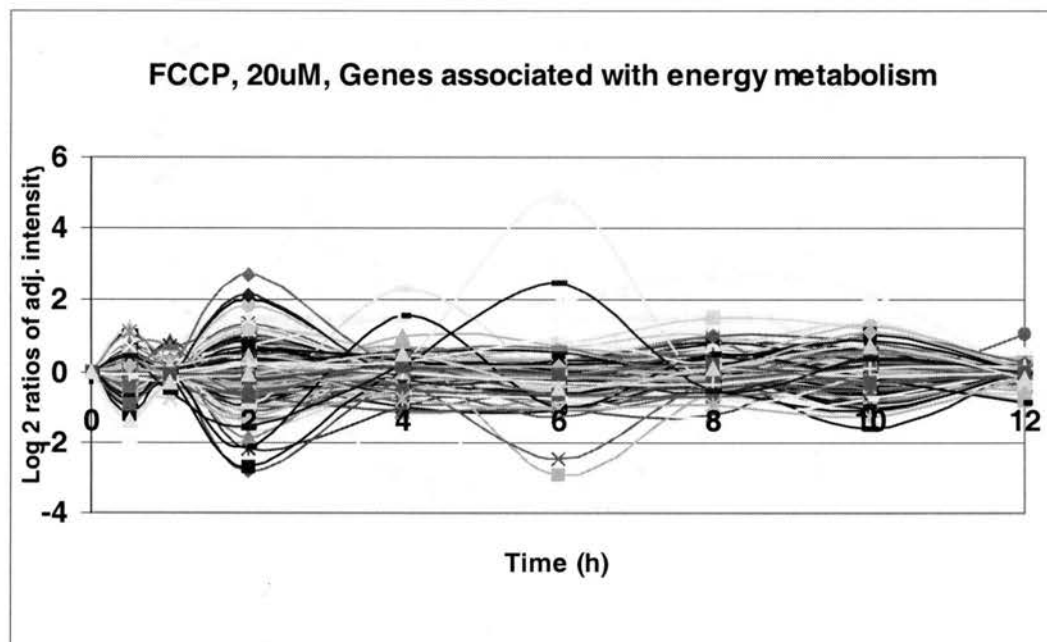FCCP, 20uM, Genes associated with energy metabolism

Fig. 1. 5:

Seven genes proposed as molecular markers for uncoupling. The genes were selected from the 10 h data for 20 μM FCCP (at 80% uncoupling). Two platforms are compared here. RT-PCR analyses of expression levels of mRNA were in confirmation with the microarray data, both in direction and magnitude, for all the genes.

Marker genes for uncoupling. RT-PCR vs microarray
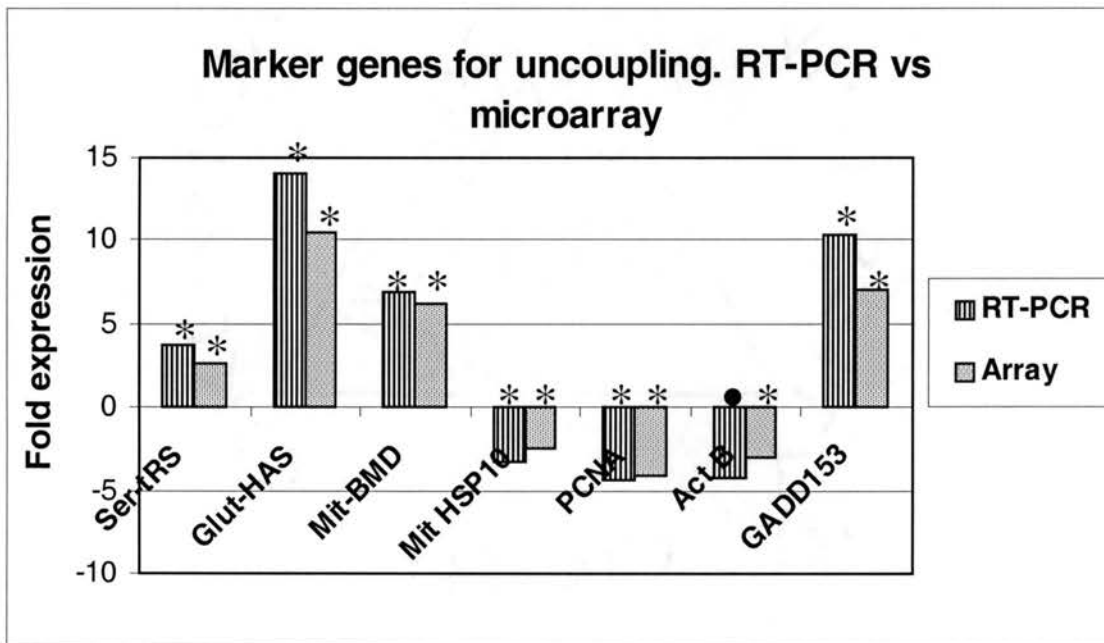
•p ≤ 0.05   *p ≤ 0.01

Fig. 1. 6:

Flow cytometric assay for cell cycle and apoptosis with BrdU and PI. Cells treated with 20 μM FCCP showed a time dependant cell cycle arrest in the G_1/G_0 and S phases, starting as early as 2 h. A small, but statistically significant percentage of cells underwent cell death, starting at 24 h.

Cell cycle assay
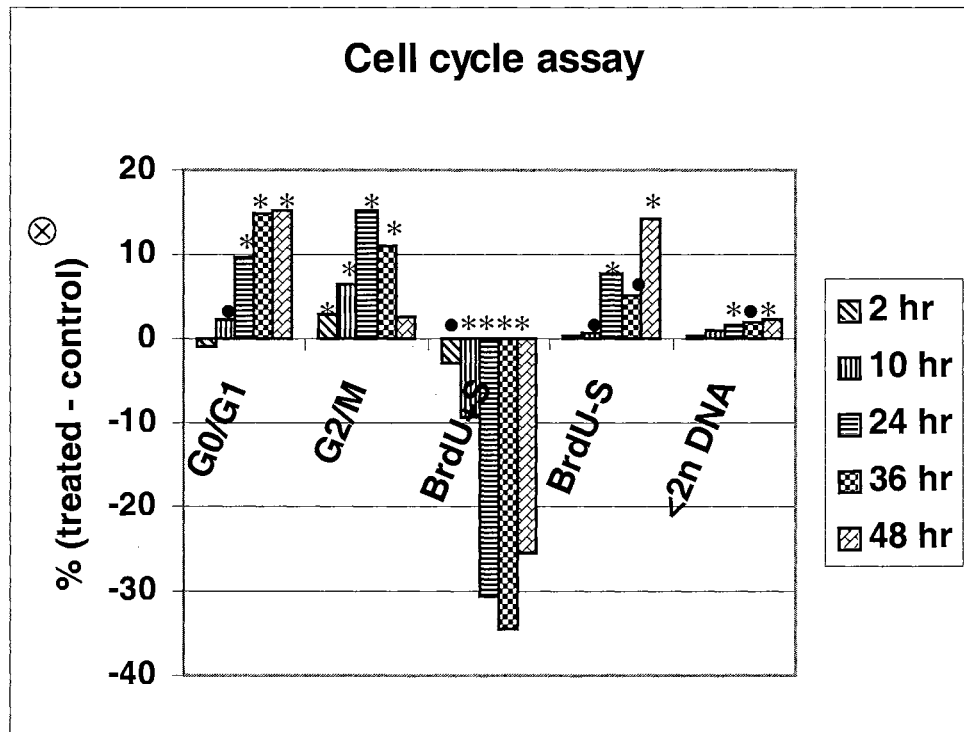
•p ≤ 0.05   *p ≤ 0.01

⊗ Control was subtracted from treated and expressed as percentage

Fig. 1. 7:

Media glucose and lactate measured from 0.5 to 24 h post treatment with 20 μM FCCP, not adjusted for cell count. O denotes no significant difference between control and time matched treatment groups (p < 0.05). Increased glucose utilization is indicative of up-regulation of metabolic activity and increased lactate output is suggestive of up-regulation of glycolytic pathways, in the treated groups.
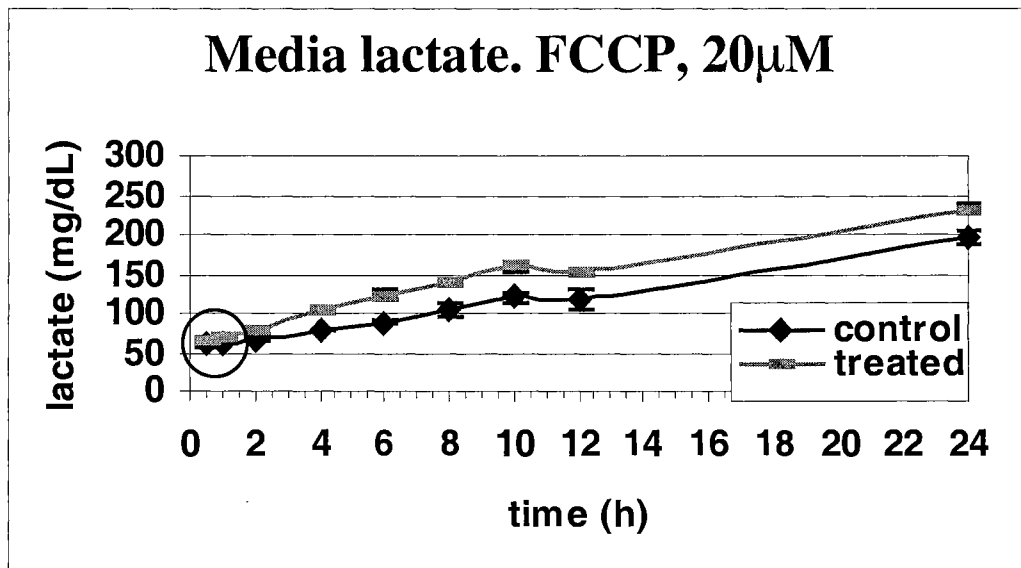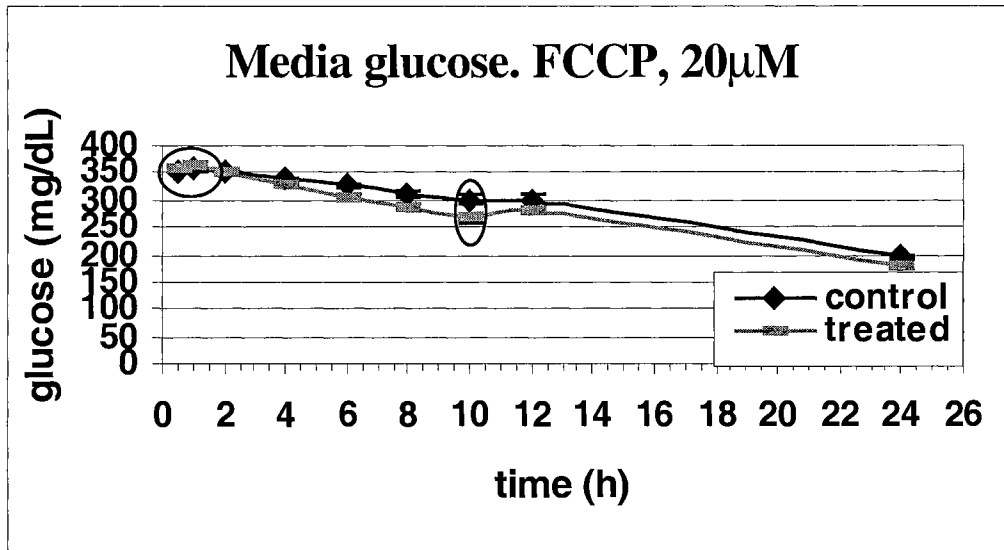
Fig. 1. 8:

Bioluminescent assay using firefly luciferase to measure intracellular ATP in response to treatment with 20 μM FCCP. O denotes no significant difference between control and time matched treated groups (p < 0.05). There was an immediate drop in ATP levels in the first 30 min that incited a compensatory response resulting in an increase in ATP levels.

ATP assay. FCCP, 20 μM

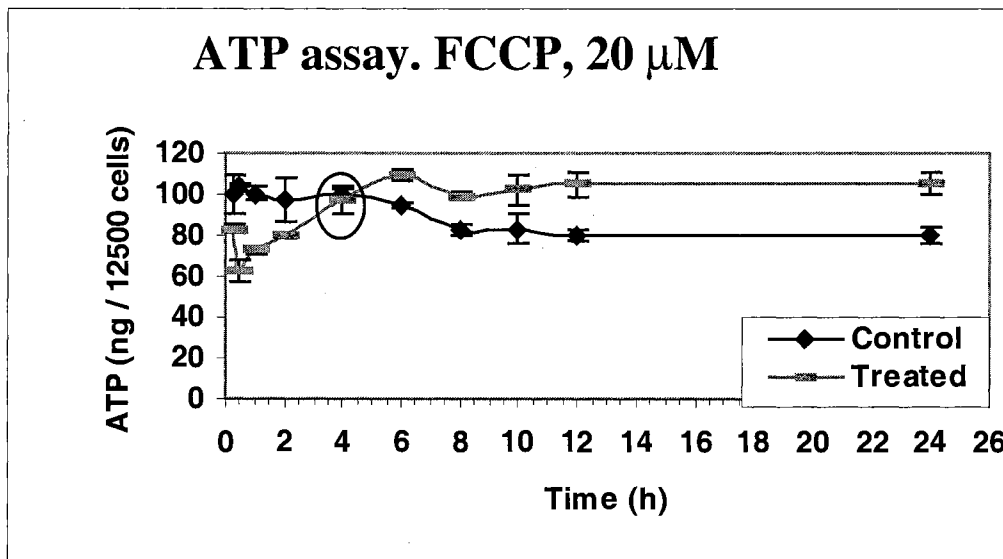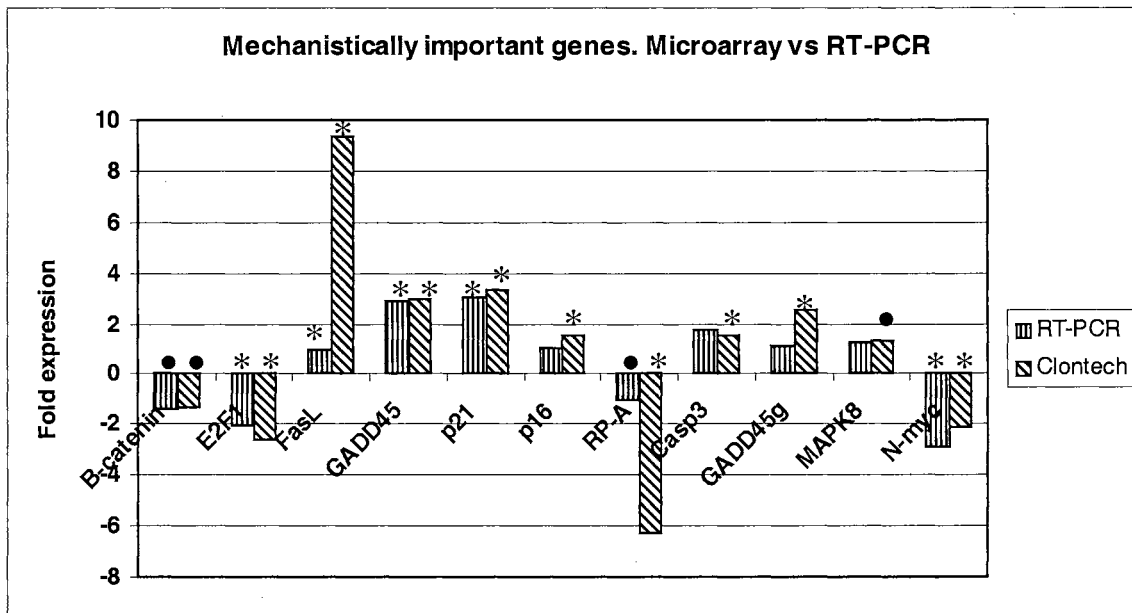**Fig. 1. 9:**

RT-PCR confirmation of 11 genes selected from pathways involved in the proposed mechanisms of action of FCCP, as outlined in fig. 1.10. The genes were chosen from the 10 h microarray data. The two platforms are compared here. Overall, there was good agreement between the platforms.

Mechanistically important genes. Microarray vs RT-PCR

$\bullet p \leq 0.05$ $*p \leq 0.01$

Fig. 1. 10:

Proposed physiological responses of FCCP, in in-vitro systems, based on reading of transcriptome. The central events were collapse of membrane potential followed by decrease in ATP, which led to down-regulation of anabolic metabolism such as protein synthesis, and DNA damage. DNA damage led to G_1 and S phase cell cycle arrest and apoptosis through modulation of several pathways involving GADD153, GADD45, p21, p16, relication protein A, PCNA and others.
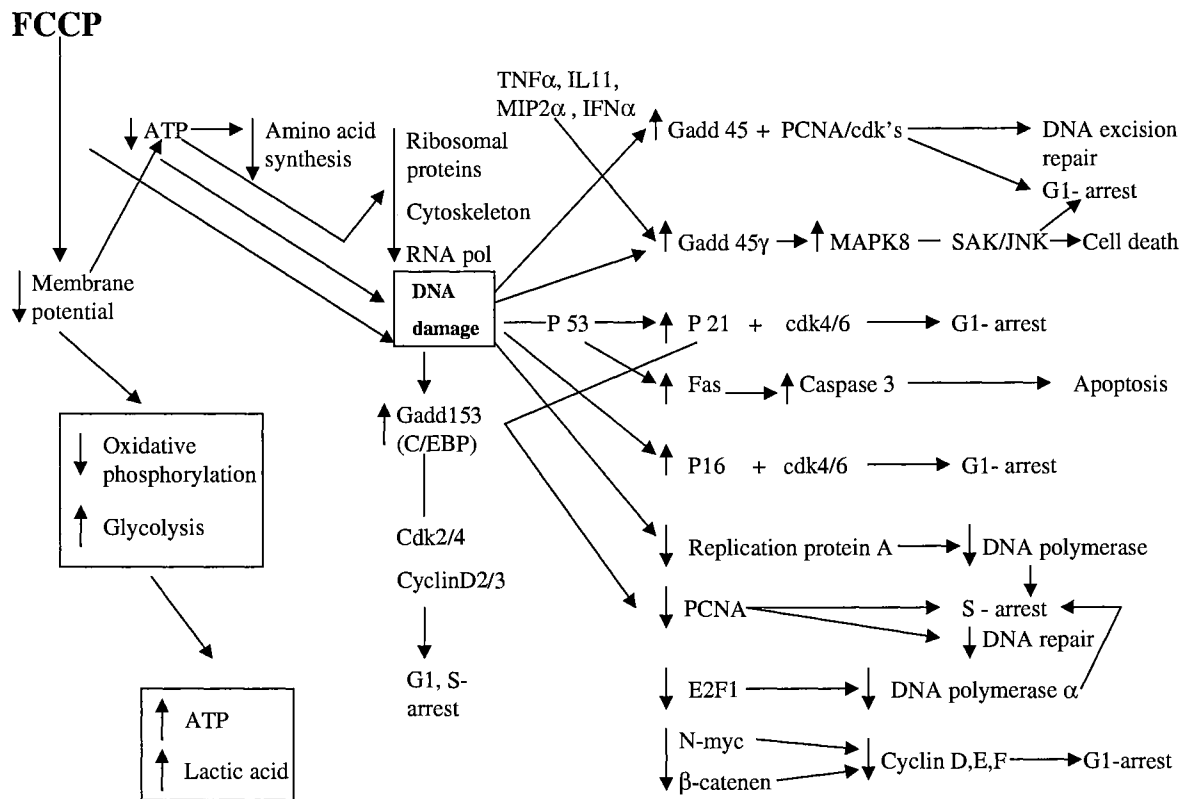
FCCP

CHAPTER 3

LARGE-SCALE DIFFERENTIAL GENE EXPRESSION DETECTS CARBONYL CYANIDE P-(TRIFLUROMETHOXY) PHENYLHYDRAZONE [FCCP]-INDUCED OXIDATIVE STRESS

Sabu Kuruvilla[1,2], Kevin T. Morgan[2,4], Roland D. Tyler[2], Lawrence W. Yoon[2], Padma K. Narayanan[3], Mark A. Tirmenstein[3], Laura M. Storck[3], Catherine X. Hu[3], Heath C. Thomas[3], Marilyn J. Easton[2], Donald R. Creech[2], Tanya Brown[2], Jerry R. Malayer[1] and Charles W. Qualls Jr.[2]

[1]*Oklahoma State University, Stillwater, OK 74078*
[2]*GlaxoSmithKline, Inc. Research Triangle Park, NC 27709*
[3]*GlaxoSmithKline, Inc. King of Prussia, PA 19406*
[4]*Present address: Aventis Pharmaceuticals, Raleigh, NC 27612*

ABSTRACT

FCCP has been known from the early 1900's as an uncoupler of oxidative phosphorylation. However, published reports about other toxic effects of this compound are scant. This work is an attempt to understand as yet unidentified toxicological mechanisms associated with this compound, using gene expression, biochemical assays and morphological evaluations as tools, in a human rhabdomyosarcoma (RD) cell line. Initial gene expression studies using cDNA microarrays with 150 µM FCCP for 10 h showed gene expression patterns consistent with oxidative stress, in addition to patterns for cell cycle arrest, stress, DNA damage, DNA repair, suppression of DNA replication, apoptosis and inflammation. The RT-PCR profile obtained using previously identified marker genes of oxidative stress confirmed FCCP-induced oxidative stress. Subsequently, biochemical tests for glutathione depletion, superoxide production and lipid peroxidation were performed and they provided further proof for FCCP-induced oxidative stress. Flow cytometric assay with annexin V and propidium iodide (PI) showed an increase in apoptosis and necrosis with increasing concentration of FCCP. Bioluminescent assay demonstrated a reduction of intracellular ATP upon treatment with FCCP, which is indicative of the uncoupling effect of the compound and its influence on energy metabolism. Histological evaluation of cells stained with hematoxylin and eosin (H&E) revealed reduced cell count and mitotic arrest at 10 h post treatment. It was concluded that FCCP is an oxidative stressor and that gene expression profile can be used effectively as a molecular marker for oxidative stress.

Key words:

Oxidative stress, gene expression, FCCP, uncoupling agent, RD cells, MTS assay, ATP, glutathione, heme oxygenase, thioredoxin reductase.

INTRODUCTION

Oxygen is necessary for all aerobic forms of life. Reduction of oxygen to water

provides the energy for the complex activities of the higher organisms. However,

reduction of oxygen is inherently associated with risks. Incompletely reduced oxygen

species during normal aerobic metabolism generates reactive oxygen species (ROS) that

can cause significant damage by nonspecifically and indiscriminately reacting with

various macromolecules, leading to a variety of metabolic impairment and cell deaths.

Reactive oxygen intermediates are normally generated by the electron transport chain

(Janssen et al., 1993), primarily in complex I (Turrens et al., 1980) and complex III

(Cadens et al., 1977; Turrens et al., 1985). They are also generated from molecular

oxygen either by exposure to ultraviolet radiation, by endogenous reduction through

cellular oxidases, peroxidases and mono - and dioxygenases or by a variety of chemicals.

Oxidative reactions are employed beneficially as a defensive mechanism by tissue cells,

and by circulating phagocytic cells of innate immune system against invading pathogens.

There exists a balance between ROS and endogenous antioxidant systems in the cells of

healthy individuals. Excess reactive oxygen either due to overproduction as a result of

toxic insult or due to decreased scavenging by the antioxidant system can lead to

perturbance in the redox balance. The importance of ROS in biological systems has been

historically recognized (Fridovich, 1975; Fridovich, 1978) and their significance has

become more apparent with the recent advances in molecular biology. For further

reading, we suggest Gille et al., 1995 and Scandalios, 1997.

Mitochondria, besides being equipped with enzymatic defensive mechanisms to

combat excessive ROS generation, are also believed to regulate cellular levels of ROS

through 'uncoupling' of oxidative phosphorylation (respiration without phosphorylation), although our knowledge of redox regulation through uncoupling is still emerging. The thermoregulatory activity of uncoupling protein 1 (UCP1) in brown fat is well recognized (Del Mar et al., 2000), but it is unclear whether other isoforms of uncoupling protein have a role in regulating heat production in tissues other than brown fat (Hagen et al., 2002). It has been postulated that uncoupling may have an antioxidant role in a variety of tissues. Extremely low concentrations of 3,5-di-tert-butyl-4-hydroxybenzylidenemalononitrile (SF6847), a potent chemical uncoupler, abolishes H_2O_2 production by heart muscle mitochondria in state 4 respiration (when the availability of respiratory substrates are low) [Korshunov et al., 1997]. The positive correlation between mitochondrial membrane potential ($\Delta\Psi$) and ROS production was described by Liu, 1997. It has been postulated that mitochondria possess a special mechanism called 'mild' uncoupling, which prevents a strong increase in proton motive force ($\Delta\bar{u}_H^+$) when ADP is exhausted. If mild uncoupling is unable to prevent superoxide formation, the next line of defense must be actuated. This might be the opening of non-specific pores in the inner mitochondrial membrane. The pore opening results in the collapse of $\Delta\bar{u}_H^+$ (Skulachev, 1998).

In 1939, the Russian biochemists Belitser and Tsibakova found that addition of arsenate to skeletal muscle mince allows respiration to occur without ATP formation (Slkulachev, 1998). In 1948 Loomis and Lipman described uncoupling activity of the chemical 2,4-p-dinitrophenol (Slkulachev, 1998). Since then many artificial uncouplers have been described. FCCP is a very potent artificial uncoupler with protonophorous activity and since it is capable of collapsing the $\Delta\Psi$, it can be theorized to possess regulatory effects on ROS generation, similar to endogenous uncouplers, but it's not clear

whether this effect is dose dependent. It is also not clear what specific mechanisms of toxicity are activated at higher exposure concentrations of FCCP. The purpose of this study was to identify FCCP-induced mechanisms of toxicity in-vitro, with special emphasis on oxidative stress, using gene expression as a source of clues to be explored.

MATERIALS AND METHODS

Chemicals:

FCCP was procured from Sigma Chemical Company (St Louis, MO) and was at least 98% pure as measured by thin layer chromatography. The compound was initially dissolved in 95% ethyl alcohol due to its poor solubility in tissue culture media. Other reagents were obtained from Clontech Laboratories (Palo Alto, CA), ResGen (Huntsville, AL), Perkin Elmer Life Sciences (Boston, MA), Promega Corporation (Madison, WI), Calbiochem-Novabiochem Corporation (San Diego, CA), Invitrogen Life Technologies (Carlsbad, CA) and Pharmingen BD Biosciences (San Diego, CA).

Cell culture:

RD cells (ATCC, CCL-136), obtained from American Type Culture Collection (ATCC), Rockville, MD were grown in Dulbeco's Modified Eagles Medium (DMEM) with Glutamax and 10% fetal bovine serum (FBS), without antibiotics and incubated at 37°C with 5% CO_2. They were cultured in collagen coated 'T175 Biocoat vented flasks' (Collagen I Cellware, Becton Dickinson Labware) and fed every 2 days, for subculture and stock expansion. For RNA preparations the cells were grown in Biocoat 150 mm

diameter petri dishes (Collagen I cellware, Becton Dickinson Labware) with 25 ml

medium, and containing a numbered collagen coated glass microscope coverslip for light

microscopic evaluation of cell morphology. For the purpose of RNA extraction, cells

were seeded at a density of 1×10^7 in 3 control and 3 treated dishes per time point. They

were fed at 24 and 38 h, and were dosed at 48 h after seeding. Cells were harvested at

multiple time points from 0 to 24 h post treatment.

Toxicity and dose selection:

As described earlier by Morgan et al. (2002) and Merrill et al. (2002), exposure

concentration of FCCP was selected using light microscopy in combination with MTS

tetrazolium assay (Cell Titer 96® Aqueous Non-radioactive Cell Proliferation Assay,

Promega), which measures the reductive capacity of the cells, largely as a function of

cellular NADPH/NADH content (Marshall et al., 1995). The concentration that caused a

50% reduction in MTS activity after 24 h (24 h MTS EC_{50}) was determined. RD cells

were plated in 96 well plates with 20,000 cells and 100 μl of DMEM + 10% FBS per

well. Following chemical exposure, 20 μl of MTS reagent was added to each well, the

plate was incubated for 1 h at 37°C and spectrophotometric absorbance read at 490 nm.

The 24 h MTS EC_{50} was determined using a series of 1-in-10 dilutions, from 100 nM or

maximum achievable concentrations, with 6 wells per concentration. This approach was

then repeated, but bracketing a narrower exposure range, until the 24 h MTS EC_{50}

concentration was determined. An exposure concentration of 150 μM was selected for

this study based on the 24 h MTS EC_{50} in combination with light microscopic evaluation

for cell viability.

Cell morphology:

Coverslips were removed from petri dishes at each time point and fixed in 95% ethanol. They were then stained with H&E and evaluated by light microscopy. Five representative 20x fields from each of the 3 controls and 3 treated coverslips were captured with a digital camera mounted on a microscope and imported into Imagepro plus™ software. The images were then enlarged as necessary and the cells from each 20x field were counted to obtain separate values for total cell counts and mitotic figures.

Gene expression assay:

Based on earlier work by Kuruvilla et al. (submitted), the 10 h time point was selected for this study. CCL-136 tissue culture cells, after removal of the media, were lysed in situ with Trizol Reagent™ (Gibco-BRL, MD) and the lysate was stored at -80°C until use. Total RNA was isolated by chloroform/ isopropanol/ ethanol extraction and RNA quality and quantity were assessed using agarose gel electrophoresis and spectrophotometric 260/ 280 nm absorbance. ^{33}P-labelled cDNA probes were prepared with total RNA from each of the triplicate samples of both control and treated groups, using a modified Clontech (Palo Alto, CA) protocol, and hybridized to Clontech Atlas™ Human 1.2-1, 1.2-3, 1.2-Toxicology and Toxicology II cDNA nylon microarrays with 1185 genes per array. Denaturation and annealing (4 µl) was carried out at 94^{0}C for 10 sec and 70°C for 10 min using 6 µg total RNA and 1 µl CDS Atlas specific primers (0.2 µM each). The extension reaction (22 µl, 35 min at 49°C) contained 0.5 mM each dATP, dGTP, dTTP; 50 mM Tris-HCl pH 8.3; 75mM KCl; 3 mM MgCl$_2$; 4.5 mM DTT; 100

μCi ^{33}P-α-dCTP (3000 Ci/ mmol, 10 μCi/ μl, NEN, NE) and 200 units Super Script II™

reverse transcriptase (Gibco-BRL, MD). Extension was terminated by heating at 94°C for

5 min. Unincorporated ^{33}P-α-dCTP was removed using G_{50} Microspin columns

(Amersham Biosciences, Inc., Piscataway, NJ). Pre-hybridization was carried out at 64°C

for 1 h, in 6.5 ml MicroHybe™, 3.25 μl poly-dA (1 μg/ μl, ResGen) and 6.5 μl Human

Cot 1 DNA (1 μg/ μl, Clontech). Heat denatured ^{33}P-cDNA was added and hybridization

carried out for 16 h. Arrays were washed at 64° following manufacturer's instructions.

The membranes were exposed to a phosphor imager screen for 60 h and optical density

was acquired using Optiquant™ software and a Cyclone scanner (Packard Biosciences

Co., Meriden, CT). Image files generated from phosphor imager scans were analyzed

using Clontech Atlas™ software. After background subtraction, data were normalized and

statistically analyzed using Normalization and Local Regression (NLR) software (Kepler

et al., 2002). NLR processed text files were used to compare control with treated groups,

generate p-values, Mean Log Intensity (MLI), and ratio of differences between groups.

The NLR output files were again subjected to data manipulation with Microsoft Excel™

software to find changes through ranking by ratios, p-values or MLI.

Real Time Quantitative RT-PCR (TaqMan™):

The expression of the 7 genes suggested as molecular markers for oxidative stress by

Morgan et al. (2002) were analyzed by real time quantitative RT-PCR (oxidative stress

plate). These genes were: Cytochrome P450 1A1 (CYP 1A1), DNA topoisomerase 2A

(TOP2A), Heme oxygenase-1 (HO1), Cyclin dependant kinase inhibitor 1 (CDKN1), γ-

Glutamyl-cysteinyl ligase regulatory subunit (GCLM), Glutathione reductase (GR) and

Thioredoxin reductase (TXNR). The Total RNA was DNAase treated (Ambion DNAase

I) according to the manufacturer's protocol. RNA was quantified using Molecular Probes

Ribogreen™ assay and a Cytofluor 2350 fluorometer. Samples were diluted to 10 ng/ µl

prior to RT-PCR (TaqMan™) analysis using Perkin Elmer ABI Prism 7700 Sequence

Detection system. Primers were designed with the use of Perkin Elmer Primer Express™

software. A 96-well assay was arranged to detect mRNA expression of 7 genes in 3

control and 3 treated RNA samples, using probes and primers from Keystone Biosource.

The arrangement of the plate included one row for each gene and one row for 18S

ribosomal RNA (rRNA) internal control. RNA samples were then arranged column-wise,

with 3 pairs of control and 3 pairs of treated samples, in duplicate to fill the 12 columns

of the plate. Forward and reverse primers were diluted to 9 µM and probe to 2 µM, and

20 µl of each was aliquoted to make the probe/primer master mix. The master mix for the

remaining component prepared according to the manufacturer's protocol (without probes

and primers) and 35 µl was aliquoted per well. Fifteen µl of probe/ primer mix was then

added using a multichannel pipette, the plate was sealed with optical grade caps, and the

reaction was carried out as follows: 48°C for 30 min (reverse transcriptase or RT step),

95°C for 10 min (Amplitaq activation and RT denaturation), 40 cycles of 94°C for 15 sec

and 60°C for 1 min. Values of fold change in expression were graphed for comparison

purpose. Statistical significance was determined for control vs. treated groups using a two

tailed t-test at $p < 0.01$ or $p < 0.05$.

Media chemistry:

Media samples were collected at 2 h intervals for up to 24 h, centrifuged at 3200xg

for 15 min at 4°C to remove floating cells and the supernatant were stored at –20°C prior

to analysis of lactate dehydrogenase (LD), at 37°C by a modified kinetic procedure, using

a Hitachi 911 analyzer (Roche Diagnostics). Differences between time points and

treatment groups were expressed as mean (± SD) and significance was assessed using a

two tailed t-test at $p < 0.01$ or $p < 0.05$.

Glutathione assay:

Reduced and oxidized glutathione (GSH and GSSG, respectively) levels were

assayed by HPLC with fluorometric detection, according to the method of Martin and

White (1991).

Superoxide radical assay:

Hydroethidine (HE), a sodium borohydride-reduced form of ethidium bromide (EB)

was used to evaluate generation of superoxide ($O_2^{\bullet}$-) in RD cells upon exposure to FCCP.

HE, a specific and sensitive indicator of $O_2^{\bullet}$- (Rothe and Valet, 1990) is cell permeable

and can be directly oxidized to EB by $O_2^{\bullet}$- produced by the cell (Carter et al., 1994).

Intracellular EB tightly binds DNA and is fluorescent (610 nm) on excitation with the

488 nm line of a FACSCalibur (Becton-Dickinson, San Jose, CA). Ten µM HE was

added to the cell suspension for dye loading. Fifteen min after incubation at 37°C with

HE, RD cells were incubated for an additional 6 h in the presence or absence of FCCP

(50, 100, 150 μM) immediately after which data aquisition commenced on the FACSCalibur bench-top flow cytometer.

Lipid peroxidation assay:

Peroxyl radicals generated during lipid peroxidation of the cell membranes upon treatment with FCCP were detected, after incorporating a lipophilic fluorescein derivative, 5-(N-dodecanoyl) aminofluorescein (C_{11}-fluor), in the cell membranes. A decrease in fluorescence of C_{11}-fluor that is propotional to the increase of peroxyl radicals was expected. A FACSCalibur bench-top flow cytometer was used to monitor C_{11} at excitation and emission wavelengths of 488 and 520 nm, respectively, using the method described by Makrigiorgos et al. (1997).

Apoptosis and necrosis assay:

Annexin V is a Ca^+ dependant phospholipid binding protein that binds with high affinity to phosphatidylserine, a lipid that is on the inner surface of the cell membrane, but translocates to the outer surface quite early in the apoptotic process. Hence annexin V can be used as a sensitive probe to detect phosphatidylserine on the cell membrane. Translocation of phosphatidylserine to external cell surface is not unique to apoptosis (apoptotic necrosis), but occurs also during cell necrosis (oncotic necrosis). However, during the initial stages of apoptosis, the cell membrane remains intact, while at the very moment cell necrosis occurs the cell membrane loses its integrity. Therefore, measurement of annexin V binding to cell surface as indicator of apoptosis has to be performed in conjunction with a dye inclusion test to establish the integrity of the cell

membrane. Propidium iodide (PI) is impermeable to cells with intact membranes, but stains DNA of cells, which have lost cell membrane integrity. Thus, cells that are positive for annexin V only are apoptotic and those that are positive for both annexin V and PI are necrotic. A flow cytometric assay, using fluorescein labelled annexin V and PI was performed, according to the method of Vermes et al. (1995), 4 h after treatment with 150 μM FCCP. For a review of the terminology and mechanisms associated with cell death, the suggested reading is Trump et al. (1997).

ATP assay:

Changes in intracellular ATP concentrations were measured at 0, 50, 100 and 150 μM FCCP at 10 h, for both control and treated cells, using Luciferin-Luciferase, as per Karamohamed et al. (1999). Bioluminescent somatic cell assay kits were purchased from Sigma Chemical Company. The cells were suspended in their original media and adjusted to 5×10^5 cells/ ml. The cells were treated with ATP releasing agent, which allowed rapid release of small molecules such as ATP, while larger molecules remained trapped inside the cells, affording protection from the ATPases. The free ATP was allowed to react with Luciferin-Luciferase and the light released was measured using a Turner Designs 20/20 luminometer. Differences between control and treated groups were expressed as mean ($\pm$ SD) and statistical significance was assessed using a 2 tailed t-test at $p < 0.01$ or $p < 0.05$.

RESULTS (Data are presented in appendices 2A and 2B)

Characterization of RD cells:

This cell line was established in 1968 from a malignant embryonal

rhabdomyosarcoma of the pelvis of a 7 year-old girl. The line consists of cells of two

cytologic features - poorly differentiated spindle cells and larger multinucleated cells. No

contractile myofilaments could be demonstrated by light or electron microscopy (data not

shown). Immunohistochemical staining failed to reveal the presence of significant

amounts myosin and myoglobin (data not shown). The cells grew as a monolayer and

showed occasional 'whorling' patterns when grown on collagen I coated plastic tissue

culture dishes, using DMEM with 10% FBS.

Cell morphology and viability:

Light microscopic examination of cells treated with 150 µM FCCP for 10 h revealed

clear morphologic changes including cell shrinkage and rounding (fig. 2.1). In the treated

group, there was a decrease of 44.9% and 100% in cell count and mitotic figures,

respectively (data not shown). There was also a marked increase in apoptosis/ necrosis

subsequent to treatment, although the apoptotic and necrotic cells could not be clearly

separated on H&E stained coverslips. A time course assay over 24 h, to measure LD

enzyme activity in the media, as an indicator of cell membrane damage with resulting

cytosolic leakage, showed no significant difference between the treated and control

groups up to 6 h. Thereafter, the treated group showed a significant increase in LD

activity ($p < 0.01$). At 10 h, the mean of the treated group was 66 units/ L higher than that of the controls and at 24 h, the difference was 179.66 units/ L more than control (fig. 2.2).

Gene expression arrays:

Statistically significant changes ($p < 0.05$) in mRNA levels of numerous genes, relative to controls, were induced by treatment of RD cells with 150 μM FCCP for 10 h. Results are presented in table 2.1. In general, statistically significant transcriptional changes were observed in genes associated with redox control, stress, cell cycle, DNA damage and replication, apoptosis, uncoupling of oxidative phosphorylation, energy metabolism and inflammation.

RT-PCR for oxidative stress:

RT-PCR platform was used to quantitate the mRNA expression changes for the 7 genes on the oxidative stress plate, after exposure to 150 μM FCCP for 10 h. The changes in gene expression ($p < 0.01$) were indicative of oxidative stress. The (fold expression) changes were as follows: CYP1A1 (-1.7), TOP2A (-7.1), HO1 (17.9), CDKN1 (3.4), GCLM (4.9), GR (1.4), and TXNR (4.6). Six of the 7 genes on the oxidative stress plate were also available on the microarray platform and a comparison was made between expression patterns on the two platforms. Direction and magnitude of the expression of transcripts of 4 genes (TOP2A, HO1, CDKN1, GR and TXNR) were similar on both platforms. The expression of GR was similar in direction. CYP1A1, however, was not statistically significant on either platform (fig. 2.3).

The FCCP time course study followed the expression of the 7 oxidative stress genes for 9 time points over a 24 h period. A pattern of oxidative stress started to emerge as early as 4 h and was clearly evident by 8 h. TOP2 and HO1 proved to be good indicators of oxidative stress as they had the highest fold changes across time points and were apparent by 2 h (fig. 2.4). The dose response study followed the expression of the same 7 genes at 7 exposure concentrations, from 0.1 μM to 150 μM FCCP at 10 h. The pattern of oxidative stress was detectable starting at 50 μM and was clearly evident at 100 and 150 μM concentrations (fig. 2.5).

GSH and GSSG:

FCCP significantly altered intracellular GSH and GSSG status (fig. 2.6) relative to time-matched controls. At 10 h, there was a statistically significant ($p < 0.01$) decrease in GSH levels of 64% for 50 uM and 71% for 100 and 150 uM concentrations. There was a significant increase ($p < 0.01$ or $p < 0.05$) in GSSG of 154%, 217% and 279% along with a concomitant decrease in the GSH: GSSG ratio of 35, 20 and 15 for the 50, 100 and 150 μM groups, respectively.

Superoxide:

Superoxide radical generation was significantly increased ($p < 0.01$) with FCCP treatment at 1 h. The increases were 170%, 161% and 160% of control for each of the groups treated with 50, 100 and 150 μM FCCP, respectively (fig. 2.7).

Lipid peroxidation:

The oxidation of unsaturated lipids in cell membranes showed a dose related increase at 4 h after treatment with 50 to 150 µM FCCP (fig. 2.8). There was approximately 20, 35 and 44% increase in lipid peroxidation relative to controls, corresponding to 50, 100 and 150 µM FCCP, respectively.

Apoptosis and necrosis:

Percentage of apoptotic and necrotic cells were measured 4 h after treatment with 50 to 150 µM FCCP. Apoptosis, as measured by annexin V positivity, increased 1.9 to 2.7 folds over the control, with the 50 µM group showing the highest percentage of apoptotic cells ($p < 0.05$). Necrosis, as measured by annexin V + PI positivity, was more marked and showed a dose dependant, statistically significant ($p < 0.01$ and $p < 0.05$) increase of 2.9 to 6.2 fold over the controls (fig. 2.9).

ATP assay:

Treatment of RD cells with 50, 100 and 150 µM FCCP was associated with statistically significant ($p < 0.01$) decreases of 64, 74 and 78%, respectively, in ATP levels at 10 h (fig. 2.10).

RT-PCR for mechanistically important genes:

RT-PCR analysis of mRNA expression of 7 genes selected from the microarray data to represent pathways that were found to be modulated at 10 h post treatment with 150

μM FCCP. Some of these genes are previously known to be affected by oxidative stress but others are not. Genes known to be associated with oxidative stress are janus kinase 1 (JAK1), cadherin 2 (CAD2), relA proto-oncogene (RELA) [Associated with NFκB], protein kinase C alpha polypeptide (PKCA) and voltage-dependent anion channel 3 (VDAC3). Genes that have not been associated with oxidative stress are Alzheimer's disease amyloid A4 protein (ALZA) and peroxisome proliferator-activated receptor alpha (PPARα). The RT-PCR results were then compared with the microarray results. Five out of 7 genes were in agreement with the microarray result, both in magnitude and direction. The observed (fold changes) were CAD2 (1.2), RELA (1.2), PKCA (3.1), PPARα (2.1) and VDAC3 (3.9). The expression of the above genes, except PPARα were statistically significant ($p < 0.01$ or $p < 0.05$). The two other genes, ALZA and JAK1, were however, not statistically significant (fig. 2.11).

DISCUSSION

The potential for developing chemical uncouplers for therapeutic use as anti-obesity drugs is well recognized, but reports on toxic effects of such compounds other than uncoupling of oxidative phosphorylation, is scant. The present study was undertaken in an attempt to fill such a void. Toxic concentrations of FCCP were used in-vitro with RD cells to elicit gene expression responses that were measured using cDNA based microarray technology. The expression profile was then screened to identify potentially toxic pathways, and patterns consistent with oxidative stress were identified.

It has been previously established that the expressions of a number of genes/ proteins are modulated by oxidative stress. Most notable are heat shock proteins; growth arrest and DNA damage inducible genes such as GADD45, GADD153; HO; cellular protooncogenes including c-fos, c-myc and c-jun; inflammatory mediators such as IL8; and antioxidant enzymes including superoxide dismutase (SOD) and catalase; GSH; GR; glutathione peroxidase and TXNR (Crawford et al., 2000; Morgan et al., 2002).

The list of genes modulated in the present study includes the genes mentioned above and other genes involved in antioxidant enzyme systems, transcriptional regulation, DNA damage, DNA replication, stress response, signal transduction, inflammation, apoptosis, electron transport, ion channels, cell adhesion, uncoupling and others. Because oxidants damage DNA, trigger signal transduction pathways and inflammatory responses, and induce pro-oxidant state, modulation of the expression of genes involved in such pathways is understandable. However, the induction of expression of some genes, like HO, is not so obvious. HO is a key enzyme in heme catabolism and its induction is a protective response against oxidative stress, detoxifying the pro-oxidant heme, leading to the production of the antioxidants biliverdin and bilirubin. HO-1, the inducible isozyme of HO, is induced not only by its substrate heme, but also by various other stimuli like hypoxia (Ogawa, 2002).

Oxidant responsive elements have been identified for several genes that are modulated by oxidative stress. These include c-fos, c-jun, HO and glutathione S-transferase (Crawford et al., 2000). Transcripts for the above genes were significantly modulated in this study. The presence of an AP-1 site in the promoter region of HO-1

suggests that induction of c-fos and c-jun mRNA and their respective protein products during oxidative stress contributes to the transcriptional induction of HO-1.

Cytosolic SOD is involved with the detoxification of superoxide anion radical, converting it into H_2O_2 and subsequently into H_2O by the glutathione redox cycle. Up-regulation of transcripts for cytoplasmic SOD was supported by biochemical assay demonstrating the increase in intracellular superoxide radical. During redox imbalance, ROS are reduced by GSH in a reaction catalyzed by glutathione peroxidase. This reaction generates GSSG (glutathione disulfide) which is then reduced by GR, consuming NADPH. In the current study, GR was 1.92 fold upregulated ($p < 0.0001$). This is an important indicator of oxidative stress and was subsequently confirmed by biochemical assays demonstrating depletion of GSH (fig. 2.6).

Transcriptional upregulation of TXNR and glutaredoxin are important observations and are considered to be indicators of oxidative stress. The former enzyme is involved with the reduction of another redox enzyme, thioredoxin. Thioredoxin and related molecules like glutaredoxin are small ubiquitous proteins that function as endogenous reductants and have cytoprotective function (Klassen, 2001).

Up-regulation of mRNA for RelA [a DNA binding subunit of NF-Kappa B (NF-$_K$B)] observed in this study, and supported by RT-PCR (fig. 2.11), is also interpreted as oxidative stress responses. Transcription factor NF-$_K$B has been recognized as a central regulator of inflammatory genes and is activated not only by the pro-inflammatory cytokines, but also by oxidative stress (Rahman, 2002). NF-$_K$B is known to bind to the regulatory DNA elements of pro-inflammatory genes (Christma et al. (2000) and a number of inflammatory mediators such as IL4, IL6, IL11, MIP2α and TGFβ were

transcriptionally up-regulated in this study, perhaps acting as an early signal for recruitment of inflammatory cells to the site of insult. Although a number of oxidants are known to activate NF-$_\kappa$B, it is not known whether these stimuli feed into cytokine induced signaling pathways of NF-$_\kappa$B activation or if there are pathways that directly activate NF-$_\kappa$B or indirectly activate through inhibitory effect on I-Kappa B (I-$_\kappa$B).

Modulation of mRNA levels of ion channels like VDAC3 (supported by RT-PCR – fig. 2.11) and others in the current study can be explained as follows. Many ion channels possess thiol-containing residues that are susceptible to oxidation. By virtue of their strategic location in a channel protein, such residues may influence the function of a channel greatly, including its ionic conductance and gating characteristics (Kourie, 1998). Thus, altering the channel activity based on the redox status of the cell depends on whether the changes in secondary structure of the protein due to oxidation holds the channel in an open or closed position.

Up-regulation of PKC mRNAs, and supported by RT-PCR (fig. 2.11), indicates involvement of Ca^{2+} signaling in response to oxidative stress. Activation of mitogen activated protein (MAP) kinase pathways as a response to cytokines or other inflammatory stimuli is evidenced by the up-regulation of mRNAs for several MAP kinases including p38 and JNK-1. MAP kinase p38 and JNK are responsive to oxidative stress and play an important role in oxidative stress induced apoptosis. Similar results were obtained by Garcia-Fernandez et al. (2002), in response to treatment with an oxidative stress inducing compound, Aplidin.

Up-regulation of transcripts for TNFα induced protein and caspases 8,7 and 3 in the current study point to the association between oxidative stress and apoptosis/ necrosis.

Experimental evidence in literature suggests that ROS are common mediators in several apoptosis signalling pathways (Chau et al., 1998). TNFα released in an inflammatory environment will transiently activate neutrophils and macrophages to release superoxide by activation of the plasma membrane NADPH oxidase, causing death of the invading organisms from lipid peroxidation and alterations of proteins and nucleic acids (Shalaby et al., 1985). Further, caspase 8 mediated apoptosis through TNFα signaling is well-recognized (Granville et al., 1998). Biochemical assays for cell death showed significant increase in necrosis and apoptosis upon treatment with FCCP, confirming the gene expression data (fig. 2.9).

Modulation of several cell adhesion molecules, such as CAD2 (supported by RT-PCR – fig. 2.11) and others, is proposed to be mediated through chemically induced oxidative stress (Sen et al., 2001). Cell adhesion molecules play a major role in inflammatory and immune functions (Cotran et al., 1999). Several stimuli such as cytokines, chemokines, oxidants and antioxidants have been shown to influence the expression of adhesion molecules (Sen et al., 2001).

Modulation of many other stress associated transcripts were observed and included the upregulation of GADD153, GADD45, DNA ligases, caspases and p21, suggesting that there was DNA damage, apoptosis and cell cycle arrest. Down-regulated genes include Proliferating cyclic nuclear antigen (PCNA), Poly (ADP-ribose) polymeraes (PARP), several cyclins, TOP2A and DNA polymerase, and this can be attributed to oxidative stress leading to DNA damage, suppressed DNA replication and cell cycle arrest (Gille et al., 1995).

Depletion of ATP subsequent to FCCP treatment, as demonstrated by

Bioluminescent assay using firefly luciferase (fig. 2.10), is attributed to loss of

mitochondrial membrane potential and its effect on energy metabolism.

Microarray gene expression platforms are relatively new technology and as such the

results could not be accepted without being supported by more conventional techniques.

Therefore, selected genes at 10 h were quantitated with RT-PCR, using the 7-gene plate

for oxidative stress, described by Morgan et al. (2002) and a comparison was made with

the array results. There was good agreement between RT-PCR and array results (fig. 2.3).

Similar RT-PCR results were obtained by Morgan et al. (2002) and Merrill et al. (2002).

A time course experiment over a 24 h period (fig. 2.4) and a dose response experiment

(fig. 2.5) were conducted to follow the expression of the genes on the 7-gene oxidative

stress plate, using RT-PCR. It was determined that FCCP-induced oxidative stress was

transcriptionally expressed from 4 to 24 h, at a concentration of 50 to 150 μM. Since

transcriptional alterations do not necessarily translate into biochemical events, relevant

biochemical assays were performed to demonstrate GSH depletion (fig. 2.6), super oxide

production (fig. 2.7), and lipid peroxidation (fig. 2.8), in addition to morphological

evaluations (fig. 2.1), to support the microarray data.

The current study demonstrates FCCP-induced oxidative stress in RD cell line.

Oxidative stress was first identified by analysis of cDNA based gene expression data and

then confirmed on a limited set of genes by RT-PCR. Multiple morphologic and

biochemical oxidative stress assays confirmed the conclusions drawn from gene

expression data. This is the first report of oxidative stress consequent to FCCP treatment.

It is also concluded that gene expression profiling can be used as a method to screen

compounds for oxidative stress and potentially for identifying other mechanisms of toxicity. The data generated suggests that gene expression profiles can provide reliable information about transcriptionally controlled modulations of biochemical processes in biological systems.

ACKNOWLEDGEMENTS

REFERENCES

Aoki, T., Suzuki, Y., Miyata, A., Oyamada, Y., Takasugi, T., Mori, M., Fujita, H., and Yamaguchi, K. (1996). Modulation of ICM-I expression by extracellular glutathione in hyperoxia-exposed human pulmonary artery endothelial cell. *Am. J. Respir. Cell. Mol. Biol.* **15**, 319-327.

Cadens, E., Boveris, A., Ragan, C.I., and Stoppani, A.O.M. (1977). Production of superoxide radicals and hydrogen peroxide by NADH-ubiquinone reductase and ubiquinol-cytochrome c reductase from beef-heart mitochondria. *Arch. Biochem. Biophys.* **180**, 248-257.

Carter, O.W., Narayanan, P.K., and Robinson, P. (1994). Intracellular hydrogen peroxide and superoxide anion detection in endothelial cells. *J. Leukoc. Biol.* **55**, 253-258.

Chau, Y.P., Shiah, S.G., Don, M.J., and Kuo, M.L. (1998). Involvement of hydrogen peroxide in topoisomerase inhibitor beta-lapachone-induced apoptosis and differentiation in human leukemia cells. *Free Radic. Biol. Med.* **24**, 660-670.

Christman, J.W., Blackwell, T.S., and Juurlink, B.H. (2000). Redox regulation of nuclear factor kappa B: therapeutic potential for attenuating inflammatory responses. *Brain Pathol.* **10**, 153-162.

Cotran, R.S., Kumar, V., and Collins, T. (1999). *Robbins Pathologic Basis of Disease.* W.B. Saunders Co., Philadelphia, PA.

Crawford, D.R., Suzuki, T., and Davies, K. (2000). Redox regulation of gene expression. *Antioxidant and Redox Regulation of Genes.* Academic Press, San Diego. 21-45

Del Mar, G. M., Ricquier, D., and Cassard-Doulcie, A.M. (2000). The human uncoupling protein-1 gene (UCP1): present status and perspectives in obesity research. *Obes. Rev.* **1,** 61-72

Fridovich, I. (1975) Oxygen: Boon and bane. *Am. Scientist* **63,** 54-59.

Fridovich, I. (1978). The biology of oxygen radicals. *Science* **201**, 875-80.

Garcia-Fernandez, L.F., Losada, A., Alcaide, V., Alvarez, A.M., Cuadrado, A., Gonzalez, L., Nakayama, K., Nakayakama, K.I., Fernandez-Sousa, J.M., Munoz, A., and Sanchez-Puelles, J.M. (2002). Aplidin induces the mitochondrial apoptotic pathway via oxidative stress-mediated JNK and p38 activation and protein kinase C delta. *Oncogene.* **21**, 7533-7544.

Gille, G., and Sigler, K. (1995). Oxidative stress and living cells. *Folia Microbiol.* **40**, 131-152.

Granville, D.J., Carthy, C.M., Hunt, W.C, and McManus, B.M. (1998). Apoptosis: Molecular aspects of cell death and disease. *Lab. Invest.* **78**, 893-913.

Hagen, T., Vidal-Puig, A. (2002). Mitochondrial uncoupling proteins in human physiology and disease. *Minerva Med..* **93,** 41-57.

Hampton, M.B., and Orrenius, S. (1997). Dual regulation of caspase activity by hydrogen peroxide: Implication of apoptosis. *FEBS Lett.* **414**, 552-556.

Janssen, Y.M.W., Van Houten, B., Borm, P.J.A., and Mossman, B.T. (1993). Cell and tissue responses to oxidative damage. *Lab. Invest.* **69**, 261-74.

Karamohamed, S., Nordstrom, T. and Nyren, P., (1999). Real-time bioluminometric method for detection of nucleoside diphosphate kinase activity. *Biotechniques.* **26,** 728-734.

Kepler, T.B., Crossby, L., Morgan, K.T. (2002). Normalization and analysis of DNA microarray data by self-consistency and local regression. *Genome biol.* **3**, 1-12.

Klassen, C.D. (2001). Casarett & Doull's Toxicology, *The Basic Science of Poisons*. McGraw-Hill, New York. 65.

Korshunov, S.S., Skulachev, V.P., Starkov, A.A. (1997). High protonic potential actuates a mechanism of production of reactive oxygen species in mitochondria. *FEBS Lett.* **416**, 15-18.

Kourie, J.I. (1998). Interaction of reactive oxygen species with ion transport mechanism. *Am. J. Physiol.* **275**, C1-C24.

Liu, S.S. (1997). Generating, partitioning, targeting and functioning of superoxide in mitochondria. *Biosci. Rep.* **17**, 259-72.

Makrigiorgos, G.M., Kassis, A.I., Mahmood, A., Bump, E. and Savvides, P. (1997). Novel fluorescein-based flow cytometric method for detection of lipid peroxidation. *Free Radic. Biol. Med.* **22**, 93-100.

Marshall, N.J., Goodwin, C.J. and Holt, S.J. (1995). A critical assessment of the use of microculture tetrazolium assays to measure cell growth and function. *Growth Regulation.* **5**, 69-84.

Martin, J., and White, I.N.H. (1991). Fluorimetric determination of oxidised and reduced glutathione in cells and tissues by high-performance liquid chromatography following derivatization with dansyl chloride. *J. Chromatogr.* **568**, 219-24.

Merrill. C.L., Ni, H., Yoon, L., Tirmenstein, M.A., Narayanan, P., Benavides, G.R., Easton, M.J., Creech, D.R., Hu, C.X., McFarland, D.C., Hahn, L., Thomas, H.C., and Morgan, K.T. (2002). Etomoxir-induced oxidative stress in HepG2 cells detected by differential gene expression is confirmed biochemically. *Toxicol. Sci.* **68**, 93-101.

Morgan, K.T., NI, H., Brown, R.H., Yoon, L., Qualls, C.W., Crossby, L.M., Reynolds, R., Gaskil, B., Anderson, P.S., Kepler, T.B., Brainard, T., Liv, N., Easton, M.J., Merrill, C.L., Creech, D.R., Sprenger, D., Cooner, G., Johnson, P., Fox, T., Stator, M., Richard, E., Kuruvilla, S., Casey, W., and Benavides, G.R. (2002). Application of cDNA microarray technology to in vitro toxicology and the selection of genes for a real-time RT-PCR-based screen for oxidative stress in hep-G2 cells. *Toxicol. Pathol.* **30**, 435-451.

Ogawa, K. (2002). Heme metabolism in stress response. *Jpn. J. Hygiene.* **56**, 615-621.

Rahman, I. (2002). Oxidative stress, transcription factors and chromatin remodelling in lung inflammation. *Biochem. Pharmacol.* **64**, 935-942.

Rothe, G., and Valet, G. (1990). Flow cytometric analysis of respiratory burst activity in phagocytes with hydroethidine and 2', 7'-Dichlorofluorescin. *J. Leukoc. Biol.* **47**, 440-448.

Sachi, Y., Hirota, K., Masutani, H., toda, K., Okamoto, T., Takigawa, M., and Yodoi, J. (1995). Induction of ADF/TRX by oxidative stress in keratinocytes and lymphoid cells. *Immunol. Lett.* **44**, 189-193.

Scandalios, J.G. (1997). *Oxidative Stress and the Molecular Biology of Antioxidant Defenses.* Cold Spring Harbor Monograph Series, Cold Spring Harbor press, New York.

Sen, C.K., and Roy, S. (2001). Antioxidant regulation of cell adhesion. *Med. Sci. Sports Exerc.* **33**, 377-381.

Shalaby, M.R., Aggarwal, B.B., Rinderknecht, E., Svedersky, L.P., Finkle, B.S., and Palladino, M.A. (1985). Activation of human polymorphonuclear neutrophil functions by interferon- and tumor necrosis factor. *J. Immunol.* **135**, 2069-2073.

Skulachev, V.P. (1998). Uncoupling: new approaches to an old problem of bioenergetics. *Biochim. Biophy. Acta* **1363**, 100-124.

Trump, B.F., Berezesky, I.K., Chang, S.H., and Phelps, P.C. (1997). The pathways of cell death: oncosis, apoptosis, and necrosis. *Toxicol. Pathol.* **25**, 82-88.

Turrens, J.F., and Boveris A. (1980). Generation of superoxide anion by the NADH dehydrogenase of bovine heart mitochondria. *Biochem. J.* **191**, 421-427.

Turrens, J.F., Alexandre, A., Lehninger, A.L. (1985). Ubisemiquinone is the electron donor for superoxide formation by complex III of heart mitochondria. *Arch. Biochem. Biophys.* **237**, 408-414.

Vermes, I., Haanen, C., Steffens-Nakken, H., and Reutelingsperger, C. (1995). A novel assay for apoptosis flow cytometric detection of phosphatidylserine expression on early apoptotic cells using fluorescein labelled annexin V. *J. Immunol. Methods* **184**, 39-51.

Table 1:

Differential gene expression profile. NLR output for Clontech Atlas™ human 1.2-1, 1.2-3, 1.2-toxicology and Toxicology II microarrays, showing important genes that have changed significantly ($p \leq 0.05$), at 10 h post FCCP treatment. In column 2, '1' denotes down-regulation and '2' denotes up-regulation. 'Fold changes' represents the ratio treated/ control. 'MLI' is mean log intensity. Genes included on the oxidative stress plate (fig. 2.3) are bold faced and italicized. Genes selected as mechanistically important (fig. 2.11) are non-bold faced italicized.

Gene	1=down 2=up	Ratio	MLI	p-value
<u>Toxicological</u>				
thioredoxin reductase (TXNR)	2	4.85	0.569	8.69E-31
glutathione S-transferase mu 4 (GSTM4)	1	3.07	-0.454	2.83E-12
glutathione reductase (GSR, GR)	2	1.92	1.32	9.76E-07
peroxisome proliferative-activated receptor alpha (PPAR-alpha)	2	1.83	-0.973	5.57E-04
glutathione S-transferase alpha 4 (GSTA4)	1	1.66	-0.23	9.17E-04
catalase (CAT)	1	1.77	-1.05	1.33E-03
glutathione peroxidase 1 (GSHPX1)	1	1.42	1.5	7.56E-03
cytochrome P450 IVA11 (CYP4A2)	1	2.27	-2.4	4.21E-02
cytochrome P450 IA2 (CYP1A2)	2	1.54	-1.39	4.52E-02
heme oxygenase 1 (HO1)	2	19.7	0.702	1.30E-47
thioredoxin peroxidase 2 (TDPX2)	1	1.58	2.29	7.13E-04
glutaredoxin	2	1.83	1.11	1.10E-04
heme oxygenase 2 (HO2)	2	3.01	-0.559	5.70E-03
endothelial nitric oxide synthase (EC-NOS)	2	2.77	0.937	1.03E-14
cytosolic superoxide dismutase 1 (SOD1)	2	1.33	2.77	3.49E-02
cytochrome P450 IA1 (CYP1A1)	2	1.2	-2.89	0.686
<u>Stress related</u>				
90-kDa heat-shock protein A (HSP90A)	2	2.46	4.4	1.63E-10
mitochondrial heat shock 10-kDa protein (HSP100)	2	1.44	2.45	5.88E-03
40-kDa heat shock protein 1 (HSP40)	2	1.41	1.34	8.87E-03
70-kDa heat shock protein 1 (HSP70.1)	2	13	1.3	1.14E-60
27-kDa heat-shock protein (HSP27)	2	2.95	4.68	7.33E-12
110-kDa heat-shock protein (HSP110)	2	2.11	2.07	1.93E-02
Janus kinase 1 (JAK1)	2	2.12	0.559	2.52E-04
STAT-induced STAT inhibitor 2	2	2.47	1.2	1.24E-11
signal transducer and activator of transcription 2 (STAT2)	2	1.46	0.935	2.77E-02

Gene	1=down 2=up	Ratio	MLI	p-value
relA proto-oncogene (RELA)	2	2.01	0.0497	2.07E-06
Alzheimer's disease amyloid A4 protein (ALZA)	2	1.5	3.35	2.68E-03
peroxisome proliferative-activated receptor alpha (PPARA)	2	1.83	-0.973	5.57E-04
amyloid-like protein 2	2	1.36	1.81	2.25E-02
mitogen-activated protein kinase p38 (MAP kinase p38)	2	1.43	0.111	1.26E-02
DNA damage and repair				
growth arrest & DNA damage-inducible protein 45g (GADD45g)	2	6.88	1.91	4.12E-41
growth arrest & DNA damage-inducible protein 153 (GADD153)	2	6.59	2.71	1.21E-39
DNA ligase IV (LIG4)	2	2.52	-0.484	8.89E-09
DNA mismatch repair protein MSH2	1	2.06	0.802	3.00E-08
DNA mismatch repair protein MSH6	1	1.57	1.62	6.92E-04
DNA ligase III (LIG3)	1	1.74	-0.756	8.93E-04
DNA excision repair protein ERCC1	2	1.45	1.62	6.12E-03
DNA replication				
DNA polymerase delta catalytic subunit	1	1.64	0.406	2.43E-04
DNA polymerase alpha catalytic subunit (POLA)	1	1.45	1.35	5.42E-03
DNA topoisomerase I (TOP1)	2	1.42	2.07	8.80E-03
DNA topoisomerase II alpha (TOP2A)	1	4.56	2.42	5.87E-26
DNA polymerase epsilon subunit B	1	2.85	0.813	9.51E-09
poly(ADP-ribose) polymerase (PARP)	1	6.35	-0.762	3.97E-05
DNA-directed RNA polymerase II 14.5 kD polypeptide.	1	1.53	2.22	2.48E-02
replication protein A 30-kDa subunit	2	1.77	-1.72	3.75E-02
replication protein A 70-kDa subunit (RPA70)	1	2.08	1.06	2.91E-02
Cell cycle				
cyclin F (CCNF)	1	6.7	-0.969	1.18E-25
cyclin A1 (CCNA1)	2	4	-0.318	1.85E-18
cyclin H (CCNH)	2	2.92	1.49	1.91E-15
cyclin-dependent kinase inhibitor 1A (CDKN1A; p21)	2	4.95	1.36	1.07E-30
cyclin D2 (CCND2)	1	1.38	2.07	1.65E-02
cyclin D1 (CCND1)	1	1.37	0.438	1.77E-02
G1/S-specific cyclin D3 (CCND3)	1	3.05	0.112	4.06E-06
G1/S-specific cyclin D2 (CCND2)	1	1.68	1.7	1.22E-04
proliferating cyclic nuclear antigen (PCNA)	1	2.3	1.71	5.57E-10
beta catenin (CTNNB)	1	1.66	1.17	8.03E-04
Signal transduction				
mitogen-activated protein kinase kinase 3 (MAPKK3)	2	3.41	-0.384	1.22E-14

Gene	1=down 2=up	Ratio	MLI	p-value
mitogen-activated protein kinase kinase 1 (MAPKK1)	1	2.85	1.92	2.52E-14
mitogen-activated protein kinase 9 (MAPK9)	2	2.56	2.88	6.18E-12
mitogen-activated protein kinase kinase 4 (MKK4)	2	1.78	-0.854	7.67E-04
mitogen-activated protein kinase 8 (MAPK8)	2	1.81	-1	8.20E-04
mitogen-activated protein kinase 6 (MAPK6)	2	1.54	0.667	8.69E-04
mitogen-activated protein kinase 7 (MAPK7)	1	1.47	0.238	6.52E-03
mitogen-activated protein kinase kinase 5 (MAPKK5)	1	1.43	0.428	7.35E-03
mitogen-activated protein kinase 3 (MAPK3)	1	2.16	-0.081	3.47E-07
protein kinase C alpha polypeptide (PKCA)	2	3.68	0.177	4.59E-19
protein kinase C zeta type (NPKC-zeta)	2	1.94	-1.19	4.41E-04
Transcription activators				
transcription factor E2-alpha (E2A)	1	1.6	1.39	4.14E-04
PRB-binding protein E2F1; retinoblastoma-binding protein 3	1	1.98	0.954	6.15E-05
transcription factor TFIIB; GTF2B	2	1.71	1.31	1.40E-04
c-jun N-terminal kinase 2 (JNK2)	1	1.75	0.022	2.82E-02
fos-related antigen (FRA1)	2	4.71	2.6	9.99E-07
c-jun proto-oncogene; transcription factor AP1	2	7.74	2.8	6.94E-39
jun-D	2	6.27	0.25	4.79E-15
fos-related antigen 2 (FRA2)	2	12.1	-0.909	3.94E-07
c-fos proto-oncogene	2	1.77	-2.59	2.19E-02
N-myc proto-oncogene	1	2.91	-1.62	3.32E-05
c-myc oncogene	2	1.35	3.56	4.18E-02
Apoptosis				
caspase 3 (CASP3)	2	3.03	1.87	7.35E-16
p53 cellular tumor antigen	1	3.09	-0.239	4.20E-13
caspase 4 (CASP4)	2	5.58	1.25	7.27E-35
caspase 8 (CASP8)	2	2.02	0.558	9.36E-08
apoptosis regulator bcl-x	2	1.92	1.41	9.61E-07
caspase 2 (CASP2)	1	1.82	1.7	6.74E-06
caspase 7 (CASP7)	2	1.87	-1	3.85E-04
caspase-6 precursor (CASP6)	1	2.55	0.323	3.46E-05
caspase-10 precursor (CASP10)	1	1.38	3.34	3.11E-02
annexin V	2	1.91	2.67	1.49E-06
Inflammatory mediators				
transforming growth factor beta 2 (TGFB2)	2	3.65	0.963	2.70E-22
interleukin 11 (IL11)	2	4.22	-0.955	6.75E-16
interleukin 4 receptor alpha subunit (IL4R-alpha)	1	2.45	-0.131	4.81E-09
interleukin 13 (IL13)	2	1.74	0.193	9.36E-05
fas-activated serine/threonine kinase (FAST)	1	1.49	0.743	1.84E-03

Gene	1=down 2=up	Ratio	MLI	p-value
macrophage inflammatory protein 2 alpha (MIP2-alpha)	2	7.55	0.366	8.88E-19
interleukin-6 receptor alpha subunit precursor (IL6R-alpha)	2	3.73	-0.393	2.32E-04
interleukin-12 alpha subunit precursor (IL12A)	2	2.08	-1.61	6.43E-03
interleukin-11 (IL11)	2	4.91	-0.6	1.04E-04
interleukin-5 receptor alpha subunit precursor (IL5R-alpha)	2	1.86	0.853	5.11E-04
interleukin-6 receptor beta subunit precursor (IL6R-beta)	2	1.68	0.105	3.04E-02
interleukin-8 precursor (IL8)	2	2.44	0.907	3.18E-07
transforming growth factor beta (TGFB)	2	1.32	3.21	3.87E-02
tumor necrosis factor alpha-induced protein 6	2	5.01	-2.19	1.27E-05
tumor necrosis factor type 1 receptor-associated protein	1	2.65	1.08	2.06E-13
tumor necrosis factor receptor superfamily member 1B	1	1.71	1.27	5.34E-05
Uncoupling proteins				
mitochondrial uncoupling protein 3 (UCP3)	1	3.33	0.184	1.24E-16
mitochondrial uncoupling protein 2 (UCP2)	1	3.91	-1.03	4.62E-14
Ion channels				
solute carrier family 12 member 4 (SLC12A4)	2	4.11	1.38	7.40E-25
sodium/potassium-transporting ATPase beta 3 subunit (ATPB3)	2	1.84	1.2	4.02E-06
water channel aquaporin 3 (AQP3)	2	1.88	0.227	6.20E-03
sodium/glucose cotransporter 2	1	3.79	-1.13	1.79E-02
aquaporin 4	2	1.92	-0.0704	1.79E-02
voltage-gated potassium channel EAGB.	2	4.22	-3	2.77E-02
sodium & chloride-dependent glycine transporter 1 (GLYT1)	2	3.55	-1.73	3.36E-06
voltage-dependent anion channel 3 (VDAC3)	1	3.03	1.84	6.27E-16
Cell adhesion				
cadherin 2 (CDH2)	2	1.71	2.86	6.45E-05
selectin P ligand	2	1.89	-1.76	2.36E-02
E-selectin precursor; endothelial leukocyte adhesion molecule 1	1	9.2	-1.8	2.13E-03
vascular cell adhesion protein 1 precursor (VCAM 1)	1	4.29	-1.52	2.89E-02
integrin alpha 7B	2	1.33	0.959	2.56E-02
integrin beta 8 precursor	2	3.22	1.13	7.65E-14
integrin alpha 6 precursor (ITG0A6)	1	1.38	1.28	2.30E-02
integrin alpha 9 (ITGA9)	1	1.77	-0.734	3.33E-02

**Fig. 2. 1:**

Light microscopic morphology of H&E stained cells treated with 150 μM FCCP at 10 h showing cell shrinkage, loss of adhesion and rounding. Cytoplasmic basophilia and hyperchromatic neclei with occasional cytoplasmic blebbing and fragmentation are seen. There is marked decrease in cell numbers and mitotic figures, along with marked increase in apoptosis/ necrosis, relative to time matched controls.

control
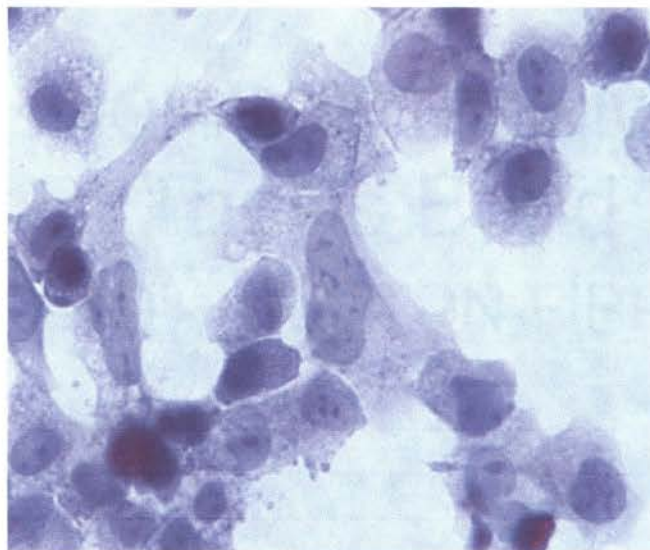
treated

Fig. 2. 2:

Time course data on LD enzyme activity in the media, as a measure of cell membrane damage with leakage of cytosolic enzymes following treatment with 150 μM FCCP. There is an increase in media LD levels in the treated group with each time point starting at 6 h, indicating increased cell injury with elapse of time.

FCCP, 150 uM. LD levels in media
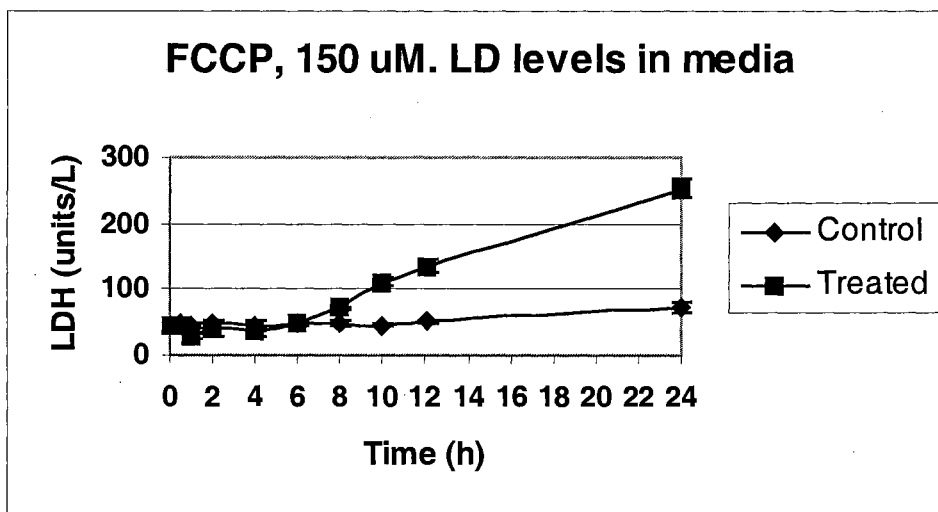
Fig. 2. 3:

RT-PCR assay of mRNA expression changes of the 7 genes on the oxidative stress plate measured as a response to treatment with 150 µM FCCP at 10 h and is compared with microarray data. Overall, there was good agreement between RT-PCR and microarray, both in magnitude and direction. Six out of seven genes were statistically significant ($p < 0.01$) and suggests FCCP-induced oxidative stress.

FCCP, 150 uM, 10 h, Oxidative stress plate
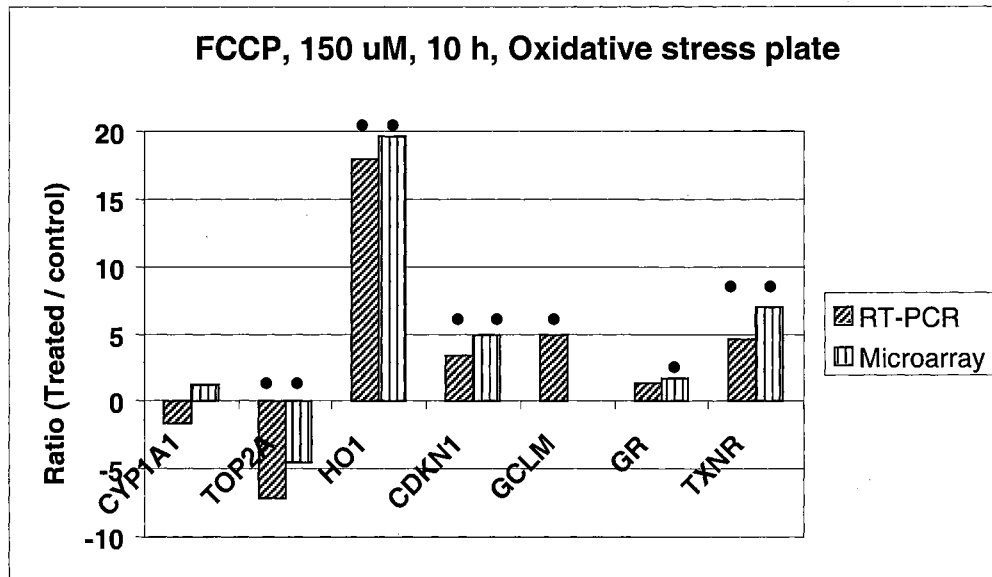
● $p < 0.01$

Fig. 2. 4:

RT-PCR time course study of transcriptional changes upon treatment with 150 μM FCCP at 10 h, using the 7 gene oxidative stress plate, over 9 time points. An oxidative stress pattern became apparent by 4 h and was clearly evident by 8 h.
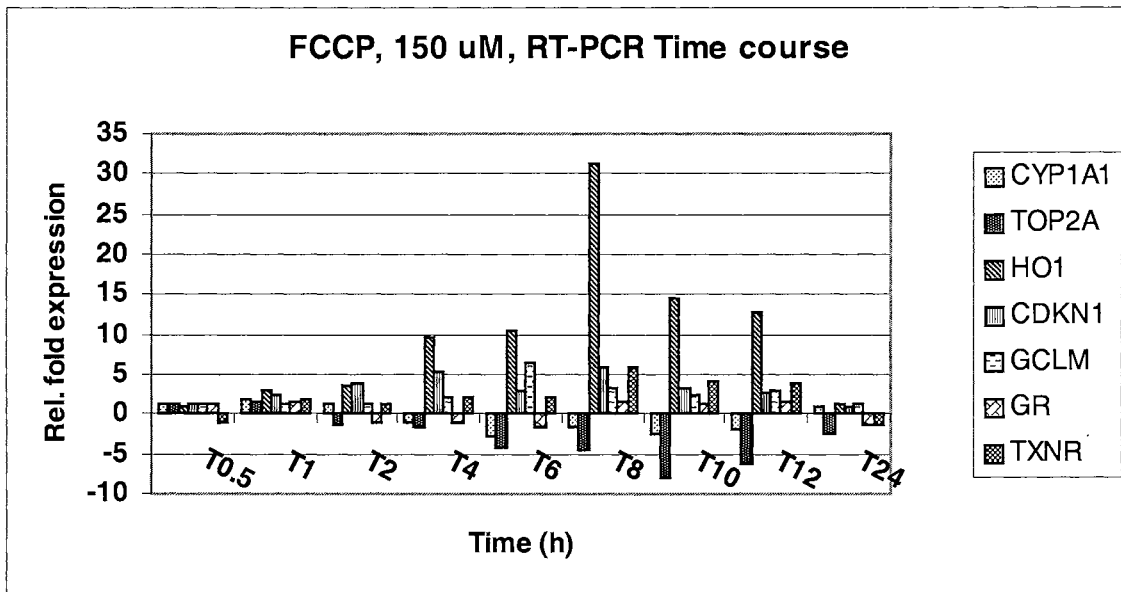
Fig. 2. 5:

RT-PCR dose response study of the expression patterns of the 7 genes on the oxidative stress plate upon treatment with 0.1 to 150 µM concentrations of FCCP for 10 h. Patterns indicative of oxidative stress were present for 50 µM and higher dose levels.

FCCP, 150 uM, 10 h, RT- PCR Dose response
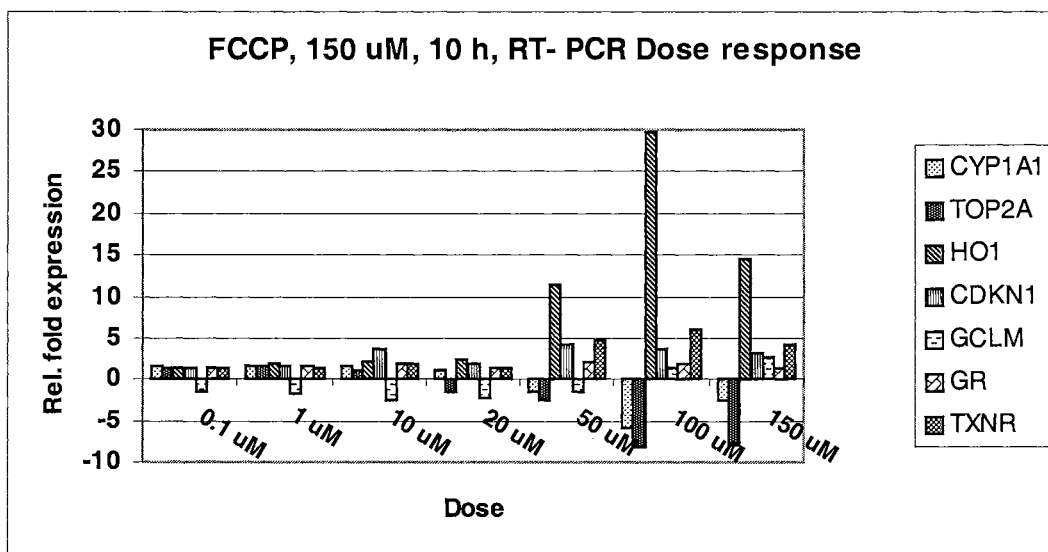
Fig. 2. 6:

Assay for levels of GSH and GSSG. There was depletion of GSH with concurrent increase of GSSG at 10 h, subsequent to treatment with 50, 100 and 150 μM FCCP, when compared with time matched controls. The GSH / GSSG ratio showed a decreasing trend with increasing dose levels. This biochemical assay confirms FCCP-induced oxidative stress and supports the gene expression analysis.
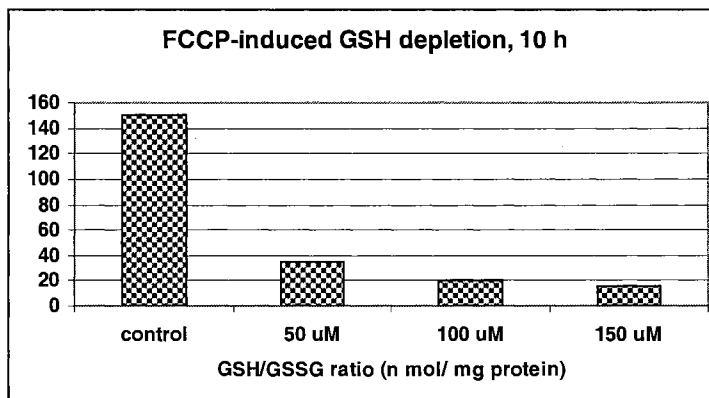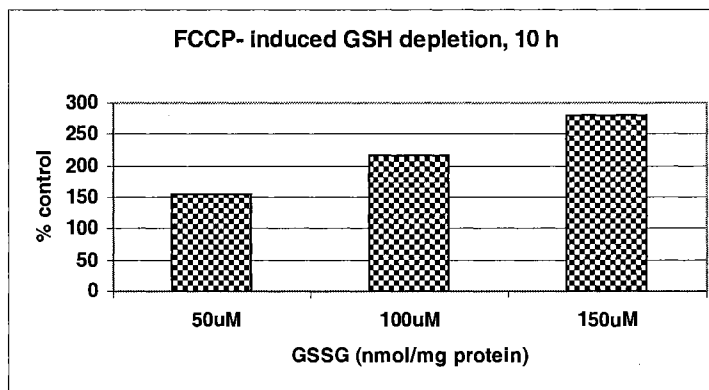

FCCP - induced GSH depletion, 10 h

• p < 0.01

FCCP- induced GSH depletion, 10 h

FCCP-induced GSH depletion, 10 h
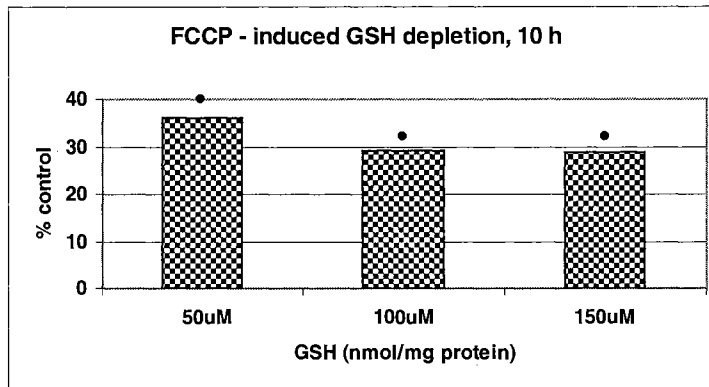
Fig. 2. 7:

Superoxide radical assay. Superoxide radical generation increased significantly ($p < 0.01$) at 1h post treatment with 50, 100 and 150 μM FCCP, relative to time matched controls. This assay suggests FCCP-induced oxidative stress and supports the gene expression analysis.
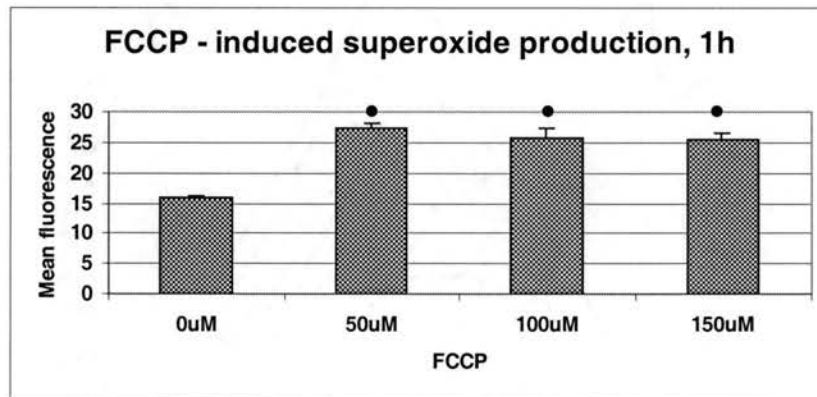
• $p < 0.01$

Fig. 2. 8:

Lipid peroxidation assay. Lipid peroxidation of cell membranes, measured as peroxyl radicals, showed a dose related increase at 4h, following treatment with 50, 100 and 150 μM FCCP and is indicative of FCCP-induced oxidative stress.
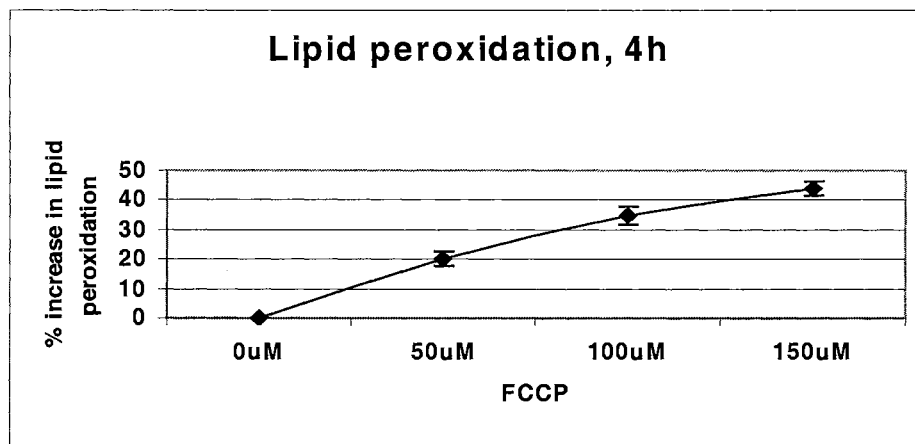
Fig. 2. 9:

Apoptosis and necrosis assay. Apoptotic cell population, measured by annexin V binding and necrotic cell population, measured by annexin V and PI positivity were determined by flow cytometry 4 h post treatment with 50 to 150 μM FCCP. There was significant (p < 0.01 and p < 0.05) increase in apoptotic and necrotic cell population with treatment. At 100 and 150 μM concentrations, the necrotic cell population was significantly higher than the apoptotic cells.

Apoptosis and necrosis, FCCP, 4 h
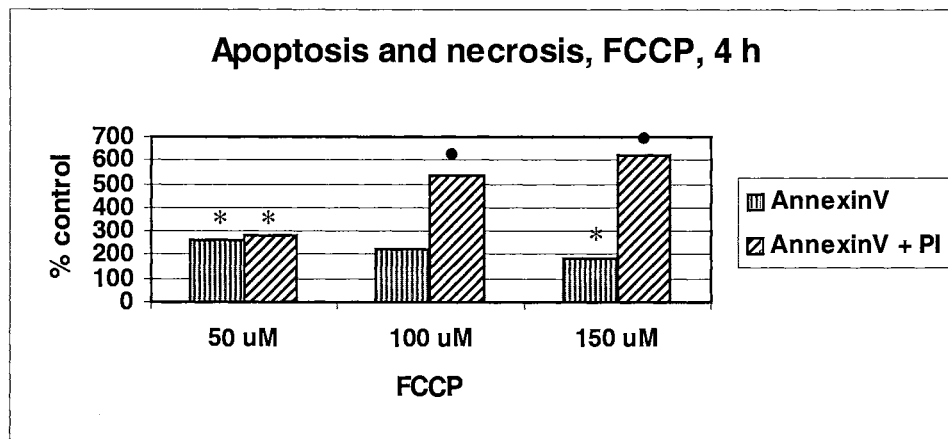
* p < 0.05   • p < 0.01

Fig. 2. 10:

ATP assay showing significant (p< 0.01) reduction of ATP levels at 10 h following treatment with 50, 100 and 150 μM FCCP, relative to time matched controls and expressed as percentage of control.

FCCP-induced ATP reduction, 10 h
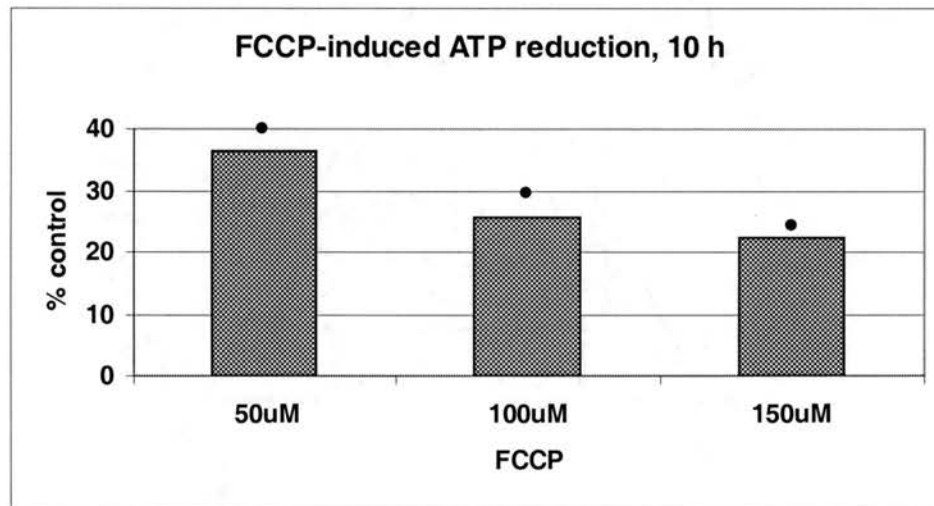
• p < 0.01

Fig. 2. 11:

RT-PCR analysis of expression of mechanistically important genes that may be associated with oxidative stress, selected from among genes in the microarray whose expressions were altered in response to treatment with 150 μM FCCP at 10 h. Microarray results are compared with RT-PCR. Five out of 7 genes were in good agreement, both in direction and magnitude, with microarray data. Two genes however, ALZA and JAK1, were statistically not significant. Expression of all 7 genes on the microarray and 5 genes on RT-PCR showed statistical significance ($p < 0.01$ and $p < 0.05$).

*$p < 0.05$ •$p < 0.01$
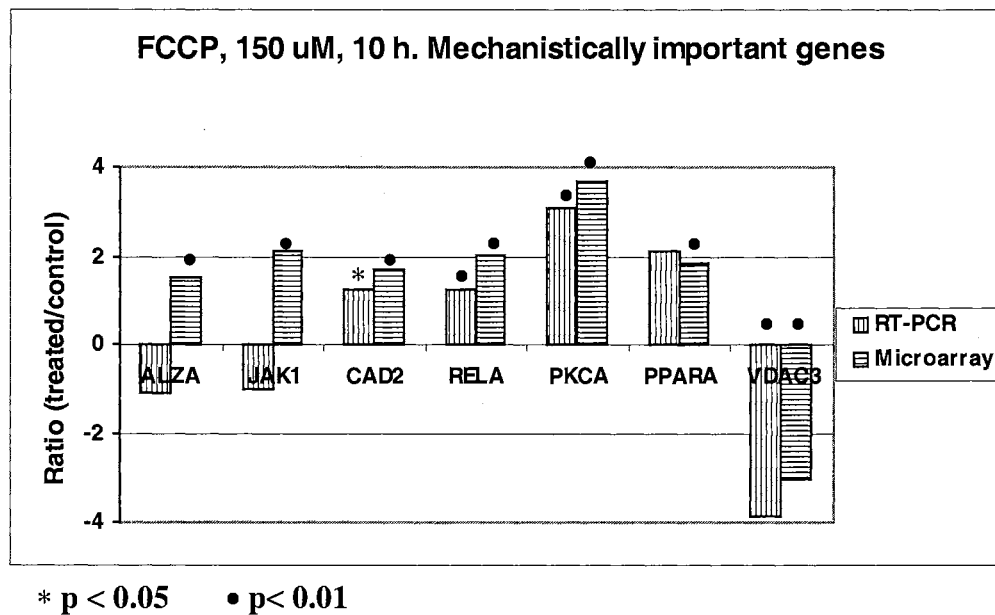
CHAPTER 4

THESIS SUMMARY

Oxidative phosphorylation (ATP synthesis driven by electron transfer to oxygen) is the culmination of energy metabolism in aerobic organisms. All the enzymatic steps in oxidative degradation of carbohydrates, fat and protein in aerobic cells converge at this final stage of cellular respiration, in which electrons flow from catabolic intermediates to dioxygen (O_2), yielding energy for generation of ATP from ADP and inorganic phosphate (Pi). Oxidative phosphorylation occurs in mitochondria and involves the reduction of O_2 to H_2O with electrons donated by NADH and $FADH_2$. The energy to drive phosphorylation of ADP is supplied by the sequential oxidation-reduction chain reaction in the electron transporting system. The transfer of electrons along the respiratory chain is accompanied by outward pumping of protons across the inner mitochondrial membrane, which results in transmembrane differences in proton concentration (gradient). The proton-motive force is subsequently used to drive the synthesis of ATP as proton flow passively back into the matrix through proton pores formed by ATP synthase. Thus, ATP is synthesized by coupling two reactions, electron transport and phosphorylation.

Synthetic compounds called uncoupling agents (uncouplers) inhibit ATP synthesis by preventing this coupling reaction. It has been known that uncoupling agents stimulate

oxidation of substrate in the absence of ADP. In the presence of an uncoupler, respiration proceeds until virtually all of the available oxygen is reduced and rapid oxidation of substrate proceeds with little or no phosphorylation of ADP. In other words, these compounds uncouple oxidation from phosphorylation. A large number of uncouplers have been discovered. Most uncouplers are lipid soluble weak acids and can cross the inner mitochondrial membrane, as both protonated and conjugate-base forms, ablating the membrane potential. Uncouplers have relevance to energy metabolism and obesity. The effects of chemical uncouplers on obesity have been known since the early 1900's. However, such compounds have not successfully been developed as therapeutic agents for intervention of clinical obesity; an important being a lack of complete understanding of the effects of such compounds on various biochemical circuitries.

The present studies represent an attempt to understand the mechanisms of action of protonophoric uncouplers at supra pharmacological doses, on biological systems, using carbonyl cyanide p- (trifluoromethoxy) phenylhydrazone [FCCP], a lipophilic weak acid uncoupler. Both conventional and newer tools in molecular biology and toxicology were used to detect various modes of toxicity. cDNA microarray technology was used to examine chemically induced alterations in gene expression in a rhabdomyosarcoma cell line. Since large-scale differential gene expression (DGE) is an evolving technology, the results were interpreted with caution, and whenever possible, other more conventional assays were performed to support microarray data. Selected genes were analyzed using real-time quantitative RT-PCR, and functional biochemical assays were performed to confirm alterations in biochemical pathways, whenever suggested by gene expression data. Overall, the results of the study suggested that large-scale analysis of gene

expression using cDNA microarrays promise the rapid detection of toxicity for drugs and other chemicals.

In the first phase of the research, the effects of minimally toxic levels of FCCP were evaluated using DGE, combined with biochemical and morphological correlation. Changes in mitochondrial membrane potential upon exposure to the compound were used as the biological dosimeter to determine the appropriate exposure concentration for the study. The cells were exposed to 100 nM – 64 μM FCCP and mitochondrial membrane potential was measured using the J-aggregate-forming, lipophilic, cationic probe, 5,5′, 6,6′-tetrachloro-1, 1', 3,3'- tetraethylbenzimidazolylcarbocyanine iodide (JC-1), with FACScan flow cytometer. There was a positive correlation between exposure concentration and membrane depolarization. The response to treatment was linear up to 2 μM and plateaued at around 32 μM. At 20 μM FCCP, there was approximately 80% depolarization and this concentration was chosen to study gene expression changes. Cytological examination of hematoxylin and eosin (H&E) stained cells exposed to the compound at the above concentration revealed arrested proliferation and minimal morphological changes. There was a 100% and 55% decrease in mitotic figures and cell counts, respectively at 24 h compared to time matched controls. At the above concentration, clear gene expression changes were observed at 1, 2 and 10 hours. The overall sequence of molecular events observed were reminiscent of ischemic (hypoxic) cell injury and this is consistent with the expected effect of chemical uncouplers on biological systems, as they essentially neutralize the physiological role of oxygen. In living organisms, the first point of hypoxia is the cell's aerobic respiration, that is, mitochondrial oxidative phosphorylation. As the oxygen tension decreases there is loss of

oxidative phosphorylation and decreased generation of ATP, resulting in widespread effects on many systems initially including decreased activity of plasma membrane sodium pump, alteration of energy metabolism by switching from oxidative phosphorylation to glycolysis with increased lactic acid production, structural disruption of protein synthesis apparatus resulting in reduced protein synthesis and disruption of cytoskeleton, leading to morphological deterioration. In the present study, upon FCCP treatment there was an immediate decrease in mitochondrial membrane potential and cellular ATP concentration. This was followed by down-regulation of protein synthesis transcripts; up-regulation of DNA damage induced transcripts; activation of stress related transcripts; G_1 arrest, presumed to be mediated through p21, p16, β-catenen and N-myc; S phase arrest, presumed to be mediated through PCNA; and apoptosis presumed to be mediated through Fas. Statistically significant transcriptional changes observed on gene expression platforms were largely associated with protein synthesis, cell cycle regulation, cytokeletal proteins, energy metabolism, apoptosis and inflammatory mediators. Bromodeoxyuridine (BrdU) and Propidium Iodide (PI) time course assay revealed cell cycle arrest to occur in the G_1 and S phases as early as 10 h. A very small but statistically significant population of cells underwent apoptosis/ necrosis at 24 h. The shift in energy metabolism from the oxidative to the anaerobic pathway, was demonstrated by media glucose and lactate assays. There was a time dependant and statistically significant (p < 0.01) decrease in media glucose and increase in media lactate across time points, following treatment. ATP concentrations were measured at the varying concentrations of FCCP referred to above, using a bioluminescent somatic cell assay kit. There was a significant decrease in the intracellular ATP concentrations starting as early as 15 min,

with a 19 and 40% decrease at 15 and 30 min respectively. The following seven genes were selected as potential molecular markers for uncouplers - seryl-tRNA synthetase, glutamine-hydrolyzing asparagine synthetase, mitochondrial bifunctional methylenetetrahydrofolate dehydrogenase, mitochondrial heat shock 10-kDa protein, proliferating cell nuclear antigen (PCNA), cytoplasmic beta-actin, growth arrest & DNA damage-inducible protein 153 (GADD153). All seven genes gave good Quantitative RT-PCR (Taqman™) confirmation, with respect to both direction and fold change and it was concluded that gene expression changes may provide a sensitive indicator of uncoupling due to chemical exposure.

In the next phase of this research, an attempt was made to understand as yet unidentified toxicological mechanisms associated with FCCP, using differential gene expression technology, biochemical assays and morphological evaluations, as tools. A markedly higher concentration of FCCP was used to elicit gene expression data. The exposure concentration was selected using light microscopy in combination with MTS tetrazolium assay (Cell Titer 96® Aqueous Non-radioactive Cell Proliferation Assay, Promega), that measures the reductive capacity of the cells, largely as a function of cellular NADPH/NADH content. The concentration that caused a 50% reduction in MTS activity after 24 h (24 h MTS EC_{50}) was determined. Based on the 24 h MTS $EC_{50,}$ in combination with light microscopic evaluation for cell viability, a concentration of 150 μM was selected for this phase of this study. Initial gene expression studies at 10 h showed gene expression patterns consistent with oxidative stress, in addition to patterns for cell cycle arrest, stress, DNA damage, DNA repair, suppression of DNA replication, apoptosis and inflammation. RT-PCR assay was performed to evaluate for oxidative

stress, using previously identified marker genes of oxidative stress. The genes on the oxidative stress panel were cytochrome P450 1A1 (CYP 1A1), DNA topoisomerase 2A (TOPO2A), heme oxygenase-1 (HO1), cyclin dependant kinase inhibitor 1 (CDKN1), γ-Glutamyl-cysteinyl ligase regulatory subunit (GCLM), glutathione reductase (GR) and thioredoxin reductase (TXNR). The RT-PCR profile obtained was consistant with oxidative stress induced expression patterns. A time course study followed the expression of the 7 oxidative stress genes for 9 time points over a 24 h period. A pattern of oxidative stress started to emerge as early as 4 h and was clearly evident by 8 h. TOP2 and HO1 proved to be good indicators of oxidative stress as they had the highest fold changes across time points and were apparent by 2 h. Similarly, a dose response study followed the expression of the same 7 gene transcripts at 7 exposure concentrations, from 0.1 µM to 150 µM FCCP at 10 h. The pattern of oxidative stress was clearly evident at 50 to 150 µM concentrations. Subsequently, biochemical tests for glutathione depletion, superoxide production and lipid peroxidation were performed and they provided further proof for FCCP-induced oxidative stress. Flow cytometric assay with Annexin V and Promidium iodide (PI) showed an increase in apoptosis and necrosis with increasing concentration of FCCP. The bioluminescent assay demonstrated a reduction of intracellular ATP concentration upon treatment with FCCP, which is indicative of the uncoupling effect of the compound and its influence on energy metabolism. Cytological evaluation of cells stained with H&E revealed reduced cell count and mitotic arrest at 10 h post treatment. RT-PCR analysis of mRNA expression of a separate set of 7 genes selected from the 10 h microarray data to represent pathways that were modulated with FCCP treatment, was also performed. Some of these genes were previously known to be affected by oxidative

stress while others were not. Genes known to be associated with oxidative stress are janus kinase 1 (JAK1), cadherin 2 (CAD2), relA proto-oncogene (RELA) [associated with NF-κB], protein kinase C alpha polypeptide (PKCA) and voltage-dependent anion channel 3 (VDAC3). Genes that have not been associated with oxidative stress are Alzheimer's disease amyloid A4 protein (ALZA) and peroxisome proliferator-activated receptor alpha (PPARα). The RT-PCR results were then compared with the microarray results. Five out of 7 genes were in agreement with the microarray result, both in magnitude and direction. The conclusion was that FCCP is a potent oxidative stressor and that gene expression profiles can be used effectively as a molecular marker for oxidative stress. This was the first report of FCCP- induced oxidative stress.

Taken together, the results of these studies can be briefly summarized as follows:

1. FCCP- induced loss of membrane potential was measured in intact cells, with the J-aggregate forming probe, JC-1

2. Gene expression changes may provide a sensitive indicator of uncoupling.

3. A set of 7 genes was identified as molecular markers for uncoupling with FCCP.

4. The genes identified as molecular markers of FCCP-induced uncoupling can be potentially used as markers of uncoupling by other agents.

5. The effect of uncouplers is reminiscent of hypoxic injury, with protein synthesis apparatus being one of the first systems to be affected.

6. The main events following uncoupling are drop in ATP, suppression of protein synthesis, DNA damage, disruption in cytoskeletal structure, increased glycolysis, increased expression of stress associated proteins, inflammatory stimulation, loss of

cell to cell adhesion, modulation of ion channel expression, cell cycle arrest and eventually apoptosis/ necrosis.

7. Cell cycle arrest owing to uncoupling occurs at G_1 and S phases.

8. FCCP is an oxidative stressor at higher doses in-vitro.

9. FCCP-induced oxidative stress is most apparent at 50 to 150 μM and at 4 to 12 h in RD cells in in-vitro systems.

10. Gene expression data was supported as and when deemed necessary, by RT-PCR and biochemical functional assays for the following: ATP, cell cycle, media glucose, media lactate, media LD, GSH and GSSG, lipid peroxidation, super oxide production, apoptosis and necrosis.

11. Large-scale analysis of gene expression using cDNA microarrays promises the rapid detection of toxicity for drugs and other chemicals.

Future directions:

Protonophoric uncouplers of oxidative phosphorylation still have the potential of being developed in to drugs for the pharmacological intervention of clinical obesity. But more work needs to be done to understand their pharmacological actions and toxicological mechanisms. Animal studies at various dose levels that incorporates monitoring of body heat output (with infrared thermal imaging system), standard metabolic rate, body weight, heart weight, body fat measurements, feed and water intake, along with assays for urinary nitrogen excretion, are in order. Tools of differential gene expression, protein expression, histopathology, metabonomics and clinical chemistry may be utilized to generate data. Parallels may be drawn between in-vitro and in-vivo studies.

A question that was not answered in the present study, but could easily be answered in an animal study, is how skeletal muscles might react to prolonged low levels of uncoupling – if there will there be an attempt to differentiate between oxidative to glycolytic myofibers.

VITAℤ

Sabu Kuruvilla

Candidate for the Degree of Doctor of Philosophy

Thesis: TRANSCRIPTIONAL RESPONSES TO TOXIC LEVELS OF
CARBONYL CYANIDE P-(TRIFLUROMETHOXY)
PHENYLHYDRAZONE [FCCP], AN UNCOUPLER OF
OXIDATIVE PHOSPHORYLATION

Major field: Veterinary Pathology

Biographical:

Education: Received Bachelor of Veterinary Sciences and Animal Husbandry from
Kerala Agricultural University, India, and a Master of Veterinary Sciences from
the University of Agricultural University, Bangalore, India, in 1976 and 1980,
respectively. Completed the requirements for the Doctor of Philosophy degree
with a major in Veterinary Pathology at Oklahoma State University in May,
2003

Experience: Worked as a member of the faculty of Kerala Veterinary College, India from
1980 to 1989. Moved to the United States in 1989 and worked for Park Poultry,
canton, Ohio until 1996, where I was responsible for hatchery management and
live production. Started graduate studies in Veterinary Pathology at Oklahoma
State University in 1996 and conducted PhD research at GlaxoSmithKline, RTP,
North Carolina.

Professional Memberships: American Veterinary Medical Association